

AD _____

Award Number: DAMD17-99-1-9518

TITLE: Role of Sphingosine Kinase in Radiation-Induced Apoptosis
of Human Prostate Cancer Cells

PRINCIPAL INVESTIGATOR: Victor Nava, M.D., Ph.D.

CONTRACTING ORGANIZATION: Georgetown University Medical Center
Washington, DC 20007

REPORT DATE: August 2001

TYPE OF REPORT: Annual Summary

PREPARED FOR: U.S. Army Medical Research and Materiel Command
Fort Detrick, Maryland 21702-5012

DISTRIBUTION STATEMENT: Approved for Public Release;
Distribution Unlimited

The views, opinions and/or findings contained in this report are those of the author(s) and should not be construed as an official Department of the Army position, policy or decision unless so designated by other documentation.

20020118 152

REPORT DOCUMENTATION PAGE			Form Approved OMB No. 074-0188	
Public reporting burden for this collection of information is estimated to average 1 hour per response, including the time for reviewing instructions, searching existing data sources, gathering and maintaining the data needed, and completing and reviewing this collection of information. Send comments regarding this burden estimate or any other aspect of this collection of information, including suggestions for reducing this burden to Washington Headquarters Services, Directorate for Information Operations and Reports, 1215 Jefferson Davis Highway, Suite 1204, Arlington, VA 22202-4302, and to the Office of Management and Budget, Paperwork Reduction Project (0704-0188), Washington, DC 20503				
1. AGENCY USE ONLY (Leave blank)	2. REPORT DATE August 2001	3. REPORT TYPE AND DATES COVERED Annual Summary (1 Aug 00 - 31 Jul 01)		
4. TITLE AND SUBTITLE Role of Sphingosine Kinase in Radiation-Induced Apoptosis of Human Prostate Cancer Cells		5. FUNDING NUMBERS DAMD17-99-1-9518		
6. AUTHOR(S) Victor Nava, M.D., Ph.D.				
7. PERFORMING ORGANIZATION NAME(S) AND ADDRESS(ES) Georgetown University Medical Center Washington, DC 20007 E-Mail: navav@gusun.georgetown.edu		8. PERFORMING ORGANIZATION REPORT NUMBER		
9. SPONSORING / MONITORING AGENCY NAME(S) AND ADDRESS(ES) U.S. Army Medical Research and Materiel Command Fort Detrick, Maryland 21702-5012		10. SPONSORING / MONITORING AGENCY REPORT NUMBER		
11. SUPPLEMENTARY NOTES				
12a. DISTRIBUTION / AVAILABILITY STATEMENT Approved for Public Release; Distribution Unlimited			12b. DISTRIBUTION CODE	
13. ABSTRACT (Maximum 200 Words) Understanding the biological mechanisms that control cell growth and cell death is a mayor goal in cancer research since it could allow the design of anti-neoplastic therapies to specifically eliminate tumor cells. The effectiveness of radiotherapy and chemotherapy relies in part in their ability to induce a genetic program of cell destruction know as apoptosis. Unfortunately, at present this conventional therapies induce cell death of both normal and cancer cells resulting in undesirable toxic effects. Furthermore, the signaling pathways that lead to apoptosis are often subverted in cancer cells resulting in resistance to radiation or chemotherapy. One mechanism by which cancer cells become resistant to radiation is by disrupting the sphigomyelin pathway that comprises a series of biochemical reactions generating lipid molecules called sphingolipids that are involved in controlling various cellular functions. The sphingolipid metabolites ceramide, sphingosine and sphingosine-1-phosphate (SPP) have recently emerged as a new class messengers that regulate cell growth and apoptosis. While intracellular accumulation of sphingosine or ceramide induces cell death, SPP promotes cell survival. Therefore, our laboratory has proposed that a dynamic balance in the level of intracellular sphingolipids serves as a signal to determine whether a cell survives or dies. In support of this hypothesis it has been found that the sensitivity of specific prostate cancer cell lines to radiation correlates with intracellular ceramide levels and with the activity of sphingosine kinase (SPHK), the enzyme that catalyzes the formation of SPP after adding a phosphate group to sphingosine. I propose to further investigate the role of sphingolipids in radiation-induced apoptosis in prostate cancer. First, prostate cancer cell lines with different susceptibility to radiation will be used to determine the mass levels of ceramide, sphingosine and SPP at different times after apoptotic stimulation. Elevated intracellular levels of ceramide and sphingosine are expected to be found in association with high radiosensitivity. Second, the levels of expression of SPHK will be experimentally enhanced or inhibited in prostate cancer cells and the susceptibility to apoptosis will be studied. Since SPHK produces SPP, decrease sensitivity to radiation is expected if high levels of this kinase are achieved. Finally, isolation of different forms of human SPHK will be attempted from known DNA sequences with similarity to murine SPHK. Achievement of this goal could facilitate characterization of role of sphingolipid metabolites in human cancer. In summary, studying the role of sphingolipids in the modulation of susceptibility of prostate cancer cells to apoptotic may provide the basis for molecular strategies that improve existing anti-neoplastic therapies.				
14. SUBJECT TERMS Prostate Cancer			15. NUMBER OF PAGES 52	
17. SECURITY CLASSIFICATION OF REPORT Unclassified			16. PRICE CODE	
18. SECURITY CLASSIFICATION OF THIS PAGE Unclassified			20. LIMITATION OF ABSTRACT Unlimited	
19. SECURITY CLASSIFICATION OF ABSTRACT Unclassified				

THIS PAGE
LEFT BLANK
INTENTIONALLY

TABLE OF CONTENTS

FRONT COVER	1
SF298	2
TABLE OF CONTENTS	4
INTRODUCTION	5
BODY	6
REPORTABLE OUTCOMES	9
CONCLUSIONS	10
REFERENCES	10
APPENDICES	12

INTRODUCTION

Recently, others and we have suggested that the sphingolipid metabolites, ceramide and sphingosine, provide proapoptotic signals, and a further metabolite, sphingosine-1-phosphate (SPP), promotes cell survival and suppresses apoptosis (1,2,7). Dysregulation of this sphingolipid biostat may be important in the acquisition of malignant phenotypes and radioresistance in which transformed cells can circumvent existing apoptotic mechanisms that would normally target the destruction of these cells. Thus, resetting this biostat could potentially be used to enhance apoptosis and overcome resistance to radiation or androgen ablation.

Previously, it has been suggested that LNCaP cells are highly resistant to induction of apoptosis by γ -irradiation due in part to a defect in ceramide generation (3,4). Likewise, resistance to apoptosis involves a defect in ceramide generation in the PC3 prostate cancer cell line. Although in LNCaP cells, irradiation did not result in ceramide generation or apoptosis, pretreatment with TPA not only enhanced radiation-induced apoptosis, but also enabled ceramide generation via activation of ceramide synthase (8). In agreement, apoptosis was abrogated by fumonisin B1, a competitive inhibitor of ceramide synthase. Most importantly, when transplanted orthotopically into the prostate of nude mice, LNCaP cells produced tumors that showed the same responses to TPA and radiation therapy (8). However, apoptosis induced by treatment with TNF and γ -irradiation was not mediated by stimulation of de novo ceramide synthesis. Similarly, apoptosis in LNCaP cells induced by the topoisomerase 1 inhibitor camptothecin, ceramide generation was also independent of the de novo pathway. A further metabolite of ceramide, sphingosine, has also been shown to induce apoptosis of androgen-independent human prostate cancer cells (5). Collectively, our previous work (10) suggest that ceramide and sphingosine generation together with inhibition of sphingosine kinase are critical components in radiation-induced apoptosis in human prostate cancer cells. Preventing ceramide and sphingosine generation and/or stimulation of sphingosine kinase may provide a selective advantage in the development of radioresistance of prostate tumors. Therefore, development of agents which specifically regulate levels of sphingolipid metabolites might provide new tools to use in conjunction with radiation therapy. Therefore, in order to further characterize the regulation of cell death by sphingolipids we established various cell lines expressing sphingosine kinase (SPHK).

BODY

Cloning and characterization of human isoforms of SPHK.

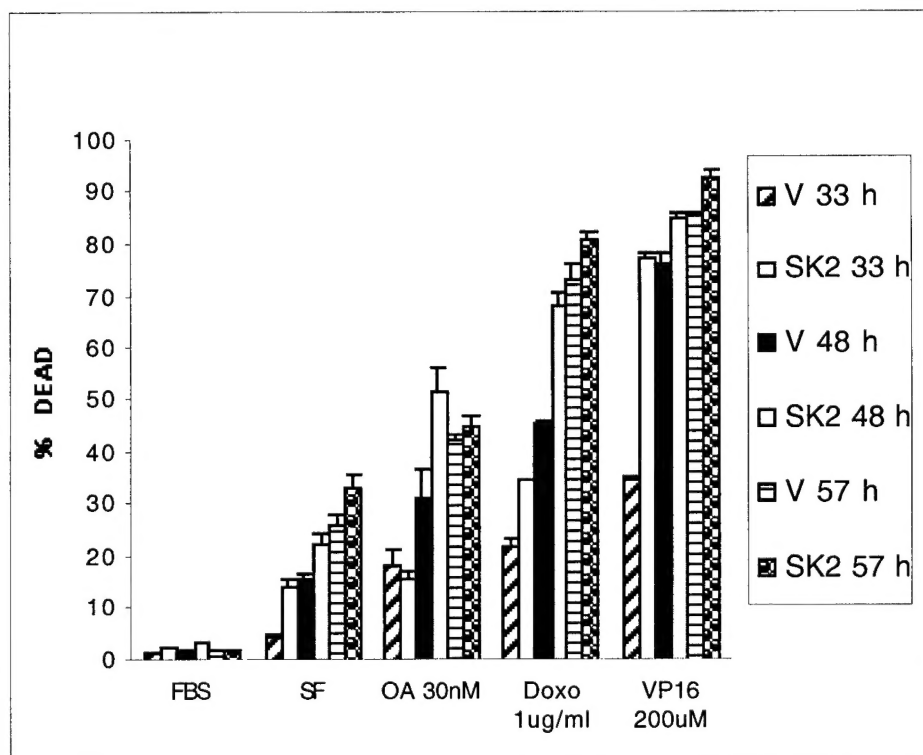
Last year we cloned and characterized human SPHK-1 and a novel sphingosine kinase isoform named SPHK-2 which we reported in the literature (11,12). This served to complete Task 3 of the grant (see Appendices).

Modulation of the expression of SPHK in human prostate cancer cell lines and characterization of their susceptibility to apoptosis.

The enhanced survival of cancer cells depends either on subversion of the apoptotic machinery by mutations or selection of genes that induce proliferation. SPP, the product of SPHK, could contribute to malignant transformation since it has mitogenic and anti-death functions. The cloning of SPHK now allows us to use genetic approaches to directly examine this hypothesis avoiding complications of exogenously added SPP, such as receptor engagement, limiting uptake, and delivery to specific cellular compartments, and is likely to succeed since previous results from our laboratory indicate that overexpression of SPHK in NIH 3T3 fibroblasts has mitogenic and anti-apoptotic effects (13). Therefore, we decided to assess whether modulation of SPHK activity by varying its expression in human prostate carcinoma cells alters their susceptibility to apoptotic stimuli, and whether SPHK expression counteracts only ceramide-mediated processes and/or also acts independently to promote survival. We selected TSU-Pr1 prostate carcinoma cells for studies of the role of SPHK regulating apoptosis for several reasons: **1.** TSU-Pr1 cells are sensitive to many apoptotic agents some of which, like Doxorubicin, are known to elevate ceramide levels. **2.** Irradiation increases ceramide levels and induces apoptosis in TSU-Pr1 cells. **3.** TSU-Pr1 cells undergo caspase-dependent apoptosis that is accessible to study using a variety of techniques used in our laboratory. **5.** TSU-Pr1 cells can readily be transfected and achieve high levels of protein expression of the transgenes. Our long-term plan is to study the role of both isoforms of SPHK in prostate cancer. However, our initial efforts were focused on SPHK-2 since it is a novel enzyme of unknown function, and since it is expressed in prostate cancer by SAGE (14). A pooled cell line overexpressing murine SPHK-2 tagged with c-myc was constructed using Lipofectamine Plus according to the instructions of the manufacturer (GIBCO-BRL). Surprisingly, we found that SPHK-2 accelerates apoptosis of TSU-Pr1 cells induced by a variety of noxious stimuli (Fig. 1A). Expression of SPHK-2 was adequate as determined by immunoblots (Fig.1B). Similar results were obtained using various cell lines after transient or stable overexpression (data not shown). In general, SPP production or SPHK-1 overexpression

has been associated with inhibition of cell death. However, some reports indicate that elevations of SPP may also be able to induce apoptosis (15). These apparently contradictory results may be reconciled considering various non-exclusive possibilities that are currently under investigation in our laboratory: 1- Differential effects of the accumulation of SPP in discrete microenvironments in a cell-type specific manner. 2- Generation of a SPP metabolite, such as dihydro-SPP, that could act in a cell-type specific fashion. Alternatively, a protein function of SPHK-2, may to activate the cell death program independently of the enzymatic ability to generate SPP . This is supported by the presence of a non-conserved region in SPHK-2 that is absent in SPHK-1, and is also the focus of our current efforts. In summary, we have made significant progress towards the completion of Task. 2 of the grant which could be completed within the allocated time of 32 months.

A



B

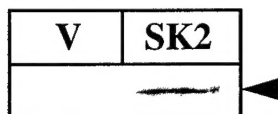


Figure 1. SPHK-2 accelerates cells death of TSU-Pr1 cells. (A) Subconfluent prostate cancer TSU-Pr1 cells stably expressing murine SPHK-2 (SK2) or a vector (V) control cell line, were treated with serum free media containing or not Okadaic acid (OA), Doxorubicin (Doxo) or Etoposide (VP16) at the indicated concentrations and cell viability was determined by blindly counting at least 400 cells at different times. Bars indicate standard error of an experiment performed in duplicate. Similar results were obtained in three independent experiments. (B) Expression of myc-SPHK-2 (SK2) in the TSU-Pr1 pooled cell line used in A, was confirmed by standard immunoblotting. Lysates from stable vector (myc-pcDNA3) transfected cells were used as a control.

REPORTABLE OUTCOMES

Publications during 2000-2001.

1. **Nava V. E.**, O. Cuvillier, L.C. Edsall, K. Kimura, E.P. Gelmann, and S. Spiegel. 2000. Sphingosine Enhances Apoptosis of Radiation Resistant Prostate Cancer Cells. Cancer Research. 60: 4305-4310.
2. Liu Y, Wada R, Yamashita T, Deng C.X., Rosenfeldt H.M. Hobson J.P., **Nava V.E.**, Chae S.S., Lee M.J., Liu C.H., Hla T, Spiegel S. and Proia R.L. 2000. Edg-1, the G-Protein-Coupled Receptor for Sphingosine-1-Phosphate, is Essential for Vascular Maturation. 2000. J. Clin. Invest. 106(8):951-961.
3. Cuvillier O.C., **V. E. Nava**, S. Murthy, L.C. Edsall, T. Levade, S. Milstien, and S. Spiegel. 2001. Sphingosine generation, cytochrome c release, and activation of caspase-7 in doxorubicin-induced apoptosis of MCF7 breast adenocarcinoma cells. Cell Death and Differentiation. 8: 162-171.
4. Rosenfeldt HM, J.P. Hobson, M. Maceyka, Y. Liu, A. Olivera, **V.E. Nava**, Milstien, R. Proia, and S. Spiegel. Transactivation of EDG-1 by PDGF is essential for SRC and Focal Adhesion Kinase activation. Submitted.

Abstracts during 2000-2001.

1. **V.E. Nava**, O. Cuvillier, E.C. Edsall, K. Kimura, S. Murthy, E.P. Gelman and S. Spiegel. 2000. Sphingosine sensitizes LNCaP cells to γ -irradiation-induced apoptosis. Fumosins Risk Assessment Workshop. FDA. University of Maryland. College Park, Maryland.
2. **V.E. Nava**, O. Cuvillier, E.C. Edsall, K. Kimura, S. Murthy, E.P. Gelman and S. Spiegel. 2000. Modulation of TNF- α and γ -irradiation-induced apoptosis of Prostate Cancer Cells by Sphingolipids. Programmed Cell Death Regulation. American Association for Cancer Research. Lake Tahoe, Nevada. B-14.
3. **V.E. Nava**, Shvetha Murthy, Ana Olivera, Samantha Poulton, Adriana Stoica, Mary Beth Martin, Robert Clarke and Sarah Spiegel. 2001 Sphingosine kinase promotes estrogen-dependent tumorigenesis of breast cancer MCF-7 cells through inhibition of apoptosis and induction of proliferation. The Molecular Basis of Cancer: Signaling to Cell Growth and Death (J2). Keystone Symposia. Taos, New Mexico. P-226.

CONCLUSIONS

Resistance to apoptosis is important in tumorigenesis and viral diseases and thus interference with apoptosis is important for development of therapeutic modalities in cancer and other human diseases. The positive and negative effects of SPP and ceramide on cell proliferation and survival may potentially be of interest in paradigms of normal growth and development, as well as in stress responses, toxicology, and tumor biology.. Disregulation of the sphingolipid biostat may be important in the acquisition of malignant phenotypes in which transformed cells can circumvent existing apoptotic mechanisms that would normally target the destruction of mutated cells. The regulation of the sphingolipid biostat may have important implications for the treatment of cancer, since many therapeutic approaches have been shown to cause accumulation of ceramide, including cytosine arabinoside, vincristine, daunorubicin, and ionizing radiation (6,9). While some therapeutic approaches that induce ceramide-mediated apoptotic pathways have had success in treating leukemias and lymphomas, many solid tumors have proven to be more resistant to apoptotic stimuli. The reasons for these differences in susceptibility to apoptotic stimuli are poorly understood. It is our hypothesis that the susceptibility of tumor cells to apoptotic stimuli can be altered by modulating the sphingolipid biostat. In support of this idea, we showed that radiation resistance of prostate cancer cells could also be altered by modulating ceramide levels. Elucidation of the role of sphingolipid metabolites, ceramide and SPP, in cancer cell biology, may also identify new targets and mechanisms for specifically interfering with proliferative, locomotive, and survival responses as a basis for therapeutic intervention based on manipulation of sphingolipid metabolite signaling.

REFERENCES

1. Hannun, Y. Functions of ceramide in coordinating cellular responses to stress, *Science*. 274: 1855-1859, 1996.
2. Kolesnick, R. N. and Kronke, M. Regulation of ceramide production and apoptosis, *Annu. Rev. Physiol.* 60: 643-665, 1998.
3. Garzotto, M., White-Jones, M., Jiang, Y., Ehleiter, D., Liao, W. C., Haimovitz-Friedman, A., Fuks, Z., and Kolesnick, R. 12-O-tetradecanoylphorbol-13-acetate-induced apoptosis in LNCaP cells is mediated through ceramide synthase, *Cancer Res.* 58: 2260-2264, 1998.
4. Kimura, K., Bowen, C., Spiegel, S., and Gelmann, E. P. TNF- α sensitizes prostate cancer cells to irradiation-induced apoptosis, *Cancer Res.* 7: 1606-1614, 1999.
5. Shirahama, T., Sakakura, C., Sweeney, E. A., Ozawa, M., Takemoto, M., Nishiyama,

- K., Ohi, Y., and Igarashi, Y. Sphingosine induces apoptosis in androgen-independent human prostatic carcinoma DU-145 cells by suppression of bcl-X(L) gene expression, *FEBS Lett.* 407: 97-100, 1997.
6. Cuvillier, O., Pirianov, G., Kleuser, B., Vanek, P. G., Coso, O. A., Gutkind, S., and Spiegel, S. Suppression of ceramide-mediated programmed cell death by sphingosine-1-phosphate, *Nature.* 381: 800-803, 1996.
 7. Spiegel, S., Foster, D., and Kolesnick, R. N. Signal transduction through lipid second messengers, *Curr. Opin. Cell Biol.* 8: 159-167, 1996.
 8. Garzotto, M., Haimovitz-Friedman, A., Liao, W. C., White-Jones, M., Huryk, R., Heston, W. D., Cardon-Cardo, C., Kolesnick, R., and Fuks, Z. Reversal of radiation resistance in LNCaP cells by targeting apoptosis through ceramide synthase, *Cancer Res.* 59: 5194-5201, 1999.
 9. Spiegel, S. and Merrill, A. H., Jr. Sphingolipid metabolism and cell growth regulation, *FASEB J.* 10: 1388-1397, 1996.
 10. Nava V. E., O. Cuvillier, L.C. Edsall, K. Kimura, E.P. Gelmann, and S. Spiegel. Sphingosine Enhances Apoptosis of Radiation Resistant Prostate Cancer Cells. *Cancer Research.* 60: 4305-4310, 2000.
 11. Liu H, Sugiura M, Nava V.E, Edsall LC, Kono K, Poulton S, Milstien S, Kohama T, Spiegel S. Molecular Cloning and Functional Characterization of a Novel Mammalian Sphingosine Kinase Type 2 Isoform. *J Biol Chem.* 275: 19513-20, 2000.
 12. Nava V. E., E. Lacana, P. Samantha, H. Liu, M. Sugiura, K. Kono, S. Milstien, Kohama and S. Spiegel. Functional Characterization of Human Sphingosine Kinase-1. *FEBS Letters.* 473: 81-84, 2000.
 13. Olivera O, T. Kohama, L. Edsall, V. Nava, O. Cuvillier, S. Poulton, and S. Spiegel. Sphingosine Kinase Expression Increases Intracellular Sphingosine-Phosphate and Promotes Cell Growth and Survival. *J. Cell Biol.* 147:545-557, 1999.
 14. Velculescu VE, Zhang L, Vogelstein B, Kinzler KW. Serial analysis of gene expression. *Science.* 371:368-9, 1995.
 15. Hung WC, Chuang LY. Induction of apoptosis by sphingosine-1-phosphate in human hepatoma cells is associated with enhanced expression of bax gene product. *Biochem Biophys Res Commun.* 229:11-5, 1996.

APPENDICES

Sphingosine Enhances Apoptosis of Radiation-resistant Prostate Cancer Cells¹

Victor E. Nava, Olivier Cuvillier, Lisa C. Edsall, Kotohiko Kimura, Sheldon Milstien, Edward P. Gelmann, and Sarah Spiegel²

Department of Biochemistry and Molecular Biology [V. E. N., O. C., S. S.], and Division of Hematology/Oncology, Department of Medicine [K. K., E. P. G.], Lombardi Cancer Center, Georgetown University Medical Center, Washington, DC 20007, and Laboratory of Cellular and Molecular Regulation, National Institute of Mental Health, Bethesda, Maryland 20892 [L. C. E., S. M.]

ABSTRACT

Ceramide has been implicated as an important component of radiation-induced apoptosis of human prostate cancer cells. We examined the role of the sphingolipid metabolites—ceramide, sphingosine, and sphingosine-1-phosphate—in susceptibility to radiation-induced apoptosis in prostate cancer cell lines with different sensitivities to γ -irradiation. Exposure of radiation-sensitive TSU-Pr1 cells to 8-Gy irradiation led to a sustained increase in ceramide, beginning after 12 h of treatment and increasing to 2.5- to 3-fold within 48 h. Moreover, irradiation of TSU-Pr1 cells also produced a marked and rapid 50% decrease in the activity of sphingosine kinase, the enzyme that phosphorylates sphingosine to form sphingosine-1-phosphate. In contrast, the radiation-insensitive cell line, LNCaP, had sustained sphingosine kinase activity and did not produce elevated ceramide levels on 8-Gy irradiation. Although LNCaP cells are highly resistant to γ -irradiation-induced apoptosis, they are sensitive to the death-inducing effects of tumor necrosis factor α , which also increases ceramide levels in these cells [K. Kimura *et al.*, *Cancer Res.*, 59: 1606-1614, 1999]. Moreover, we found that although irradiation alone did not increase sphingosine levels in LNCaP cells, tumor necrosis factor α plus irradiation induced significantly higher sphingosine levels and markedly reduced intracellular levels of sphingosine-1-phosphate. The elevation of sphingosine levels either by exogenous sphingosine or by treatment with the sphingosine kinase inhibitor *N,N*-dimethylsphingosine induced apoptosis and also sensitized LNCaP cells to γ -irradiation-induced apoptosis. Our data suggest that the relative levels of sphingolipid metabolites may play a role in determining the radiosensitivity of prostate cancer cells, and that the enhancement of ceramide and sphingosine generation could be of therapeutic value.

INTRODUCTION

Prostate cancer is the most common malignancy and the second leading cause of cancer deaths in men (1). Radiation therapy that causes growth inhibition and apoptosis is often used for treatment of both primary and metastatic prostate cancer. However, despite using high doses of radiation, about 20-25% of prostate cancer patients with noninvasive disease (stages T₁-T₂) relapse. A major reason for failure to eradicate local disease is the intrinsic radioresistance of the tumors. Ionizing radiation mediates cell death, in part, through chromosomal damage and also by the induction of apoptosis. Although apoptosis seems to be less prevalent than clonogenic cell death, one mechanism by which cancer cells become resistant to radiation or chemotherapy is by the disruption of pathways leading to apoptosis.

Abundant evidence suggests that the sphingolipid metabolite, ceramide, is a critical component of ionizing radiation-induced apoptosis (2-5). This apoptotic pathway is initiated by hydrolysis of sphingo-

myelin, a membrane lipid, attributable to the activation of sphingomyelin-specific forms of phospholipase C, termed sphingomyelinases SMases,³ to generate ceramide. Ceramide, in turn, can activate several pathways important for the induction of apoptosis (reviewed in Refs. 6, 7). Both neutral and acidic SMases, distinguishable by their pH optima, have been reported to be involved in the induction of apoptosis after ionizing radiation (reviewed in Refs. 8, 9). Acidic SMase may play an essential role in radiation-induced apoptosis because lymphocytes from individuals with Niemann-Pick disease (who have an inherited deficiency of acidic SMase) and from acidic SMase-deficient mice, do not generate ceramide and have defective apoptotic responses to ionizing radiation (4). These deficits are reversible on restoration of acidic SMase activity, which further substantiates the obligatory role for ceramide generation in these apoptotic responses. However, ionizing radiation-triggered apoptosis of sensitive, but not resistant, human myeloid leukemic cell lines correlated with sphingomyelin hydrolysis and ceramide generation through activation of neutral, but not acidic, SMase (10). Similarly, loss of ceramide production from a neutral SMase confers resistance to radiation-induced apoptosis of lymphocytes (5). Moreover, depletion of glutathione, an endogenous inhibitor of neutral SMase (11), may also contribute to its activation, because glutathione depletion occurs in a variety of cells during radiation-induced apoptosis (12, 13). In addition, it has been suggested that *de novo* synthesis of ceramide as a result of increased ceramide synthase activity may also be involved in apoptosis (14), particularly in radiation-insensitive LNCaP prostate cancer cells that are induced to die by the phorbol ester PMA (15). LNCaP cells express androgen receptor, and their growth is increased by androgen. However, because they do not undergo apoptosis after androgen withdrawal, these cells can be used as an *in vitro* model to study strategies for treating prostate cancers that are resistant to androgen ablation. LNCaP cells are highly resistant to apoptosis induced by γ -irradiation, although somewhat sensitive to the death-inducing effects of TNF- α . Recently, we have shown that TNF- α sensitizes LNCaP cells to γ -irradiation-induced apoptosis by elevating ceramide levels (16). Moreover, exogenous C₂-cer also sensitized LNCaP cells to irradiation, which lends further support to the notion that ceramide generation might be important for radiation-induced apoptosis in human prostate cancer.

One metabolite of ceramide, sphingosine, formed by ceramidase, has also been implicated in cell growth arrest and apoptosis. Sphingosine is rapidly produced during TNF- α -mediated apoptosis in human neutrophils (17) and cardiac myocytes (18). Recently, it has been shown that sphingosine and other long-chain sphingoid bases induce apoptosis in hepatoma cells by the activation of caspase-3-like proteases (19). Moreover, in androgen-independent human prostatic carcinoma DU-145 cells that express bcl-X_L, sphingosine but not its metabolites induced apoptosis by down-regulation of bcl-X_L, independently of PKC inhibition (20). In contrast to the growth-suppressing and pro-apoptotic roles of ceramide

Received 12/8/99; accepted 6/7/00.

The costs of publication of this article were defrayed in part by the payment of page charges. This article must therefore be hereby marked advertisement in accordance with 18 U.S.C. Section 1734 solely to indicate this fact.

¹ This work was supported by NIH Grants CA61774 (to S. S.) and CA/AG79912 (to E. P. G.). V. E. N. was supported by Postdoctoral Fellowship BC961968 from the United States Army Medical Research and Materiel Command, Prostate Cancer Research Program.

² To whom requests for reprints should be addressed, at Department of Biochemistry and Molecular Biology, Georgetown University Medical Center, 353 Basic Science Building, 3900 Reservoir Road, NW, Washington, DC 20007. Phone: (202) 687-1432; Fax: (202) 687-0260; E-mail: spiegel@bc.georgetown.edu.

³ The abbreviations used are: SMase, sphingomyelinase; TNF- α , tumor necrosis factor α ; C₂-cer, C₂-ceramide (*N*-acetylsphingosine); IMEM, Richter's improved minimal essential medium; ISEL, *in situ* end labeling; PKC, protein kinase C; SPP, sphingosine-1-phosphate; DMS, *N,N*-dimethylsphingosine; PMA, phorbol 12-myristate 13-acetate; PARP, poly(ADP-ribose) polymerase; FB1, fumonisin B1.

and sphingosine, SPP, formed from sphingosine by activation of sphingosine kinase (21), has been implicated in cellular proliferation and survival induced by platelet-derived growth factor, serum, nerve growth factor, and vitamin D₃, and protects cells from apoptosis resulting from elevations of ceramide (22–26). In this report, we examined the role of ceramide, sphingosine, and sphingosine kinase in the sensitization of radio-resistant LNCaP prostate cells to γ -irradiation-induced apoptosis.

MATERIALS AND METHODS

Materials. Human TNF- α and poly-D-lysine were purchased from Boehringer Mannheim (Indianapolis, IN). *Staphylococcus aureus* SMase and FBI were purchased from Sigma (St. Louis, MO). Sphingosine and DMS were from Biomol Laboratories (Plymouth Meeting, PA). *Escherichia coli* diacylglycerol kinase was from Calbiochem (La Jolla, CA). Insulin/transferrin/selenium was from Biofluids (Rockville, MD).

Cell Culture. LNCaP and TSU-Pr1 human prostate cancer cells were maintained at 37°C in IMEM (Life Technologies, Gaithersburg, MD) supplemented with 5% fetal bovine serum (27). LNCaP cells were plated on poly-D-lysine-coated dishes and grown for 5 days. Twenty-four h before treatment, cells were starved in serum-free IMEM medium without phenol red, supplemented with insulin (5 μ g/ml), transferrin (5 μ g/ml), and selenium (5 ng/ml). Cells were treated as indicated without or with γ -irradiation (8 Gy), using a JL Shepherd Mark 1 Irradiator [¹³⁷Cs] source with a dose rate of 209 cGy/min.

Apoptosis Measurement. ISEL was used to determine the extent of apoptosis as described previously (27). In some experiments, apoptotic morphology was also examined by staining cells with Hoechst 33258 (Calbiochem, San Diego, CA) as previously described (24). At least 500 cells were scored to calculate the percentage of apoptotic cells.

Extraction of Lipids. Cells were harvested in 1 ml of 25 mM HCl/methanol, and lipids were extracted with 2 ml of chloroform/1 M NaCl (1:1, v/v) plus 100 μ l 3N NaOH for the extraction of SPP and phases separated. Phospholipid, ceramide, and sphingosine levels were determined in aliquots of the organic layer, whereas SPP levels were determined from aqueous phase extracts (23).

Measurement of Total Cellular Phospholipids. Total phospholipids in cellular lipid extracts were quantified as described previously (28).

Measurements of Ceramide, Sphingosine, and SPP Levels. Mass amounts of ceramide and sphingosine in cellular extracts were measured by the diacylglycerol kinase and sphingosine kinase enzymatic methods, respectively, exactly as described previously (23). Labeled ceramide-1-phosphate and SPP were resolved by TLC with chloroform/acetone/methanol/acetic acid/water (10:4:3:2:1) and quantified with a Molecular Dynamics Storm phosphorimager (Sunnyvale, CA). SPP levels were measured essentially as described previously (29). Briefly, 500 μ l of buffer A [200 mM Tris-HCl (pH 7.4), 75 mM MgCl₂ in 2 M glycine (pH 9.0)] and 50 units of alkaline phosphatase were added to the aqueous phase containing extracted SPP. After incubating 1 h at 37°C, 50 μ l concentrated HCl were added, and sphingosine was extracted and quantitated with sphingosine kinase as described previously (29). For each experiment, known amounts of SPP were used to generate a standard curve.

Sphingosine Kinase Activity. Cells were harvested in buffer B [20 mM Tris (pH 7.4), 20% glycerol, 1 mM mercaptoethanol, 1 mM EDTA, 1 mM sodium orthovanadate, 40 mM -glycerophosphate, 0.5 mM 4-deoxyripyridoxine, 15 mM NaF, 10 μ g/ml leupeptin, 10 μ g/ml aprotinin and 1 mM phenylmethylsulfonyl fluoride] and lysed by freeze-thawing. Supernatants were collected after centrifugation at 100,000 \times g for 30 min at 4°C. Cytosolic sphingosine kinase activity was determined as described previously (23).

Immunoblotting. Cells were harvested in buffer C [10 mM HEPES-KOH (pH 7.4), 2 mM EDTA, 0.1% (w/v) CHAPS, 5 mM DTT, 1 mM phenylmethylsulfonyl fluoride, 10 μ g/ml pepstatin A, 10 μ g/ml aprotinin, and 20 μ g/ml leupeptin] and Western blotting was carried out as described previously (24). Clone 7D3-6 mouse monoclonal anti-PARP (PharMingen, San Diego, CA; 0.5 μ g/ml), rabbit polyclonal anti-caspase-7 (Oncogene, Cambridge, MA; 2.5 μ g/ml), rabbit anti-caspase-3 (gift of Dr. Donald Nicholson), and mouse anti-caspase-8 (gift of Dr. Markus Peter), were used as primary antibodies. Proteins were visualized with SuperSignal-enhanced chemiluminescent reagent (Pierce, Rockford, IL) using antirabbit or antimouse horseradish peroxidase-conjugated IgG (Bio-Rad).

RESULTS

Sphingomyelinase Treatment Sensitizes LNCaP Cells to γ -Irradiation-induced Apoptosis. Previously, we have shown that treatment with C₂-cer synergizes with γ -irradiation to induce cell death in LNCaP cells (16). In agreement, we have found that increasing endogenous long-chain ceramide levels in LNCaP cells by pretreatment with SMase induces apoptosis and sensitizes the cells to a dose of γ -irradiation (8 Gy) sufficient to trigger apoptosis of TSU-Pr1 but not of LNCaP cells (Fig. 1). Apoptosis increased in a time-dependent manner, and at least 48 h were required for significant cell death. To confirm the induction of apoptosis, we also examined DNA fragmentation and nuclear condensation by staining with the DNA-specific fluorochrome bisbenzimidazole (Hoechst 33258). Substantially more DNA ladder formation and fragmented nuclei were seen after 72 h than after 48 h (data not shown).

To examine whether there was a correlation between ceramide levels and radiation sensitivity, we measured changes in ceramide levels after irradiation of these two cell lines. Exposure of radiation-sensitive TSU-Pr1 cells to 8 Gy irradiation led to acute, but small, increases in ceramide levels within 30 min, followed by a sustained elevation in ceramide 12 h after irradiation, which reached a 3-fold increase by 48 h (Fig. 2A). This generation of ceramide preceded the appearance of nuclear fragmentation that was evident only after 48 h (Fig. 1). In contrast, ceramide levels did not change in radio-resistant LNCaP cells (Fig. 2A). In addition, irradiation induced a rapid and sustained decrease in sphingosine kinase activity in TSU-Pr1 cells but not in LNCaP cells (Fig. 2B). A surge in sphingosine levels was detected in TSU-Pr1 cells in correspondence with the inhibition of sphingosine kinase (Fig. 2C). SPP levels in the radiosensitive TSU-Pr1 cells were below the detection limit (<0.01 pmol/nmol phospholipid), and we were, thus, unable to detect any increases after irradiation. Interestingly, levels of SPP in TSU-Pr1 cells were much lower than in LNCaP cells (0.12 pmol/nmol phospholipid), which are more resistant to γ -radiation. Thus, there seems to be a reciprocal relationship between ceramide/sphingosine and sphingosine kinase in radiation-sensitive prostate cancer cells.

Sphingosine Generation in Apoptosis-sensitized LNCaP Cells. Because it has been suggested that sphingosine, a breakdown product of ceramide, might also be a mediator of programmed cell death (19), it was of interest to determine whether sphingosine could be involved in the sensitization of LNCaP cells to apoptosis that was induced by irradiation. Treatment with bacterial SMase, which markedly sensitizes these cells to radiation (Fig. 1), as expected, induced a rapid 4- to 5-fold elevation in ceramide levels, which remained elevated at 24 h and declined thereafter (Fig. 3A). Interestingly, SMase treatment

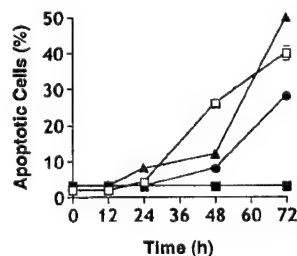


Fig. 1. Effect of γ -irradiation and sphingomyelinase on apoptosis in prostate cancer cells. LNCaP (■, ▲, ●) and TSU-Pr1 (□) cells (1.5×10^4 per well) were seeded in 6-well plates coated with poly-D-lysine and grown until ~40% confluent. Cells were treated without (□, ■) or with 100 mU/ml SMase (▲, ●) for 1 h and then irradiated with 8 Gy (□, ▲) as indicated. Apoptotic cells were assayed by ISEL at the indicated times, as described in "Materials and Methods." Results are means \pm SD of triplicate determinations from one of three representative experiments. ▲, LNCaP (SMase + 8 Gy); □, TSU-Pr1 (8 Gy); ●, LNCaP (SMase); ■, LNCaP (8 Gy).

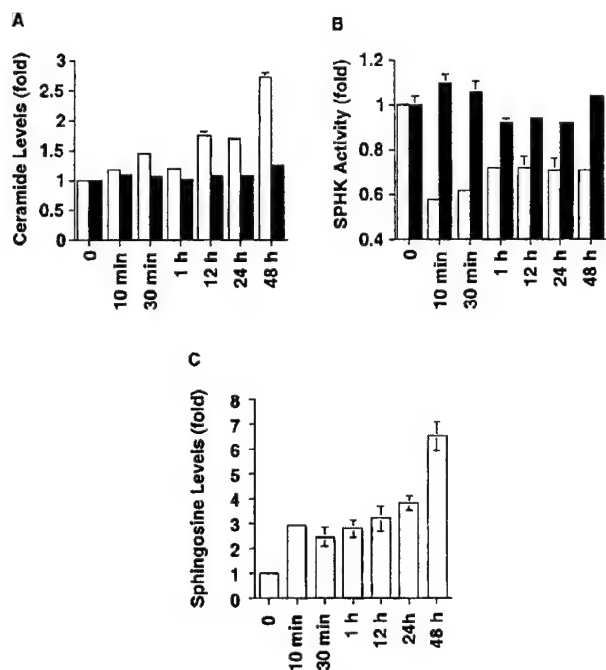


Fig. 2. γ -Irradiation-induced ceramide elevation and decreased sphingosine kinase activity in TSU-Pr1 but not in LNCaP cells. LNCaP cells (■) or TSU-Pr1 cells (□) were seeded at 2×10^5 per well and grown in 10-cm dishes. At the indicated time after exposure to 8 Gy of irradiation, ceramide levels (A), sphingosine kinase activity (B), and sphingosine levels (C, □) were measured as described in "Materials and Methods." Results are means \pm SD of triplicate determinations from a representative experiment and are expressed as fold-changes relative to zero time. The basal sphingosine level in TSU-Pr1 cells was 0.23 ± 0.07 pmol/nmol phospholipid. Similar results were found in three independent experiments. However, the small acute ceramide increase at 30 min observed in A was not statistically significant.

also increased intracellular sphingosine after 24 h (Fig. 3B). It is likely that this increase in sphingosine results from degradation of ceramide, inasmuch as the ceramide increase preceded that of sphingosine. It should be pointed out that the elevation of these two sphingolipid metabolites precedes the onset of apoptosis (Fig. 1). As previously shown (16), we found that TNF- α also sensitized LNCaP cells to irradiation with a concomitant increase in ceramide levels (Fig. 4A and 5A). Although irradiation alone did not increase sphingosine levels in LNCaP cells, irradiation together with TNF- α induced significantly higher sphingosine levels than TNF- α alone (Fig. 4B). The increase in sphingosine was detected 24 h after treatment, coinciding with elevation in ceramide levels and preceding nuclear fragmentation that was evident 48 h after treatment (16). In LNCaP cells that were sensitized to die by irradiation and TNF- α , there was a marked decrease in SPP levels 48 h after treatment, whereas no significant changes in SPP levels were detected in cells treated with γ -irradiation alone (Fig. 4C). It should be noted that SPP levels in LNCaP cells (0.12 ± 0.01 pmol/nmol phospholipid) are greater than in other normal and cancer cells (29), including HL60 cells (0.01 ± 0.001 pmol/nmol phospholipid), PC12 pheochromocytoma cells (0.02 ± 0.001 pmol/nmol phospholipid), and human breast cancer MCF7 cells (0.05 ± 0.001 pmol/nmol phospholipid), which might explain the high resistance of LNCaP cells to apoptotic stimuli.

De novo synthesis of ceramide has been implicated in the apoptosis of LNCaP cells induced by treatment with phorbol ester (15). Thus, it was of interest to examine whether the increased ceramide levels was attributable to stimulation of ceramide synthase. The mycotoxin, FB1, a known inhibitor of ceramide synthase, alone did not induce apoptosis, nor did it affect the extent of apoptosis induced by TNF and

γ -irradiation (Fig. 5B), although in agreement with a recent study (15), it almost completely blocked the increase in PMA-induced apoptosis in LNCaP cells. These results suggest that the *de novo* ceramide generation pathway does not play a role in the apoptosis that is induced by TNF- α and γ -irradiation. The increase in ceramide preceded that of sphingosine, which suggested that sphingosine might arise from ceramidase-catalyzed metabolism of ceramide. This is a

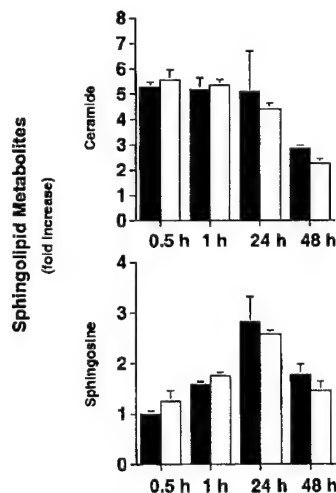


Fig. 3. Changes in ceramide and sphingosine levels after γ -irradiation of sphingomyelinase-treated LNCaP cells. Cells were seeded and grown as described in Fig. 2 and treated without or with SMase (100 mU/ml; ■) and then irradiated with 8 Gy as indicated (□). At the indicated times, ceramide, sphingosine, and phospholipid levels were determined as described in "Materials and Methods." Data are expressed as fold-increases relative to untreated controls, and are means \pm SD of triplicate determinations from a representative experiment.

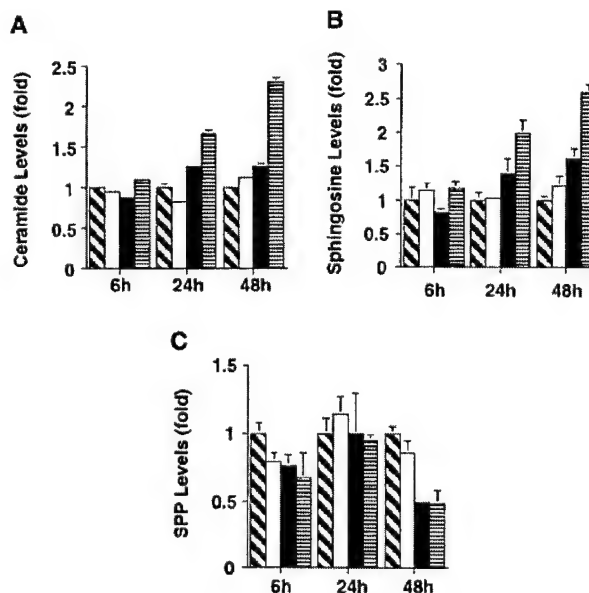


Fig. 4. Changes in levels of the sphingolipid metabolites ceramide, sphingosine, and SPP after treatment of LNCaP cells with γ -irradiation and TNF- α . Cells were seeded and grown as described in Fig. 2. Cells were treated without (control) or with TNF- α (100 ng/ml) for 1 h before irradiation with 8 Gy as indicated. Ceramide (A), sphingosine (B), SPP (C), and phospholipid levels were measured after 6, 24, and 48 h as described in "Materials and Methods." Results are means \pm SD of triplicate determinations from a representative experiment and are expressed as fold-changes relative to control. Levels of ceramide, sphingosine, and SPP in untreated LNCaP cells were 19 ± 2 , 0.23 ± 0.03 , and 0.29 ± 0.06 pmol/nmol phospholipid, respectively. □, control; ▨, γ radiation (8 Gy); ■, TNF- α ; ■, TNF- α + 8 Gy.

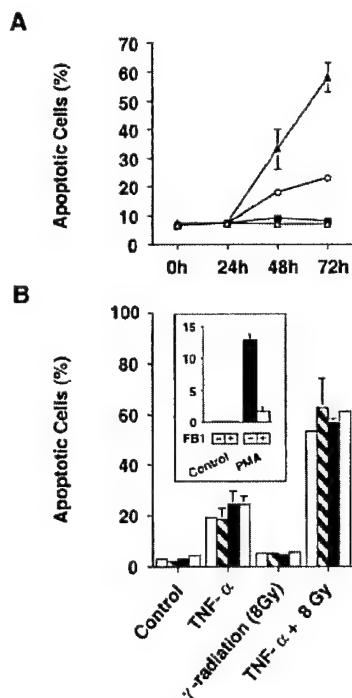


Fig. 5. Effect of FB1 on TNF- α and γ -irradiation-induced apoptosis. In A, cells were treated without (■) or with 100 ng/ml TNF- α (▲, ○) followed by irradiation (▲, ■), and apoptosis was assayed by ISEL at the indicated times. ▲, TNF- α + 8 Gy; ○, TNF- α ; ■, γ radiation (8 Gy); Δ, control. B, cells were treated with the indicated concentrations of FB1 in the absence or presence of TNF- α and/or 8 Gy irradiation as indicated, and apoptosis was determined after 72 h. □, 0 μ M FB1; ▨, 50 μ M FB1; ■, 100 μ M FB1; ▩, 150 μ M FB1. Inset, the effect of FB1 (100 μ g/ml) on PMA-induced apoptosis 48 h after treatment.

likely possibility because sphingosine is not synthesized *de novo*, and can only be produced from ceramide (30, 31). However, *N*-oleoylethanolamine, a proposed acidic ceramidase inhibitor (32), by itself, even at a relatively low concentration (0.1 mM), markedly induced LNCaP cell death. It should be pointed out that *N*-oleoylethanolamine may not be a specific acidic ceramidase because it did not inhibit acidic ceramidase activity in an *in vitro* assay.

Sphingosine and DMS Sensitize LNCaP Cells to γ -Irradiation-induced Apoptosis. Sphingosine, but not ceramide, induced apoptosis of the androgen-independent human prostatic carcinoma cell line DU-145 (17, 20). To further examine whether sphingosine generation might also be important to sensitize LNCaP cells to irradiation, we used exogenously added sphingosine, which is efficiently taken up by cells. Significant apoptosis was induced by treatment with 20 μ M sphingosine that was detectable only after 72 h (Fig. 6). Sphingosine also markedly sensitized LNCaP cells to γ -radiation in a dose-dependent manner (Fig. 6), which was evident even at 48 h. After irradiation in the presence of 20 μ M sphingosine, most (>60%) of the cells were apoptotic by 72 h.

Another means to increase sphingosine levels is by the inhibition of sphingosine kinase. Recently, we (33) and others (34) have shown that DMS is a specific competitive inhibitor of sphingosine kinase which is effective at concentrations that do not inhibit PKC. DMS, at concentrations of 10 and 20 μ M, induced 20 and 60% apoptosis, respectively, after 72 h (Fig. 7). Moreover, DMS also sensitized LNCaP cells to apoptosis induced by γ -irradiation in a dose-dependent manner.

Activation of Caspases in Sphingosine and DMS-induced Sensitization of LNCaP Cells to γ -Irradiation. The broad-specificity tetrapeptide caspase inhibitor z-VAD-fluoromethyl ketone blocks

apoptosis induced by sphingosine or DMS in HL-60 (35) and Hep3B hepatoma cells (19), which suggests that a protease of the caspase-3 subfamily is activated. Thus, we examined whether elevation of sphingosine resulted in the activation of caspases-3 and -7, which drive the effector phase of apoptosis by cleaving key proteins, particularly the DNA repair enzyme PARP. As previously shown (16), treatment with 30 nM okadaic acid for 48 h resulted in apoptosis and PARP cleavage in LNCaP cells (Fig. 8). In agreement with our previous studies (16), when compared with okadaic acid, sphingolipid

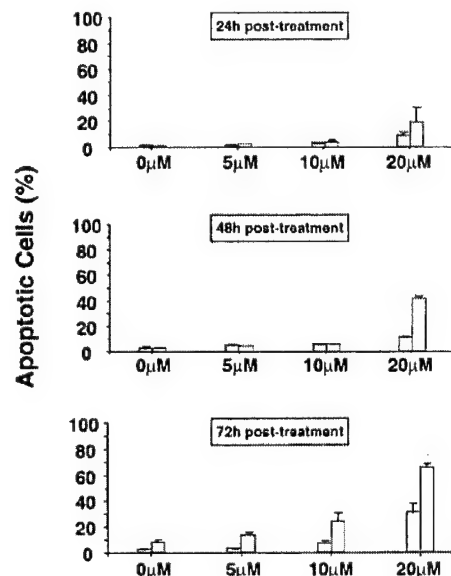


Fig. 6. Sphingosine sensitizes LNCaP cells to γ -irradiation-induced apoptosis. LNCaP cells were treated without or with the indicated concentrations of sphingosine for 1 h and then either not irradiated (□) or irradiated with 8 Gy (▨). Apoptotic cells were assayed by ISEL at the indicated times. Data are means \pm SD of triplicate determinations from one of three representative experiments.

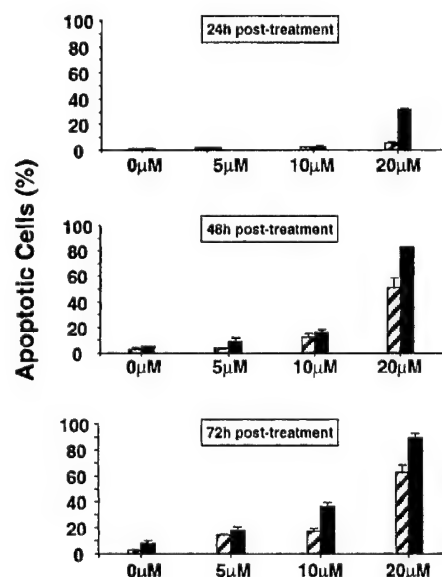


Fig. 7. The sphingosine kinase inhibitor, DMS, induces apoptosis and sensitizes LNCaP cells to γ -irradiation-induced apoptosis. LNCaP cells were treated without or with the indicated concentrations of DMS for 1 h and then either not irradiated (□) or irradiated with 8 Gy (▨). Apoptotic cells were assayed by ISEL at the indicated times. Data are means \pm SD of triplicate determinations from one of three representative experiments.

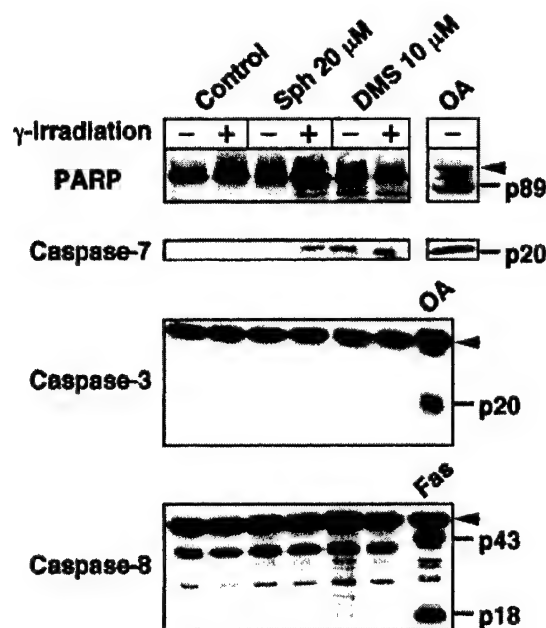


Fig. 8. Cleavage of PARP and caspase-7 in γ -irradiated LNCaP cells treated with sphingosine or DMS. LNCaP cells were treated for 72 h with 20 μ M sphingosine (Sph) or 10 μ M DMS without or with 8 Gy γ -irradiation. Cell lysates were prepared and equal amounts of proteins were immunoblotted with anti-PARP, anti-caspase-7, anti-caspase-3, or anti-caspase-8 antibodies after separation by SDS-PAGE (10% SDS gels for PARP and 15% for the others). Arrowheads, the migration of full-length PARP, caspase-3, and caspase-8. Left, PARP cleavage product (M_r 89,000), the large active subunits of caspase-7 (M_r 20,000), caspase-3 (M_r 20,000), and caspase-8 (M_r 18,000), and the intermediate cleavage fragment of caspase-8 (M_r 43,000). Lysate from LNCaP cells treated with okadaic acid (30 nM) for 48 h served as positive control for cleavage of PARP, caspase-7, and caspase-3. H9 T cells treated with anti-Fas antibody (50 ng/ml) for 24 h were used as a positive control for caspase-8 processing. Similar results were obtained in three independent experiments.

metabolites were less effective in inducing PARP cleavage, even in the presence of radiation. Barely detectable PARP cleavage was seen after cells were exposed to sphingosine alone at 20 μ M, a concentration that induced 30% apoptosis at 72 h (Fig. 6). PARP cleavage activity was increased in cells treated with sphingosine and 8 Gy irradiation after 72 h (Fig. 8), in agreement with the enhanced apoptosis. Interestingly, DMS alone was able to induce PARP cleavage in LNCaP cells without irradiation (Fig. 8), in agreement with its ability to induce apoptosis. Proteolytic processing of procaspases-3 and -7 was examined by Western blotting using antisera specific for caspase-3 and the active p20 caspase-7 subunit, respectively (Fig. 8). In agreement with our previous study (16), the procaspases-3 and -7 were cleaved into their active forms after treatment with okadaic acid, whereas no significant activation of caspase-3 could be detected in extracts from irradiated cells treated with sphingosine or DMS (Fig. 8). However, the activation of caspase-7 in the presence of sphingosine and DMS, especially after irradiation, was detected by the appearance of the M_r 20,000 large subunit (Fig. 8). In contrast, no activation of the initiator caspase-8 could be detected after treatment with sphingosine or DMS, in the absence or presence of irradiation (Fig. 8).

DISCUSSION

Recently, we and others (6, 7, 36) have suggested that the sphingolipid metabolites, ceramide and sphingosine, provide proapoptotic signals, and an additional metabolite, SPP, promotes cell survival and suppresses apoptosis. Dysregulation of this sphingolipid biostat may be important in the acquisition of malignant phenotypes and radio-

resistance in which transformed cells can circumvent existing apoptotic mechanisms that would normally target the destruction of these cells. Thus, resetting this biostat could potentially be used to enhance apoptosis and overcome resistance to radiation or androgen ablation.

Previously, it has been suggested that LNCaP cells are highly resistant to induction of apoptosis by γ -irradiation attributable in part to a defect in ceramide generation (15, 16). Likewise, resistance to apoptosis involves a defect in ceramide generation in the PC3 prostate cancer cell line (37). However, radiation-induced apoptosis is not solely dependent on ceramide signaling, and there are other ceramide-independent pathways leading to apoptosis. Although in LNCaP cells, irradiation did not result in ceramide generation or apoptosis, pretreatment with PMA not only enhanced radiation-induced apoptosis, but also enabled ceramide generation via activation of ceramide synthase (38). In agreement, apoptosis was abrogated by FB1, a competitive inhibitor of ceramide synthase. Most importantly, when transplanted orthotopically into the prostate of nude mice, LNCaP cells produced tumors that showed the same responses to PMA and radiation therapy (38). However, apoptosis induced by treatment with TNF and γ -irradiation was not mediated by stimulation of *de novo* ceramide synthesis. Similarly, apoptosis in LNCaP cells induced by the topoisomerase I inhibitor camptothecin, ceramide generation was also independent of the *de novo* pathway (37).

A further metabolite of ceramide, sphingosine, has also been shown to induce apoptosis of androgen-independent human prostate cancer cells (20). Indeed, we found that ceramide production after TNF- α treatment in irradiated LNCaP cells or after SMase treatment is followed by a surge in sphingosine that precedes caspase activation and the onset of apoptosis. Furthermore, whereas addition of exogenous sphingosine induced modest apoptosis by itself, it significantly sensitized LNCaP cells to γ -irradiation. Irradiation of TSU-Pr1 cells, but not LNCaP cells, also produced a marked decrease in the activity of sphingosine kinase, the enzyme that phosphorylates sphingosine to form SPP, with a corresponding increase in sphingosine levels. In addition, a correlation between cell death and decreased SPP levels was observed in LNCaP cells treated with TNF- α plus γ -irradiation. Interestingly, SPP levels also decreased after treatment with TNF- α alone, which induces only modest elevations of sphingosine and ceramide, and which suggests that the balance between these sphingolipid metabolites may regulate LNCaP cell survival. These results raise the possibility that the individual enzymes in sphingolipid metabolism can be differentially regulated. In agreement, it has recently been shown that sphingosine kinase can be activated independently of sphingomyelinase or ceramidase (39). Furthermore, inhibition of sphingosine kinase by DMS blocked the increase in SPP, induced apoptosis, and sensitized prostate cancer cells to γ -irradiation. Thus, the regulation of the sphingolipid biostat may also have important implications for the treatment of prostate cancer, because many therapeutic approaches have been shown to cause accumulation of ceramide and sphingosine, including chemotherapy and ionizing radiation (6, 7, 36).

Ceramide generation in response to apoptotic stimuli is complex (6, 7). In LNCaP cells, neither SMase nor ceramide synthase are activated after irradiation alone (40). In agreement, we failed to detect changes in ceramide levels in γ -irradiated LNCaP cells (Fig. 2 and Ref. 16). However, TNF- α induced an \sim 2-fold ceramide elevation that was potentiated by irradiation. TNF- α recruitment of the adaptor protein FADD is required for stimulation of acidic SMase (41), which suggests a possible mechanism for ceramide generation in LNCaP cells. Alternatively, ceramide can be generated by the activation of ceramide synthase as has been shown for apoptosis in LNCaP cells mediated by PKC activation induced by the phorbol ester PMA (15). Interestingly, sphingosine, which has been shown to inhibit PKC in

several types of cells (30, 31), triggers apoptosis in LNCaP cells, thus excluding the possibility that sphingosine is acting through PKC inhibition in LNCaP cells. The effects of TNF- α , like those of PMA, are pleiotropic (42). TNF- α has a pro-apoptotic effect in numerous tumor cells or virally infected cells, whereas, in some normal cells, such as in human endothelial cells, TNF- α is not cytotoxic. A recent study demonstrated that in these cells, TNF- α simultaneously and independently regulated sphingomyelinase and sphingosine kinase activity, which leads to the suggestion that the balance of these two antagonistic biochemical signaling pathways could regulate the fate of cells in response to TNF- α stimulation (39).

Protease inhibitor studies indicate that ceramide and sphingosine may act independently to induce cell death, and it is argued that sphingosine induces activation of upstream caspases (19, 35). However, ceramide generated by upstream caspases, has been shown to activate additional downstream caspases necessary for apoptosis (6, 43–47). Moreover, ceramide could also induce cell death by a caspase-independent pathway (48). We found that caspase-7, but not caspase-3, was activated in sphingosine-sensitized γ -irradiation-induced apoptosis of LNCaP cells, in agreement with previous reports suggesting that activation of caspase-7, but not caspase-3, is an important step in the execution of apoptosis in LNCaP cells (49). The fact that LNCaP cell lines stably overexpressing crmA are resistant to sphingolipid induced-apoptosis⁴ may place crmA-inhibitable caspases downstream of sphingolipid metabolites. Interestingly, elevation of ceramide and/or sphingosine in LNCaP cells only had a modest effect on caspase activation (Ref. 16) and Fig. 7), whereas okadaic acid induced robust activation of several caspases while triggering a similar extent of apoptosis in comparison with γ -irradiation combined with TNF- α or with sphingolipid metabolites. This underscores the specificity of the apoptotic response to different stimuli in LNCaP cells and may indicate the participation of other death proteases, such as serine proteases, that cooperate with caspases in the execution of cell death (16, 50). This may be especially important for sensitization of radiation-induced apoptosis by sphingosine and DMS, because they were able to enhance apoptosis with a limited degree of caspase activation.

Different caspases are known to be activated in LNCaP and TSU-Pr1 cells, depending on the apoptotic stimuli. In LNCaP cells, caspases-3, -6, -7, and -8 are activated after okadaic acid treatment. In contrast, caspase-3 is not involved in TNF- α - or γ -radiation-induced death in LNCaP cells, but is markedly activated in TSU-Pr1 cells. This could explain the fact that LNCaP cells are highly resistant to radiation-induced apoptosis compared with TSU-Pr1 cells (16, 51). Recent studies have demonstrated that caspase-7 and -3 are critical mediators of apoptosis in LNCaP cells. Moreover, overexpression of caspase-7 induced apoptosis even in LNCaP cells that overexpressed the oncoprotein bcl-2 (51). However, in addition to the differential activation of unique caspases (16), our recent study suggests the involvement of additional cell-type specific signaling events in prostate cancer cell death, including activation of the JNK/SAPK pathway (27), which is thought to be involved in ceramide (52) and sphingosine-induced apoptosis (53). Interestingly, expression of bcl-2 not only protected prostate carcinoma cells against the induction of apoptosis by exogenous C2-cer but also blocked its ability to activate JNK1, which indicated that bcl-2 functions at the level of JNK1 or upstream of JNK1 in the ceramide/JNK pathway (54).

Collectively, our results suggest that ceramide and sphingosine generation, together with the inhibition of sphingosine kinase, are critical components in radiation-induced apoptosis in human prostate

cancer cells. Preventing ceramide and sphingosine generation and/or stimulation of sphingosine kinase may provide a selective advantage in the development of radioresistance of prostate tumors. Therefore, development of agents that specifically regulate levels of sphingolipid metabolites may provide new tools to use in conjunction with radiation therapy.

ACKNOWLEDGMENTS

We thank Shvetha Murthy for excellent technical assistance and Drs. Markus Peter and Donald Nicholson for providing antibodies.

REFERENCES

- Wheeler, J. A., Zagars, G. K., and Ayala, A. G. Dedifferentiation of locally recurrent prostate cancer after radiation therapy. Evidence for tumor progression. *Cancer (Phila.)*, 71: 3783–3787, 1993.
- Haimovitz-Friedman, A., Kan, C. C., Ehleiter, D., Persaud, R. S., McLoughlin, M., Fuks, Z., and Kolesnick, R. Ionizing radiation acts on cellular membranes to generate ceramide and initiate apoptosis. *J. Exp. Med.*, 180: 525–535, 1994.
- Quintans, J., Kilkus, J., McShan, C. L., Gottschalk, A. R., and Dawson, G. Ceramide mediates the apoptotic response of WEHI 231 cells to anti-immunoglobulin, corticosteroids and irradiation. *Biochem. Biophys. Res. Commun.*, 202: 710–714, 1994.
- Santana, P., Peña, L. A., Haimovitz-Friedman, A., Martin, S., Green, D., McLoughlin, M., Cordon-Cardo, C., Schuchman, E. H., Fuks, Z., and Kolesnick, R. Acid sphingomyelinase-deficient human lymphoblasts and mice are defective in radiation-induced apoptosis. *Cell*, 86: 189–199, 1996.
- Chinura, S. J., Nodzenski, E., Beckett, M. A., Kufe, D. W., Quintans, J., and Weichselbaum, R. R. Loss of ceramide production confers resistance to radiation-induced apoptosis. *Cancer Res.*, 57: 1270–1275, 1997.
- Hannun, Y. Functions of ceramide in coordinating cellular responses to stress. *Science (Washington DC)*, 274: 1855–1859, 1996.
- Kolesnick, R. N., and Kronke, M. Regulation of ceramide production and apoptosis. *Annu. Rev. Physiol.*, 60: 643–665, 1998.
- Kolesnick, R., and Fuks, Z. Ceramide: a signal for apoptosis or mitogenesis? *J. Exp. Med.*, 181: 1949–1952, 1995.
- Levade, T., and Jaffrezou, J. P. Signalling sphingomyelinases: which, where, how and why? *Biochim. Biophys. Acta*, 1438: 1–17, 1999.
- Bruno, A. P., Laurent, G., Averbeck, D., Demur, C., Bonnet, J., Betteieb, A., Levade, T., and Jaffrezou, J. P. Lack of ceramide generation in TF-1 human myeloid leukemic cells resistant to ionizing radiation. *Cell Death Differ.*, 5: 172–182, 1998.
- Liu, B., Andrieu-Abadie, N., Levade, T., Zhang, P., Obeid, L. M., and Hannun, Y. A. Glutathione regulation of neutral sphingomyelinase in tumor necrosis factor- α -induced cell death. *J. Biol. Chem.*, 273: 11313–11320, 1998.
- Bump, E. A., and Brown, J. M. Role of glutathione in the radiation response of mammalian cells *in vitro* and *in vivo*. *Pharmacol. Ther.*, 47: 117–136, 1990.
- Mirkovic, N., Voehringer, D. W., Story, M. D., McConkey, D. J., McDonnell, T. J., and Meyn, R. E. Resistance to radiation-induced apoptosis in Bel-2-expressing cells is reversed by depleting cellular thiols. *Oncogene*, 15: 1461–1470, 1997.
- Bose, R., Verheij, M., Haimovitz-Friedman, A., Scotto, K., Fuks, Z., and Kolesnick, R. Ceramide synthase mediates daunorubicin-induced apoptosis: an alternative mechanism for generating death signals. *Cell*, 82: 405–414, 1995.
- Garzotto, M., White-Jones, M., Jiang, Y., Ehleiter, D., Liao, W. C., Haimovitz-Friedman, A., Fuks, Z., and Kolesnick, R. 12-O-Tetradecanoylphorbol-13-acetate-induced apoptosis in LNCaP cells is mediated through ceramide synthase. *Cancer Res.*, 58: 2260–2264, 1998.
- Kimura, K., Bowen, C., Spiegel, S., and Gelmann, E. P. Tumor necrosis factor- α sensitizes prostate cancer cells to γ -irradiation-induced apoptosis. *Cancer Res.*, 59: 1606–1614, 1999.
- Ohta, H., Yatomi, Y., Sweeney, E. A., Hakomori, S., and Igarashi, Y. A possible role of sphingosine in induction of apoptosis by tumor necrosis factor- α in human neutrophils. *FEBS Lett.*, 355: 267–270, 1994.
- Krown, K. A., Page, M. T., Nguyen, C., Zechner, D., Gutierrez, V., Comstock, K. L., Glembofski, C. C., Quintana, P. J., and Sabbadini, R. A. Tumor necrosis factor α -induced apoptosis in cardiac myocytes. Involvement of the sphingolipid signaling cascade in cardiac cell death. *J. Clin. Invest.*, 98: 2854–2865, 1996.
- Hung, W. C., Chang, H. C., and Chuang, L. Y. Activation of caspase-3-like proteases in apoptosis induced by sphingosine and other long-chain bases in Hep3B hepatoma cells. *Biochem. J.*, 338: 161–166, 1999.
- Shirahama, T., Sakakura, C., Sweeney, E. A., Ozawa, M., Takemoto, M., Nishiyama, K., Ohi, Y., and Igarashi, Y. Sphingosine induces apoptosis in androgen-independent human prostatic carcinoma DU-145 cells by suppression of *bcl-X_L* gene expression. *FEBS Lett.*, 407: 97–100, 1997.
- Kohama, T., Olivera, A., Edsall, L., Nagice, M. M., Dickson, R., and Spiegel, S. Molecular cloning and functional characterization of murine sphingosine kinase. *J. Biol. Chem.*, 273: 23722–23728, 1998.
- Cuvillier, O., Pirianov, G., Kleuser, B., Vanek, P. G., Coso, O. A., Gutkind, S., and Spiegel, S. Suppression of ceramide-mediated programmed cell death by sphingosine-1-phosphate. *Nature (Lond.)*, 381: 800–803, 1996.
- Edsall, L. C., Pirianov, G. G., and Spiegel, S. Involvement of sphingosine 1-phosphate in nerve growth factor-mediated neuronal survival and differentiation. *J. Neurosci.*, 17: 6952–6960, 1997.

⁴ K. Kimura, unpublished data.

24. Cuvillier, O., Rosenthal, D. S., Smulson, M. E., and Spiegel, S. Sphingosine 1-phosphate inhibits activation of caspases that cleave poly(ADP-ribose) polymerase and lamins during Fas- and ceramide-mediated apoptosis in Jurkat T lymphocytes. *J. Biol. Chem.*, 273: 2910-2916, 1998.
25. Kleuser, B., Cuvillier, O., and Spiegel, S. 1 α ,25-dihydroxyvitamin D₃ inhibits programmed cell death in HL-60 cells by activation of sphingosine kinase. *Cancer Res.*, 58: 1817-1824, 1998.
26. Perez, G. I., Knudson, C. M., Leykin, L., Korsmeyer, S. J., and Tilly, J. L. Apoptosis-associated signaling pathways are required for chemotherapy-mediated female germ cell destruction. *Nat. Med.*, 3: 1228-1232, 1997.
27. Bowen, C., Spiegel, S., and Gelmann, E. P. Radiation-induced apoptosis mediated by retinoblastoma protein. *Cancer Res.*, 58: 3275-3281, 1998.
28. Van Veldhoven, P. P., and Mannaerts, G. P. Inorganic and organic phosphate measurements in the nanomolar range. *Anal. Biochem.*, 161: 45-48, 1987.
29. Edsall, L. C., and Spiegel, S. Enzymatic measurement of sphingosine 1-phosphate. *Anal. Biochem.*, 272: 80-86, 1999.
30. Hannun, Y. A., and Bell, R. M. Lysosphingolipids inhibit protein kinase C: implications for the sphingolipidoses. *Science (Washington DC)*, 235: 670-674, 1987.
31. Spiegel, S., and Merrill, A. H., Jr. Sphingolipid metabolism and cell growth regulation. *FASEB J.*, 10: 1388-1397, 1996.
32. Kim, C. N., Wang, X., Huang, Y., Ibrado, A. M., Liu, L., Fang, G., and Bhalla, K. Overexpression of Bel-x₁ inhibits Ara-C-induced mitochondrial loss of cytochrome c and other perturbations that activate the molecular cascade of apoptosis. *Cancer Res.*, 57: 3115-3120, 1997.
33. Edsall, L. C., Van Brocklyn, J. R., Cuvillier, O., Kleuser, B., and Spiegel, S. N,N-Dimethylsphingosine is a potent competitive inhibitor of sphingosine kinase but not of protein kinase C: modulation of cellular levels of sphingosine 1-phosphate and ceramide. *Biochemistry*, 37: 12892-12898, 1998.
34. Yang, L., Yatomi, Y., Satoh, K., Igarashi, Y., and Ozaki, Y. Sphingosine 1-phosphate formation and intracellular Ca²⁺ mobilization in human platelets: evaluation with sphingosine kinase inhibitors. *J. Biochem. (Tokyo)*, 126: 84-89, 1999.
35. Sweeney, E. A., Inokuchi, J., and Igarashi, Y. Inhibition of sphingolipid induced apoptosis by caspase inhibitors indicates that sphingosine acts in an earlier part of the apoptotic pathway than ceramide. *FEBS Lett.*, 425: 61-65, 1998.
36. Spiegel, S., Foster, D., and Kolesnick, R. N. Signal transduction through lipid second messengers. *Curr. Opin. Cell Biol.*, 8: 159-167, 1996.
37. Wang, X.-Z., Beebe, J. R., Pwiti, L., Bielawska, A., and Smyth, M. J. Aberrant sphingolipid signaling is involved in the resistance of prostate cancer cell lines to chemotherapy. *Cancer Res.*, 59: 5842-5848, 1999.
38. Garzotto, M., Haimovitz-Friedman, A., Liao, W.-C., White-Jones, M., Huryk, R., Heston, W. D. W., Cardon-Cardo, C., Kolesnick, R., and Fuks, Z. Reversal of radiation resistance in LNCaP cells by targeting apoptosis through ceramide synthase. *Cancer Res.*, 59: 5194-5201, 1999.
39. Xia, P., Wang, L., Gamble, J. R., and Vadas, M. A. Activation of sphingosine kinase by tumor necrosis factor- α inhibits apoptosis in human endothelial cells. *J. Biol. Chem.*, 274: 34499-34505, 1999.
40. Liao, W. C., Haimovitz-Friedman, A., Persaud, R. S., McLoughlin, M., Ehleiter, D., Zhang, N., Giatci, M., Lavin, M., Kolesnick, R., and Fuks, Z. Ataxia telangiectasia-mutated gene product inhibits DNA damage-induced apoptosis via ceramide synthase. *J. Biol. Chem.*, 274: 17908-17917, 1999.
41. Wiegmann, K., Schwandner, R., Krut, O., Yeh, W. C., Mak, T. W., and Kronke, M. Requirement of FADD for tumor necrosis factor-induced activation of acid sphingomyelinase. *J. Biol. Chem.*, 274: 5267-5270, 1999.
42. Beg, A. A., and Baltimore, D. An essential role for NF- κ B in preventing TNF- α -induced cell death. *Science (Washington DC)*, 274: 782-784, 1996.
43. Dbaibo, G. S., Perry, D. K., Gamard, C. J., Platt, R., Poirier, G. G., Obeid, L. M., and Hannun, Y. A. Cytokine response modifier A (CrmA) inhibits ceramide formation in response to tumor necrosis factor (TNF)- α : CrmA and Bel-2 target distinct components in the apoptotic pathway. *J. Exp. Med.*, 185: 481-490, 1997.
44. Bose, R., Chen, P., Locanti, A., Grölich, C., Abrams, J. M., and Kolesnick, R. N. Ceramide generation by the reaper protein is not blocked by the caspase inhibitor. *p35. J. Biol. Chem.*, 273: 28852-28859, 1998.
45. Chen, L., Kim, T. J., and Pillai, S. Inhibition of caspase activity prevents anti-IgM induced apoptosis but not ceramide generation in WEHI 231 B cells. *Mol. Immunol.*, 35: 195-205, 1998.
46. Tepper, A. D., Cock, J. G., de Vries, E., Borst, J., and van Blitterswijk, W. J. CD95/Fas-induced ceramide formation proceeds with slow kinetics and is not blocked by caspase-3/CPP32 inhibition. *J. Biol. Chem.*, 272: 24308-24312, 1997.
47. Smyth, M. J., Perry, D. K., Zhang, J., Poirier, G. G., Hannun, Y. A., and Obeid, L. M. pRICE: a downstream target for ceramide-induced apoptosis and for the inhibitory action of Bel-2. *Biochem. J.*, 316: 25-28, 1996.
48. Jones, B. E., Lo, C. R., Srinivasan, A., Valentino, K. L., and Czaja, M. J. Ceramide induces caspase-independent apoptosis in rat hepatocytes sensitized by inhibition of RNA synthesis. *Hepatology*, 30: 215-222, 1999.
49. Marcelli, M., Cunningham, G. R., Haidacher, S. J., Padayatty, S. J., Sturgis, L., Kagan, C., and Denner, L. Caspase-7 is activated during lovastatin-induced apoptosis of the prostate cancer cell line LNCaP. *Cancer Res.*, 58: 76-83, 1998.
50. Schmitt, E., Sane, A. T., Steyaert, A., Cimoli, G., and Bertrand, R. The Bcl-x₁ and Bax- α control points: modulation of apoptosis induced by cancer chemotherapy and relation to TPCK-sensitive protease and caspase activation. *Biochem. Cell Biol.*, 75: 301-314, 1997.
51. Marcelli, M., Cunningham, G. R., Walkup, M., He, Z., Sturgis, L., Kagan, C., Mannucci, R., Nicoletti, I., Teng, B., and Denner, L. Signaling pathway activated during apoptosis of the prostate cancer cell line LNCaP: overexpression of caspase-7 as a new gene therapy strategy for prostate cancer. *Cancer Res.*, 59: 382-390, 1999.
52. Verheij, M., Bose, R., Lin, X. H., Yao, B., Jarvis, W. D., Grant, S., Birrer, M. J., Szabo, E., Zon, L. I., Kyriakis, J. M., Haimovitz-Friedman, A., Fuks, Z., and Kolesnick, R. N. Requirement for ceramide-initiated SAPK/JNK signalling in stress-induced apoptosis. *Nature (Lond.)*, 380: 75-79, 1996.
53. Jarvis, W. D., Fornari, F. A., Jr., Auer, K. L., Freemanman, A. J., Szabo, E., Birrer, M. J., Johnson, C. R., Barbour, S. E., Dent, P., and Grant, S. Coordinate regulation of stress- and mitogen-activated protein kinases in the apoptotic actions of ceramide and sphingosine. *Mol. Pharmacol.*, 52: 935-947, 1997.
54. Herrmann, J. L., Menter, D. G., Beham, A., von Eschenbach, A., and McDonnell, T. J. Regulation of lipid signaling pathways for cell survival and apoptosis by bel-2 in prostate carcinoma cells. *Exp. Cell Res.*, 234: 442-451, 1997.

Functional characterization of human sphingosine kinase-1

Victor E. Nava^{a,1}, Emanuela Lacana^{a,1}, Samantha Poulton^a, Hong Liu^a, Masako Sugiura^b, Keita Kono^b, Sheldon Milstien^c, Takafumi Kohama^{b,1}, Sarah Spiegel^{a,1,*}

^aDepartment of Biochemistry and Molecular Biology, Georgetown University Medical Center, 353 Basic Science Building, 3900 Reservoir Road NW, Washington, DC 20007, USA

^bPharmacology and Molecular Biology Research Laboratories, Sankyo Co., Ltd., Tokyo 140-8710, Japan

^cLCMR, NIMH, Bethesda, MD 20892, USA

Received 9 March 2000; received in revised form 10 April 2000

Edited by Guido Tettamanti

Abstract Sphingosine kinase catalyzes the phosphorylation of sphingosine to form sphingosine 1-phosphate (SPP), a novel lipid mediator with both intra- and extracellular functions. Based on sequence identity to murine sphingosine kinase (mSPHK1a), we cloned and characterized the first human sphingosine kinase (hSPHK1). The open reading frame of hSPHK1 encodes a 384 amino acid protein with 85% identity and 92% similarity to mSPHK1a at the amino acid level. Similar to mSPHK1a, when HEK293 cells were transfected with hSPHK1, there were marked increases in sphingosine kinase activity resulting in elevated SPP levels. hSPHK1 also specifically phosphorylated *D-erythro*-sphingosine and to a lesser extent sphinganine, but not other lipids, such as *D,L-threo*-dihydrosphingosine, *N,N*-dimethylsphingosine, diacylglycerol, ceramide, or phosphatidylinositol. Northern analysis revealed that hSPHK1 was widely expressed with highest levels in adult liver, kidney, heart and skeletal muscle. Thus, hSPHK1 belongs to a highly conserved unique lipid kinase family that regulates diverse biological functions.

© 2000 Federation of European Biochemical Societies.

Key words: Human sphingosine kinase; Sphingosine 1-phosphate

1. Introduction

The metabolic product of sphingosine kinase (SPHK), sphingosine 1-phosphate (SPP), is a lipid signaling molecule that acts both intra- and extracellularly to affect many biological processes. These include mitogenesis [1,2], apoptosis [3], atherosclerosis [4] and inflammatory responses [5,6]. Specific members of the EDG-1 family of G protein-coupled receptors bind SPP (reviewed in [7,8]) and modulate chemotaxis [9,10], angiogenesis [10–12], neurite retraction and cell rounding [13]. Because SPP levels are mainly regulated by the activity of SPHK, cloning and characterization of this enzyme are important for understanding its role in normal and patho-

logical processes. Previously, we purified SPHK to homogeneity from rat kidneys [14] and subsequently identified mouse cDNAs encoding two forms of SPHK, designated mSPHK1a and mSPHK1b, whose predicted proteins differ by only 10 amino acids at their N-terminus [15]. The corresponding mRNAs may arise by alternative splicing. In this study, sequence homologies to the mSPHK1a cDNAs were used to identify and clone the first human homologue, hSPHK1. hSPHK1 is ubiquitously expressed in adult tissues with highest levels in liver, kidney, lung and skeletal muscle. Our results suggest that hSPHK1 belongs to a family of highly conserved enzymes which differ from other known lipid kinases.

2. Materials and methods

2.1. Materials

SPP, sphingosine, and *N,N*-dimethylsphingosine (DMS) were from Biomol Research Laboratory Inc. (Plymouth Meeting, PA). All other lipids were purchased from Avanti Polar Lipids (Birmingham, AL). [γ -³²P]ATP (3000 Ci/mmol) was purchased from Amersham (Arlington Heights, IL). Poly-L-lysine was from Boehringer Mannheim (Indianapolis, IN). Alkaline phosphatase from bovine intestinal mucosa, type VII-NT, was from Sigma (St. Louis, MO). Restriction enzymes were from New England Biolabs (Beverly, MA). Lipofectamine Plus was from Life Technologies (Gaithersburg, MD).

2.2. Human sphingosine kinase cDNA cloning

BLAST searches using mSPHK1a sequences identified an EST clone (AA026479) which contained sequences homologous to several conserved domains of mSPHK [15]. To obtain a full-length cDNA, the 5'-end of hSPHK1 was extended by rapid amplification of cDNA ends/polymerase chain reaction (RACE-PCR; Life Technologies). First, cDNA was synthesized from HEK293 poly(A)⁺ RNA with a gene-specific antisense primer hspk1-GSP1 (5'-ACCATGTGCCAGT-GAG). Then two consecutive PCR reactions using LA Taq (TaKaRa) were performed. First PCR: 5'RACE Abridged Anchor Primer and the antisense primer hspk1-GSP2 (5'-TTCCTACAGGGAGG-TAGGCC) at 94°C for 2 min followed by 30 cycles of amplification (94°C for 1 min, 55°C for 1 min, 72°C for 2 min) and primer extension at 72°C for 5 min. Second PCR: Abridged Universal Amplification Primer and the antisense primer hspk1-GSP3 (5'-GGCTGCCA-GACGCAGGAAGG) using a program similar to the first PCR but with annealing at 65°C. The PCR products were cloned into pCR 2.1 (TA Cloning, Invitrogen) and sequences confirmed by automated sequencing. To make expression constructs, a primer set was designed as follows: sense primer containing a Kozak sequence and ATG start codon, sphk1-GSP4 (5'-GCCACCATGGATCCAGCGGGCGGCC-CC); antisense primer, sphk1-GSP5 (5'-TCATAAGGGCTCTTCTG-GCGGTGGCATCTG). The PCR reaction was performed using human fetus Marathon-Ready cDNA (Clontech) as template with the above primers, and the amplification product was subcloned into pCR3.1 (Eukaryotic TA Cloning, Invitrogen). In addition, hSPHK1 was tagged at the N-terminus by subcloning into a pcDNA-c-myc vector [2] using high fidelity taq polymerase (Pfu, Stratagene). hSPHK1 accession number is AF238083.

*Corresponding author. Fax: (1)-202-687 0260.
E-mail: spiegel@bc.georgetown.edu

¹ These authors contributed equally to this report.

Abbreviations: BSA, bovine serum albumin; DMS, *N,N*-dimethylsphingosine; DHS, *D,L-threo*-dihydrosphingosine; SPHK, sphingosine kinase; SPP, sphingosine 1-phosphate; PCR, polymerase chain reaction; RACE, rapid amplification of cDNA ends

2.3. Cell culture and expression of sphingosine kinase

Human embryonic kidney cells (HEK293, ATCC CRL-1573) were grown in high glucose Dulbecco's modified Eagle's medium (DMEM) containing 100 U/ml penicillin, 100 µg/ml streptomycin and 2 mM L-glutamine supplemented with 10% fetal bovine serum [15]. Cells were transfected with either pcDNA3.1 or pCR3.1 containing hSPHK1 using Lipofectamine Plus according to the manufacturer's protocol. Transfection efficiencies were typically about 40%.

2.4. Measurement of sphingosine kinase activity

Cytosolic sphingosine kinase activity was determined with 50 µM sphingosine, dissolved in 5% Triton X-100 (final concentration 0.25%), and [γ - 32 P]ATP (10 µCi, 1 mM) containing MgCl₂ (10 mM) as previously described [15]. In some experiments, sphingosine was added as a complex with bovine serum albumin (BSA) as previously described [15]. Specific activity is expressed as pmol SPP formed per min per mg protein.

2.5. Lipid extraction and measurement of SPP, sphingosine, and ceramide

Cells were washed with phosphate buffered saline and scraped in 1 ml of methanol containing 2.5 µl concentrated HCl. Lipids were extracted by adding 2 ml chloroform/1 M NaCl (1:1, v/v) and 100 µl 3 N NaOH and phases were separated. The basic aqueous phase containing SPP, and devoid of sphingosine, ceramide, and the majority of phospholipids, was transferred to a siliconized glass tube. The organic phases were re-extracted with 1 ml methanol/1 M NaCl (1:1, v/v) plus 50 µl 3 N NaOH, and the aqueous fractions combined. Mass measurements of SPP in the aqueous phase were carried out as previously described [16]. Sphingosine and ceramide in the organic phase were determined by enzymatic methods using sphingosine kinase and diacylglycerol kinase, respectively [17]. Total phospholipids present in lipid extracts were also quantified [17].

2.6. Northern blotting analysis

Poly(A)⁺ RNA blots containing 2 µg of poly(A)⁺ RNA per lane from multiple adult human tissues (Clontech) were hybridized with the 0.6 kb *EcoRV/SphI* fragment of pCR3.1-hSPHK1, which was gel-purified and labeled with [32 P]dCTP by random priming. Hybridization in ExpressHyb buffer (Clontech) was carried out at 65°C overnight according to the manufacturer's protocol. Blots were reprobated with a human β -actin control probe (Clontech). Bands were quantified using a Molecular Dynamics Phosphorimager.

3. Results and discussion

3.1. Cloning of hSPHK1

BLAST searches of the EST database identified a human homologue of murine SPHK, EST AA026479, with similarity to the 3' end of mSPHK1a. This sequence was used to design specific primers and 5' RACE was performed on mRNA extracted from HEK293 cells to obtain the full-length cDNA of hSPHK1. The open reading frame encodes a protein with 384 amino acids, and 85% identity and 92% similarity to mSPHK1a at the amino acid level (Fig. 1). We previously found by sequence alignment that SPHKs from mouse, yeast and *Caenorhabditis elegans* share several conserved blocks of amino acids [15]. Similarly, hSPHK1 contains these conserved regions (C1–C5, Fig. 1), including the invariant positively charged motif, GGKGGK, in the C1 domain, which may be part of the ATP binding site of this novel class of lipid kinases.

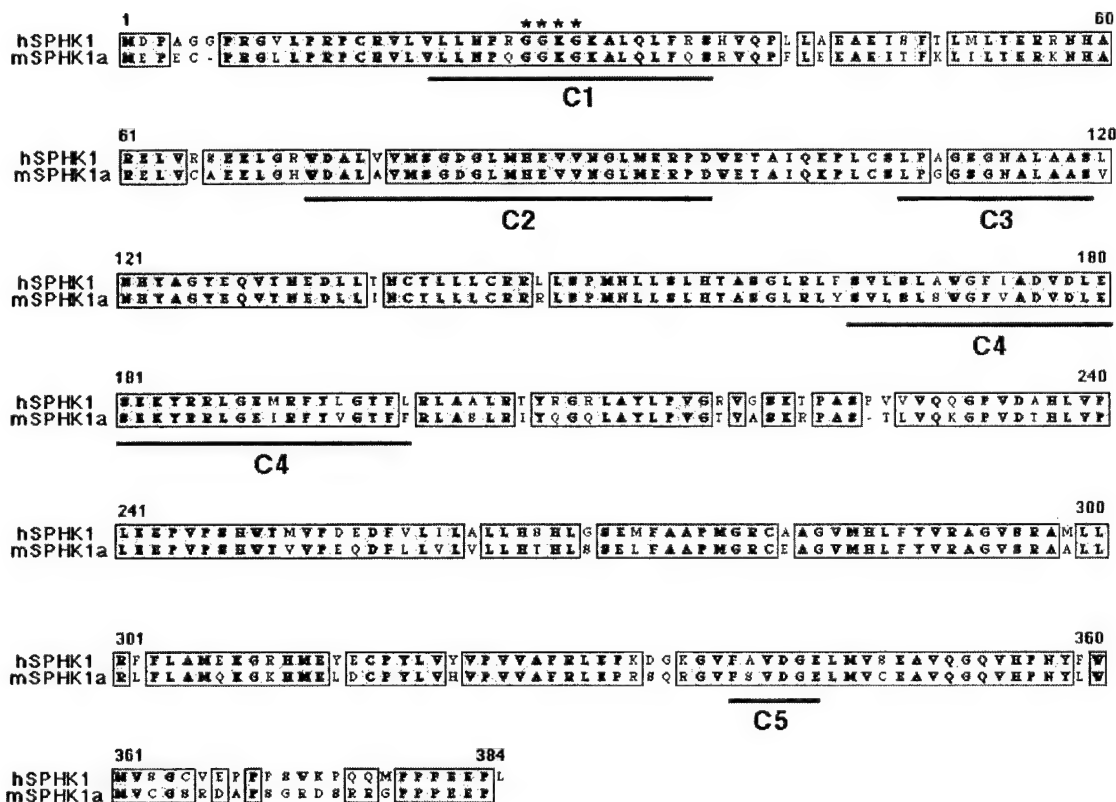


Fig. 1. Predicted amino acid sequence of hSPHK1 and alignment of the conserved domains. ClustalW alignment of SPHKs from mouse and human. Identical and conserved amino acid substitutions are shaded dark and light gray, respectively. The conserved domains (C1–C5) are indicated by lines and the invariant positively charged motif GGKGGK by asterisks.

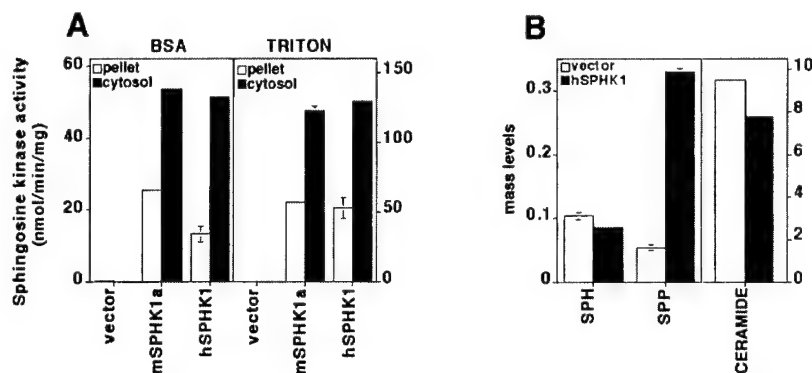


Fig. 2. Activity of hSPHK1 expressed in HEK293 cells. A: HEK293 cells were transiently transfected with empty vector or vector containing either mSPHK1a or hSPHK1. SPHK activity was measured in cytosol (filled bars) and particulate pellet (open bars) 24 h after transfection using sphingosine-BSA complexes or sphingosine-Triton X-100 micelles as substrate as indicated. SPHK activity in vector transfected cells was 84 ± 2 and 134 ± 27 pmol/min/mg using sphingosine-BSA complexes or sphingosine-Triton X-100 micelles as substrate, respectively. Data are means \pm S.D. and are representative of two independent experiments performed in triplicate. B: Changes in mass levels of SPP, sphingosine, and ceramide. Mass levels of SPP, sphingosine and ceramide in cells transfected with empty vector (open bars) or vector containing hSPHK1 (filled bars) were measured after 24 h. Data are expressed as pmol/nmol phospholipid and are means \pm S.D. of triplicate determinations.

3.2. hSPHK1 encodes a functional sphingosine kinase

HEK293 cells were transfected with expression vectors containing hSPHK1 to determine whether it encodes a bona fide SPHK. Modest levels of endogenous SPHK activity were detected in cells transfected with an empty vector (Fig. 2A). Twenty-four hours after transfection with pcDNA3.1-hSPHK1, the SPHK activity increased approximately 600-fold and remained at this level for at least 2 days. For comparison, a similar increase in activity was observed after transfection with mSPHK1a (Fig. 2A). Similar results were obtained when cells were transfected with hSPHK1 in pCR3.1. In agreement with previous results with mSPHK1a [15], hSPHK1 was stimulated by Triton X-100. Both membrane-associated and cytosolic SPHK activity have been described in

mammalian tissues and cell lines [1,18–21]. In cells transfected with hSPHK1, approximately 70% of the SPHK activity was found in the cytosol and only about 30% was membrane-associated (Fig. 2A). Similarly, we previously found that the majority of mSPHK1a activity was also expressed in the cytosol [2,15]. Kyte-Doolittle hydropathy plots did not suggest the presence of any potential hydrophobic membrane spanning domains in the primary structure of hSPHK1.

Transfection of HEK293 cells with hSPHK1 also resulted in changes in levels of sphingolipid metabolites (Fig. 2B). Mass levels of SPP increased 5.7-fold compared to cells transfected with vector alone, with a 18% decrease in levels of both sphingosine and ceramide. However, because intracellular ceramide pools are much larger than sphingosine pools, the absolute decrease of ceramide was greater than the decrease in sphingosine mass. These results suggest that transfected hSPHK1 is active in intact cells, and that kinase overexpression can alter the intracellular balance of sphingolipid metabolites.

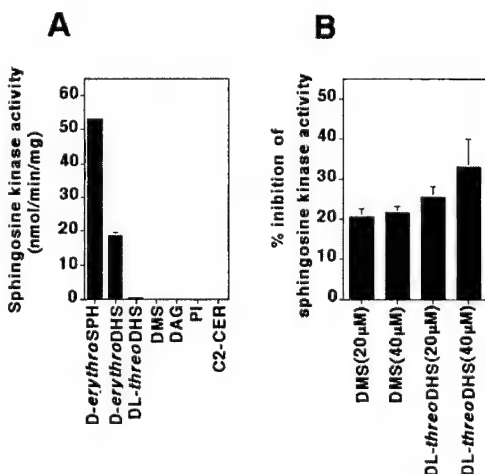


Fig. 3. A: Substrate specificity of hSPHK1. HEK293 cells were transfected with hSPHK1 and SPHK-dependent phosphorylation of various sphingosine analogs or other lipids (50 μ M) was measured using cell lysates as enzyme source. DAG, diacylglycerol; PI, phosphatidylinositol; C2-CER, N-acetyl-sphingosine. B: DMS and DHS are inhibitors of hSPHK1. SPHK activity in HEK293 cell lysates 24 h after transfection with hSPHK1 was measured with 10 μ M SPP in the absence or presence of 20 μ M and 40 μ M DMS or DHS. Data are means \pm S.D. of triplicate determinations and are expressed as percent inhibition.

3.3. Substrate specificity of hSPHK1

The naturally occurring D-(+)-erythro-trans-isomer of sphingosine and erythro-dihydrosphingosine (sphinganine) were the best substrates for hSPHK1 (Fig. 3A). However, similar to the specificity of mSPHK1a [15], sphingosine was more efficiently phosphorylated than sphinganine. Moreover, other sphingo-

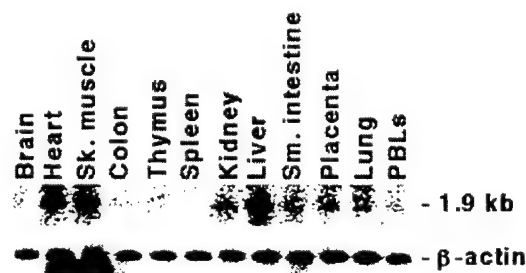


Fig. 4. Tissue-specific expression of hSPHK1 by Northern blot analysis. Top panel: A hSPHK1 probe was hybridized to a poly(A)⁺ RNA blot with the human tissues indicated at the top of each lane as described in Section 2. Bottom panel: A β -actin probe was used to reprobe the blot.

lipids, including D,L-*threo*-dihydrosphingosine (DHS) and C2-ceramide, as well as diacylglycerol and phosphatidylinositol were not substrates (Fig. 3A). With D-*erythro*-sphingosine as substrate, half-maximal velocity was found at 5 μ M, in excellent agreement with K_m values previously determined with rat kidney SPHK [14] and recombinant mSPHK1a [15]. DMS and DHS have previously been used to inhibit SPHK and block increases in SPP induced by various physiological stimuli [1,3,22]. Both of these sphingolipids also inhibited hSPHK1 and similar to their inhibitory effects on mSPHK1a [15], DHS was slightly more potent than DMS (Fig. 3B).

3.4. Tissue distribution of hSPHK1 expression

The tissue distribution of SPHK1 mRNA expression in adult human tissues was analyzed by Northern blotting (Fig. 4). In most tissues, including adult brain, heart, spleen, lung, kidney, and testis, a predominant 1.9 kb mRNA species was detected. Expression was highest in adult liver, heart and skeletal muscle. In comparison, we previously showed that mSPHK1a expression is greatest in mouse spleen, lung, kidney, testis and heart, with much lower expression in skeletal muscle [15].

In summary, hSPHK1 is the human homolog of mSPHK1. Based on EST sequences, hSPHK1 has been localized on chromosome 17q25.2 at the marker stSG28540 (D17S785-D17S836 Reference Interval, UniGene cluster Hs. 68061, URL: <http://www.ncbi.nlm.nih.gov/unigene/clust.cgi?org=hs> and cid=68061). hSPHK1 belongs to a conserved family of genes that is distinct from other known lipid kinases. Molecular cloning and characterization of members of the SPHK family should help to clarify their potential roles in various human diseases as their product, SPP, has been implicated as an important regulatory component of biological processes including growth, survival, allergy, chemotaxis, and angiogenesis.

Acknowledgements: This work was supported by a grant from the National Institutes of Health GM43880 (to S.S.) and a Postdoctoral Fellowship BC961968 from the United States Army Medical Research and Materiel Command, Prostate Cancer Research Program (V.E.N.).

We thank Ayako Yamamoto for excellent technical assistance and Dr. Lisa C. Edsall for measurements of ceramide.

References

- [1] Olivera, A. and Spiegel, S. (1993) *Nature* 365, 557–560.
- [2] Olivera, A., Kohama, T., Edsall, L.C., Nava, V., Cuvillier, O., Poulton, S. and Spiegel, S. (1999) *J. Cell Biol.* 147, 545–558.
- [3] Cuvillier, O., Pirianov, G., Kleuser, B., Vanek, P.G., Coso, O.A., Gutkind, S. and Spiegel, S. (1996) *Nature* 381, 800–803.
- [4] Xia, P., Vadas, M.A., Rye, K.A., Barter, P.J. and Gamble, J.R. (1999) *J. Biol. Chem.* 274, 33143–33147.
- [5] Xia, P., Wang, L., Gamble, J.R. and Vadas, M.A. (1999) *J. Biol. Chem.* 274, 34499–34505.
- [6] Prieschl, E.E., Csonga, R., Novotny, V., Kikuchi, G.E. and Baumrucker, T. (1999) *J. Exp. Med.* 190, 1–8.
- [7] Spiegel, S. (1999) *J. Leukocyte Biol.* 65, 341–344.
- [8] Goetzl, E.J. and An, S. (1998) *FASEB J.* 12, 1589–1598.
- [9] Sadahira, Y., Ruan, F., Hakomori, S. and Igarashi, Y. (1992) *Proc. Natl. Acad. Sci. USA* 89, 9686–9690.
- [10] Wang, F., Van Brocklyn, J.R., Edsall, L., Nava, V.E. and Spiegel, S. (1999) *Cancer Res.* 59, 6185–6191.
- [11] Lee, O.H., Kim, Y.M., Lee, Y.M., Moon, E.J., Lee, D.J., Kim, J.H., Kim, K.W. and Kwon, Y.G. (1999) *Biochem. Biophys. Res. Commun.* 264, 743–750.
- [12] Lee, M.J., Lee, M.J., Thangada, S., Claffey, K.P., Ancellin, N., Liu, C.H., Kluk, M., Volpi, M., Sha'afi, R.I. and Hla, T. (1999) *Cell* 99, 301–312.
- [13] Van Brocklyn, J.R., Tu, Z., Edsall, L.C., Schmidt, R.R. and Spiegel, S. (1999) *J. Biol. Chem.* 274, 4626–4632.
- [14] Olivera, A., Kohama, T., Tu, Z., Milstien, S. and Spiegel, S. (1998) *J. Biol. Chem.* 273, 12576–12583.
- [15] Kohama, T., Olivera, A., Edsall, L., Nagiec, M.M., Dickson, R. and Spiegel, S. (1998) *J. Biol. Chem.* 273, 23722–23728.
- [16] Edsall, L.C. and Spiegel, S. (1999) *Anal. Biochem.* 272, 80–86.
- [17] Edsall, L.C., Pirianov, G.G. and Spiegel, S. (1997) *J. Neurosci.* 17, 6952–6960.
- [18] Stoffel, W., Heimann, G. and Hellenbroich, B. (1973) *Hoppe-Seyler's Z. Physiol. Chem.* 354, 562–566.
- [19] Buehrer, B.M. and Bell, R.M. (1992) *J. Biol. Chem.* 267, 3154–3159.
- [20] Olivera, A., Rosenthal, J. and Spiegel, S. (1994) *Anal. Biochem.* 223, 306–312.
- [21] Ghosh, T.K., Bian, J. and Gill, D.L. (1994) *J. Biol. Chem.* 269, 22628–22635.
- [22] Choi, O.H., Kim, J.-H. and Kinet, J.-P. (1996) *Nature* 380, 634–636.

Molecular Cloning and Functional Characterization of a Novel Mammalian Sphingosine Kinase Type 2 Isoform*

Received for publication, March 31, 2000
Published, JBC Papers in Press, April 5, 2000, DOI 10.1074/jbc.M002759200

Hong Liu[‡]§, Masako Sugiura[¶], Victor E. Nava[‡], Lisa C. Edsall^{||}, Keita Kono[¶], Samantha Poulton[‡], Sheldon Milstien^{||}, Takafumi Kohama[¶], and Sarah Spiegel[‡]§§**

From the [‡]Department of Biochemistry and Molecular Biology, Georgetown University Medical Center, Washington, D. C. 20007, [¶]Pharmacology and Molecular Biology Research Laboratories, Sankyo Co., Ltd., Tokyo 140-8710, Japan, and ^{||}Laboratory of Cellular and Molecular Regulation, National Institute of Mental Health, Bethesda, Maryland 20892

Sphingosine-1-phosphate (SPP) has diverse biological functions acting inside cells as a second messenger to regulate proliferation and survival, and extracellularly, as a ligand for G protein-coupled receptors of the endothelial differentiation gene-1 subfamily. Based on sequence homology to murine and human sphingosine kinase-1 (SPHK1), which we recently cloned (Kohama, T., Oliver, A., Edsall, L., Nagiec, M. M., Dickson, R., and Spiegel, S. (1998) *J. Biol. Chem.* 273, 23722–23728), we have now cloned a second type of mouse and human sphingosine kinase (mSPHK2 and hSPHK2). mSPHK2 and hSPHK2 encode proteins of 617 and 618 amino acids, respectively, both much larger than SPHK1, and though diverging considerably, both contain the conserved domains found in all SPHK1s. Northern blot analysis revealed that SPHK2 mRNA expression had a strikingly different tissue distribution from that of SPHK1 and appeared later in embryonic development. Expression of SPHK2 in HEK 293 cells resulted in elevated SPP levels. *D-erythro*-dihydrosphingosine was a better substrate than *D-erythro*-sphingosine for SPHK2. Surprisingly, *D, L-threo*-dihydrosphingosine was also phosphorylated by SPHK2. In contrast to the inhibitory effects on SPHK1, high salt concentrations markedly stimulated SPHK2. Triton X-100 inhibited SPHK2 and stimulated SPHK1, whereas phosphatidylserine stimulated both type 1 and type 2 SPHK. Thus, SPHK2 is another member of a growing class of sphingolipid kinases that may have novel functions.

Sphingosine-1-phosphate (SPP)¹ is a bioactive sphingolipid

* This work was supported by Grant GM43880 from the National Institutes of Health (to S. S.) and Postdoctoral Fellowship BC961968 from the United States Army Medical Research and Material Command, Prostate Cancer Research Program (to V. E. N.). The costs of publication of this article were defrayed in part by the payment of page charges. This article must therefore be hereby marked "advertisement" in accordance with 18 U.S.C. Section 1734 solely to indicate this fact.

The nucleotide sequence(s) reported in this paper has been submitted to the GenBank[™]/EBI Data Bank with accession number(s) AF245447 and AF245448.

§ Contributed equally to this work.

** To whom correspondence should be addressed: Dept. of Biochemistry and Molecular Biology, Georgetown University Medical Cntr., 353 Basic Science Bldg., 3900 Reservoir Rd. NW, Washington, D. C. 20007. Tel.: 202-687-1432; Fax: 202-687-0260; E-mail: spiegel@bc.georgetown.edu.

¹ The abbreviations used are: SPP, sphingosine-1-phosphate; SPHK, sphingosine kinase; EDG, endothelial differentiation gene; mSPHK, mouse SPHK; EST, expressed sequence tag; PCR, polymerase chain reaction; RACE, rapid amplification of cDNA ends; hSPHK, human SPHK; BSA, bovine serum albumin; kb, kilobase; DMS, *N,N*-dimethyl-

metabolite that regulates diverse biological processes, acting both inside and outside cells (reviewed in Refs. 1 and 2). SPP plays important roles as a second messenger to regulate cell growth and survival (3, 4). Many external stimuli, particularly growth and survival factors, activate sphingosine kinase (SPHK), the enzyme that forms SPP from sphingosine. This rapidly growing list includes platelet-derived growth factor (3, 5–7), nerve growth factor (8, 9), vitamin D3 (10), muscarinic acetylcholine agonists (11), tumor necrosis factor- α (12), and cross-linking of the immunoglobulin receptors Fc ϵ R1 (13) and Fc γ R1 (14). Intracellular SPP, in turn, mobilizes calcium from internal stores independently of inositol triphosphate (11, 15), as well as eliciting diverse signaling pathways leading to proliferation (16, 17) and suppression of apoptosis (4, 8, 17–19). Moreover, competitive inhibitors of SPHK block the formation of SPP and selectively inhibit calcium mobilization, cellular proliferation, and survival induced by these various stimuli (reviewed in Ref. 1). Thus, it has been suggested that the dynamic balance between levels of the sphingolipids metabolites, ceramide and SPP, and consequent regulation of opposing signaling pathways, is an important factor that determines the fate of cells (19). For example, stress stimuli increase ceramide levels leading to apoptosis, whereas survival factors stimulate SPHK leading to increased SPP levels, which suppress apoptosis (19). Moreover, the SPHK pathway, through the generation of SPP, is critically involved in mediating tumor necrosis factor- α -induced endothelial cell activation (12), and the ability of high density lipoproteins to inhibit cytokine-induced adhesion molecule expression has been correlated with its ability to reset this sphingolipid rheostat (12). This has important implications for the protective function of high density lipoproteins against the development of atherosclerosis and associated coronary heart disease. Recent data have also connected the sphingolipid rheostat to allergic responses (20).

Interest in SPP has accelerated recently with the discovery that it is a ligand of the G protein-coupled cell surface receptor EDG-1 (17, 21). This rapidly led to the identification of several other related receptors, named EDG-3, -5, -6, and -8, which are also specific SPP receptors (reviewed in Refs. 2 and 22). Sphinganine-1-phosphate, which is structurally similar to SPP and only lacks the trans double bond at the 4 position, but not lysophosphatidic acid or sphingosylphosphorylcholine, also binds to these receptors (23), demonstrating that EDG-1 belongs to a family of G protein-coupled receptors that bind SPP with high affinity and specificity (reviewed in Refs. 2 and 22). The EDG-1 family of receptors are differentially

sphingosine; *threo*-DHS, *D, L-threo*-dihydrosphingosine; TLC, thin layer chromatography; MES, 4-morpholineethanesulfonic acid.

expressed, mainly in the cardiovascular and nervous systems, and are coupled to a variety of G proteins and thus can regulate diverse signal transduction pathways culminating in pleiotropic responses depending on the cell type and relative expression of EDG receptors. Although the biological functions of the EDG-1 family of G protein-coupled receptors are not completely understood, recent studies suggest that binding of SPP to EDG-1 stimulates migration and chemotaxis (24, 25) and as a consequence may regulate angiogenesis (24, 26, 27). EDG-5 may play a role in cytoskeletal reorganization during neurite retraction, which is important for neuronal differentiation and development (23, 28).

Critical evaluation of the role of SPP requires cloning of the enzymes that regulate its metabolism. Recently, we purified rat kidney SPHK to apparent homogeneity (29) and subsequently cloned the first mammalian SPHK, designated mSPHK1 (30). Independently, two genes, termed LCB4 and LCB5, were also shown to code for SPHKs in *Saccharomyces cerevisiae* (31). Moreover, data base searches identified homologues of mSPHK1 in numerous widely disparate organisms, including worms, plants, and mammals, demonstrating that the enzyme is encoded by a member of a highly conserved gene family (30). Comparison of the predicted amino acid sequences of the known SPHKs revealed five blocks of highly conserved amino acids (30). However, several lines of evidence indicate that there may be multiple mammalian SPHK isoforms. The finding that SPHK activity in platelets could be chromatographically fractionated into several forms with differing responses to detergents and inhibition by known SPHK inhibitors suggested the presence of multiple enzyme forms in human platelets (32). Moreover, homology searches against a comprehensive nonredundant data base revealed that several of the expressed sequence tags (dbEST) at NCBI had significant homology to conserved domains of mSPHK1 (30), yet they had substantial sequence differences. Thus, we embarked on an effort to clone other SPHK isoforms. We report here the cloning, functional characterization, and tissue distribution of a second type of mammalian SPHK (SPHK2) that has distinct sequence, properties, and tissue distribution.

EXPERIMENTAL PROCEDURES

Materials—SPP, sphingosine, and *N,N*-dimethylsphingosine were from Biomol Research Laboratory Inc. (Plymouth Meeting, PA). All other lipids were purchased from Avanti Polar Lipids (Birmingham, AL). [γ - 32 P]ATP (3000 Ci/mmol) was purchased from Amersham Pharmacia Biotech. Poly-L-lysine and collagen were from Roche Molecular Biochemicals (Indianapolis, IN). Restriction enzymes were from New England Biolabs (Beverly, MA). Poly(A)⁺ RNA blots of multiple mouse adult tissues were purchased from CLONTECH (Palo Alto, CA). LipofectAMINE PLUS and LipofectAMINE were from Life Technologies, Inc.

cDNA Cloning of Murine Sphingosine Kinase-2 (mSPHK2)—BLAST searches of the EST data base identified a mouse EST clone (GenBankTM accession number AA839233), which had significant homology to conserved domains of mSPHK1 (30) yet had substantial sequence differences. Using this EST, a second isoform of SPHK, denoted mSPHK2, was cloned by two different PCR approaches.

In the first, we used the method of PCR cloning from a mouse cDNA library (Stratagene). Approximately 1×10^6 phages were plated on twenty 150-mm plates, plaques were collected, and plasmids were isolated using standard procedures (33). An initial PCR reaction was carried out with a sequence specific primer (M-3-1, 5'-CCTGGGTG-CACCTGCGCCTGTATTGG) and the M13 reverse primer. The longest PCR products were gel-purified and used as the template for a second PCR, which contained a sequence-specific antisense primer (M-3-2, 5'-CCAGTCTTGGGGCAGTGGAGAGCC-3') and the T3 primer. The final PCR products were subcloned by TOPO TA cloning (Invitrogen) and then sequenced. Platinum high fidelity DNA polymerase (Life Technologies, Inc.) was used for the PCR amplifications with the following cycling parameters: 30 cycles of 94 °C for 30 s, 55 °C for 45 s, and 72 °C for 2 min with a final primer extension at 72 °C for 5 min.

In a second approach, 5'-RACE PCR was performed with the 5'-RACE System for rapid amplification of cDNA ends according to the manufacturer's protocol (Life Technologies, Inc.). Poly(A)⁺ RNA was isolated from Swiss 3T3 fibroblasts using a Quick Prep mRNA purification kit (Amersham Pharmacia Biotech). First strand cDNA was synthesized at 42 °C for 50 min with 5 μ g of Swiss 3T3 poly(A)⁺ RNA using a target antisense primer designed from the sequence of AA839233 (m-GSP1, 5'-AGGTAGAGGCTTCTGG) and SuperScript II reverse transcriptase (Life Technologies, Inc.). Two consecutive PCR reactions using this cDNA as a template and LA Taq polymerase (TaKaRa) were carried out as follows: first PCR, 94 °C for 2 min followed by 30 cycles of 94 °C for 1 min, 55 °C for 1 min, 72 °C for 2 min, and primer extension at 72 °C for 5 min with 5'-RACE Abridged Anchor Primer, 5'-GGCCACGCGTCGACTAGTACGGGIGGGIIGGGIG and the target-specific antisense primer m-GSP2, 5'-GCGATGGGTGAAA-GCTGAGCTG; second PCR, same conditions except that the annealing temperature was 65 °C, with Abridged Universal Amplification Primer, 5'-GGCCACGCGTCGACTAGTAC and m-GSP3, 5'-AGTCTCCAGTCA-GCTCTGGACC. PCR products were cloned into pCR2.1 and sequenced, and final PCR products were subcloned into pCR3.1 and pcDNA 3 expression vectors.

cDNA Cloning of Human Sphingosine Kinase-2 (hSPHK2)—Poly(A)⁺ RNA from HEK293 cells was used for a 5'-RACE reaction. Target-specific antisense primers (h-GSP1, 5'-CCCACTCACTCAGG-CT; h-GSP2, 5'-GAAGGACAGCCGCTCAGAG; h-GSP3, 5'-ATTGACCAATAGAAGCAACC) were designed according to the sequence of a human EST clone (accession number AA295570). First strand cDNA was synthesized with 5 μ g of HEK293 mRNA and h-GSP1. This cDNA was used as a template in an initial PCR reaction using 5'-RACE Abridged Anchor Primer and h-GSP2. Then, nested PCR was carried out using the Abridged Universal Amplification Primer and h-GSP3. The resulting PCR products were cloned and sequenced as described above.

Overexpression and Measurement of Activity of SPHK2—HEK293 cells (ATCC CRL-1573) and NIH 3T3 fibroblasts (ATCC CRL-1658) were cultured as described previously (34). HEK293 cells were seeded at 6×10^5 /well in poly-L-lysine-coated 6-well plates. After 24 h, cells were transfected with 1 μ g of vector alone or with vectors containing sphingosine kinase constructs and 6 μ l of LipofectAMINE PLUS reagent plus 4 μ l of LipofectAMINE reagent/well. 1–3 days after transfection, cells were harvested and lysed by freeze-thawing as described previously (30). In some experiments, cell lysates were fractionated into cytosol and membrane fractions by centrifugation at 100,000 $\times g$ for 60 min. SPHK activity was determined in the presence of sphingosine, prepared as a complex with 4 mg/ml BSA and [γ - 32 P]ATP in kinase buffer (35) containing 200 mM KCl, unless indicated otherwise. 32 P-SPP was separated by TLC and quantified with a phosphorimager as described previously (30).

Lipid Extraction and Measurement of SPP—Cells were washed with phosphate-buffered saline and scraped in 1 ml of methanol containing a 2.5- μ l conc. HCl. Lipids were extracted by adding 2 ml of chloroform, 1 M NaCl (1:1, v/v) and 100 μ l of 3N NaOH, and the phases were separated. The basic aqueous phase containing SPP, and devoid of sphingosine, ceramide, and the majority of phospholipids, was transferred to a siliconized glass tube. The organic phase was re-extracted with 1 ml of methanol, 1 M NaCl (1:1, v/v) plus 50 μ l of 3N NaOH, and the aqueous fractions were combined. Mass measurements of SPP in the aqueous phase and total phospholipids in the organic phase were carried out exactly as described (8, 36).

Northern Blotting Analysis—Poly(A)⁺ RNA blots containing 2 μ g of poly(A)⁺ RNA/lane from multiple adult mouse and human tissues, and mouse embryos were purchased from CLONTECH. Blots were hybridized with the 1.2-kb *Pst*I fragment of mouse EST AA389187 (mSPHK1 probe), the 1.5-kb *Eco*RI fragment of pCR3.1-mSPHK2, the 0.3-kb *Pvu*II fragment of pCR3.1-hSPHK1, or the 0.6-kb *Eco*RV-*Sph*I fragment of human EST AA295570 (hSPHK2 probe), after gel-purification and labeling with [α - 32 P]dCTP. Hybridization in ExpressHyb buffer (CLONTECH) at 65 °C overnight was carried out according to the manufacturer's protocol. Blots were reprobbed with β -actin as a loading control (CLONTECH). Bands were quantified using an imaging analyzer (BAS2000, Fuji film).

RESULTS AND DISCUSSION

Cloning of Type 2 Sphingosine Kinase

Blast searches of the EST data base identified several ESTs that displayed significant homology to our recently cloned mSPHK1 sequence (30). Specific primers were designed from

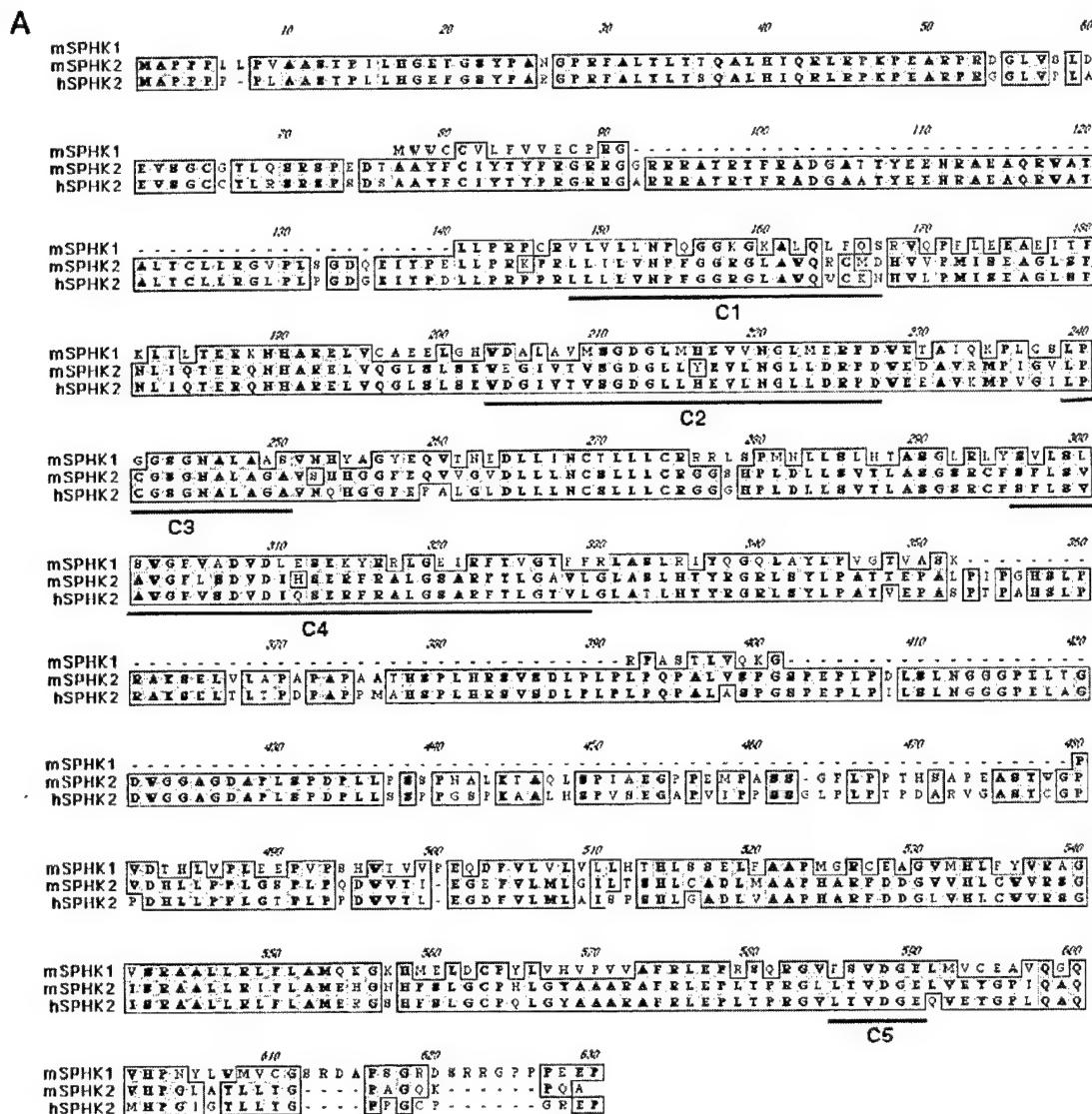


FIG. 1. Predicted amino acid sequences of murine and human type 2 SPHK. A, ClustalW alignment of the predicted amino acid sequences of mSPHK2 and hSPHK2. Identical and conserved amino acid substitutions are shaded dark and light gray, respectively. The dashes represent gaps in sequences, and numbers on the right refer to the amino acid sequence of mSPHK2. The conserved domains (C1–C5) are indicated by lines. B, schematic representation of conserved regions of SPHK1 and SPHK2. The primary sequence of mSPHK2 is compared with that of mSPHK1.

the sequences of these ESTs and were used to clone a new type of mouse and human SPHK (named mSPHK2 and hSPHK2) by the approaches of PCR cloning from a mouse brain cDNA library and 5'-RACE PCR.

ClustalW alignment of the amino acid sequences of mSPHK2

and hSPHK2 is shown in Fig. 1A. The open reading frames of mSPHK2 and hSPHK2 encode polypeptides of 617 and 618 amino acids, respectively, with 83% identity and 90% similarity. Five highly conserved regions (C1–C5), identified previously in SPHK1s (30), are also present in both type 2 kinases.

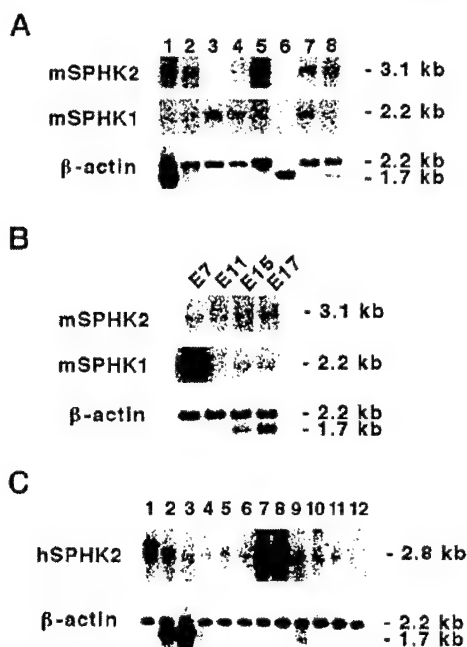


FIG. 2. Tissue-specific expression of type 1 and type 2 SPHK. A, mSPHK2 (upper panel) and mSPHK1a (middle panel) probes were end-labeled and hybridized to poly(A)⁺ RNA blots from the indicated mouse tissues as described under "Experimental Procedures." Lane 1, heart; lane 2, brain; lane 3, spleen; lane 4, lung; lane 5, liver; lane 6, skeletal muscle; lane 7, kidney; lane 8, testis. A β-actin probe (lower panel) was used as a loading control. B, expression of mSPHK1a and mSPHK2 during mouse embryonic development. Poly(A)⁺ RNA blots from embryonic days (E) 7, 11, 15, and 17 mouse embryos were probed as in A. C, tissue-specific expression of hSPHK2. Lane 1, brain; lane 2, heart; lane 3, skeletal muscle; lane 4, colon; lane 5, thymus; lane 6, spleen; lane 7, kidney; lane 8, liver; lane 9, small intestine; lane 10, placenta; lane 11, lung; lane 12, leukocyte.

Interestingly, the invariant GGKGGK positively charged motif in the C1 domain of SPHK1 is modified to GGRGL in SPHK2, suggesting that it may not be part of the ATP binding site as previously proposed (30). A motif search also revealed that a region beginning just before the conserved C1 domains of mSPHK2 and hSPHK2 (amino acid 147–284) also has homology to the diacylglycerol kinase catalytic site.

Compared with SPHK1, both SPHK2s encode much larger proteins containing 236 additional amino acids (Fig. 1B). Moreover, their sequences diverge considerably from SPHK1 in the center and at the amino termini. However, after amino acid 140 of mSPHK2, the sequences of type 1 and type 2 mSPHK have a large degree of similarity. These sequences (amino acids 9–226 for mSPHK1 and 141–360 for mSPHK2), which encompass domains C1–C4, have 47% identity and 79% similarity (Fig. 1B). In the carboxyl-terminal portion of the proteins there are also large homologous regions, which include the C5 domain, from amino acids 227–381 for mSPHK1 and 480–617 for mSPHK2, with 43% identity and 78% similarity (Fig. 1B). The overall divergence suggests that SPHK2 probably did not arise as a simple gene duplication event.

Tissue Distribution of Sphingosine Kinase Type 2

The tissue distribution of SPHK2 mRNA expression in adult mouse was compared with that of SPHK1 by Northern blotting (Fig. 2A). In most tissues, including adult liver, heart, kidney, testis, and brain, a predominant 3.1-kb SPHK2 mRNA species was detected, indicating ubiquitous expression. However, the level of expression was markedly variable

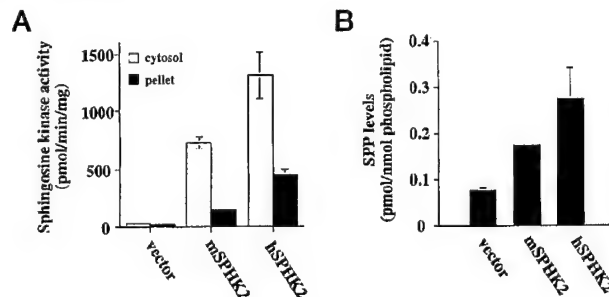


FIG. 3. Enzymatic activity of recombinant SPHK2. A, HEK293 cells were transiently transfected with empty vector or with mSPHK2 or hSPHK2 expression vectors. After 24 h, SPHK activity was measured in cytosol (open bars) and particulate fractions (filled bars). The data are mean \pm S.D. Parental and vector-transfected cells had basal SPHK activities of 26 and 37 pmol/min/mg, respectively. B, changes in mass levels of SPP after transfection with SPHK2. Mass levels of SPP in HEK293 cells transfected with empty vector, with mSPHK2 (filled bars), or with hSPHK2 were measured as described under "Experimental Procedures." The data are expressed as pmol/nmol phospholipid.

and was highest in adult liver and heart and barely detectable in the skeletal muscle and spleen (Fig. 2A). In contrast, the expression pattern of mSPHK1 is quite different, with highest mRNA expression of a 2.2-kb transcript in adult lung, spleen, and liver, although expression in liver does not predominate as with mSPHK2. mSPHK1 and mSPHK2 were both temporally and differentially expressed during embryonic development. mSPHK1 was expressed highly at mouse embryonic day 7 and decreased dramatically after embryonic day 11 (Fig. 2B). In contrast, at embryonic day 7, mSPHK2 expression was much lower than mSPHK1 and gradually increased up to embryonic day 17. The hSPHK2 2.8-kb mRNA transcript was mainly expressed in adult kidney, liver, and brain, with much lower expression in other tissues (Fig. 2C). Interestingly, expression of SPHK2 in human kidney is very high and relatively much lower in the mouse kidney, whereas the opposite pattern holds for the liver.

Activity of Recombinant Sphingosine Kinase Type 2

To investigate whether mSPHK2 and hSPHK2 encode *bona fide* SPHKs, HEK293 cells were transiently transfected with expression vectors containing the corresponding cDNAs. Because previous studies have indicated that SPHK might be present in cells in both soluble and membrane-associated forms (3, 32, 37–39), recombinant SPHK2 activity was measured both in cytosol and in membrane fractions of transfected cells. As described previously (30), untreated or vector-transfected HEK293 cells have low levels of SPHK activity (Fig. 3A). 24 h after transfection with mSPHK2 or hSPHK2, *in vitro* SPHK activity was increased by 20- and 35-fold, respectively, and then decreased thereafter (Fig. 3A). In contrast, SPHK activity in cells transfected with mSPHK1 was much higher, 610-fold greater than basal levels 24 h after transfection and remained at this level for at least 3 more days (data not shown). As in HEK293 cells, transfection of NIH 3T3 fibroblasts with mSPHK1 resulted in much higher SPHK activity than with mSPHK2. We previously found that, similar to untransfected cells, the majority of SPHK activity in cells transfected with mSPHK1 was cytosolic (30). Similarly, in cells transfected with either mSPHK2 or hSPHK2, 17 and 26%, respectively, of the SPHK activity was membrane-associated (Fig. 3A), although Kyte-Doolittle hydropathy plots did not suggest the presence of hydrophobic membrane-spanning domains.

Transfection of HEK293 cells with mSPHK2 and hSPHK2 also resulted in 2.2- and 3.3-fold increases, respectively, in

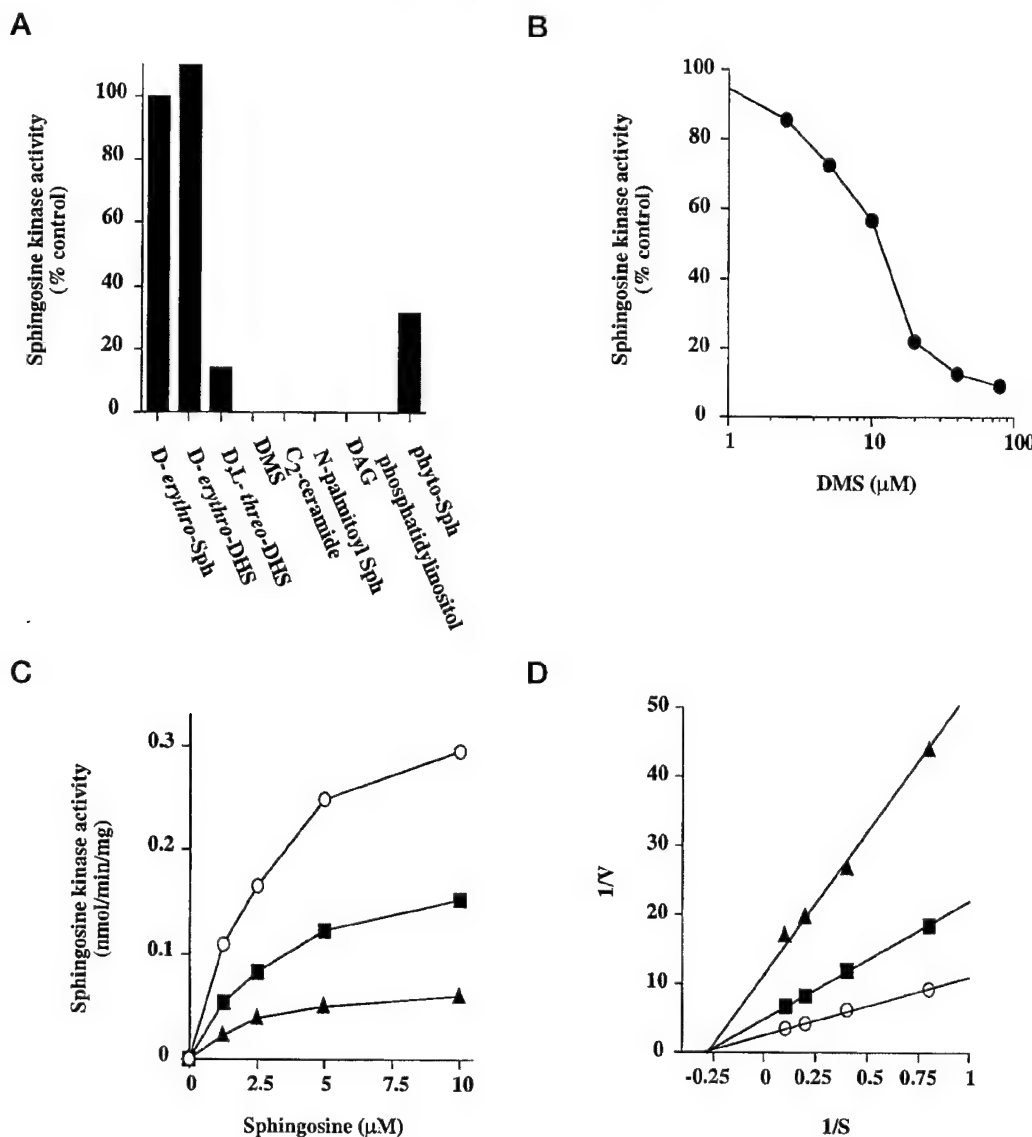


FIG. 4. **Substrate specificity of mSPHK2.** A, SPHK-dependent phosphorylation of various sphingosine analogs or other lipids (50 μ M) was measured in cytosol from HEK293 cells transfected with mSPHK2. Data are expressed as percentage of phosphorylation of D-erythro-Sph. B–D, noncompetitive inhibition of recombinant SPHK2 by *N,N*-dimethylsphingosine. B, dose-dependent inhibition of mSPHK2 by DMS. SPHK activity in HEK293 cell lysates after transfection as in A was measured with 10 μ M D-erythro-sphingosine in the presence of increasing concentrations of DMS. C, kinetic analysis of DMS inhibition. SPHK activity was measured with varying concentrations of D-erythro-sphingosine in the absence (open circles) or presence of 10 (filled squares) or 20 μ M DMS (filled triangles). D, Lineweaver-Burk plots. The K_m value for D-erythro-sphingosine was 3.4 μ M. The K_i value for DMS was 12 μ M.

SPP, the product formed by SPHK (Fig. 3B), in agreement with previous studies of sphingolipid metabolite levels after transfection with mSPHK1, which showed a lack of correlation of fold increases in SPP levels and *in vitro* SPHK enzyme activity (30, 34).

Characteristics of Recombinant mSPHK2

Substrate Specificity—Although SPHK2 is highly homologous to SPHK1, there are substantial sequence differences. Therefore, it was of interest to compare their enzymatic properties. Typical Michaelis-Menten kinetics were observed for recombinant SPHK2 (data not shown). The K_m for D-erythro-sphingosine as substrate is 3.4 μ M, almost identical to the K_m previously found for SPHK1 (29). Although the naturally occurring D-erythro-sphingosine isomer was the best substrate for SPHK1 (30), D-erythro-dihydrosphingosine was a better substrate for

SPHK2 than D-erythro-sphingosine (Fig. 4A). Moreover, although D,L-threo-dihydrosphingosine and phytosphingosine were not phosphorylated at all by SPHK1, they were significantly phosphorylated by SPHK2, albeit much less efficiently than sphingosine. Like SPHK1, other lipids including *N,N*-dimethylsphingosine (DMS), C₂- or C16-ceramide, diacylglycerol, or phosphatidylinositol, were not phosphorylated by SPHK2 (Fig. 4A), suggesting high specificity for the sphingoid base.

DMS and threo-DHS have previously been shown to be potent competitive inhibitors of SPHK1 (40) and have been used to block increases in intracellular SPP levels resulting from various physiological stimuli (3, 4, 8, 11, 13, 14, 41). However, because threo-DHS is a substrate for SPHK2, it is not useful as a tool to investigate the role of SPHK2/SPP signaling. Thus, it was important to characterize the inhibitory potential of the nonsubstrate DMS on SPHK2. Surprisingly, we found that

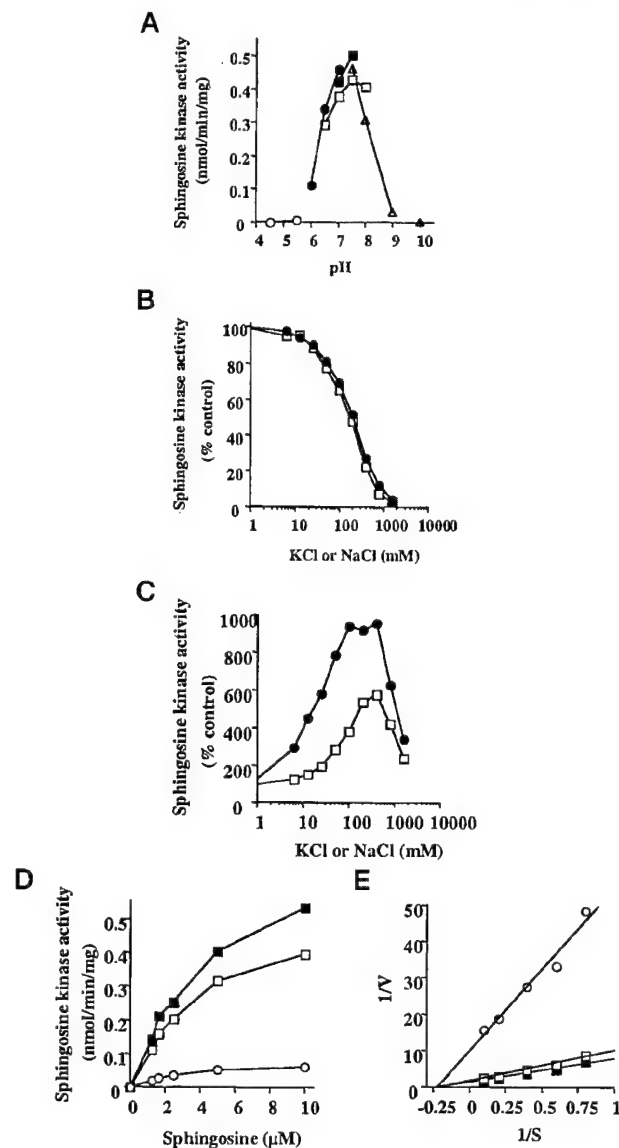


FIG. 5. pH dependence and salt effects on mSPHK2. A, cytosolic SPHK2 activity in transfected HEK293 cells was measured in kinase buffer with the pH adjusted using the following buffers: 200 mM sodium acetate (pH 4.5–5.5, open circles); 200 mM MES (pH 6–7, filled circles); 200 mM potassium phosphate (pH 6.5–8, open squares); 200 mM HEPES (pH 7–7.5, filled squares); 200 mM Tris-HCl (pH 7.5–9, open triangles); and 200 mM borate (pH 10, filled triangle). B–E, salts stimulate SPHK2 but inhibit SPHK1. B and C, SPHK activity in HEK293 cell lysates was measured 24 h after transfection with mSPHK1 (B) or mSPHK2 (C) in the absence or presence of increasing concentrations of NaCl (open squares) or KCl (filled circles). D, kinetic analysis of SPHK2 activation by KCl. mSPHK2 activity was measured with varying concentrations of D-erythro-sphingosine in the absence (open circles) or presence of 50 (open squares) or 200 mM KCl (filled circles). E, Lineweaver-Burk plots of data from D. The K_m value is not affected by the presence of KCl. V_{max} values were 0.1, 0.3, and 1 (nmol/min/mg) in the presence of 0, 50, and 200 mM KCl, respectively.

although DMS was also a potent inhibitor of SPHK2 (Fig. 4B), it acted in a noncompetitive manner (Fig. 4, C and D). The K_i for DMS with SPHK2 was 12 μ M, slightly higher than the K_i of 4 μ M with SPHK1, suggesting that it can be used to inhibit both types of SPHK.

mSPHK2 had highest enzymatic activity in the neutral pH range from 6.5 to 8 with optimal activity at pH 7.5 (Fig. 5A), a

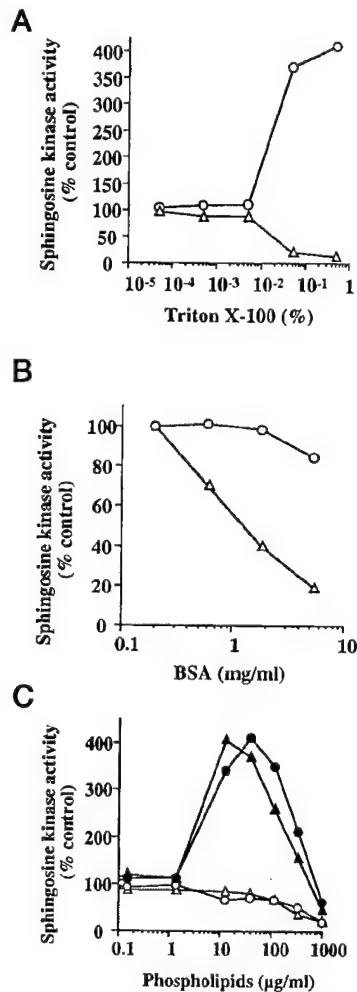


FIG. 6. Triton X-100 and BSA, but not phosphatidylserine, have differential effects on activity of SPHK1 and SPHK2. HEK293 cells were transfected with mSPHK1 (circles) or mSPHK2 (triangles) and the activities of each in cell lysates were measured after 24 h in the presence of the indicated concentrations of Triton X-100 (A), BSA (B), or phosphatidylserine (filled symbols) or phosphatidylcholine (open symbols) (C). Data are expressed as percentage of control activity measured without any additions.

pH dependence similar to that of SPHK1 (data not shown). The activity decreased markedly at pH values below and above this range.

Effects of KCl and NaCl—Most of the SPHK activity in human platelets is membrane-associated and extractable with 1 M NaCl (32). Furthermore, the salt extractable SPHK from platelets has different properties than the cytosolic enzyme. It was thus of interest to determine the effect of high salt concentrations on recombinant SPHK1 and SPHK2. Interestingly, we found that high ionic strength had completely opposite effects on their activities. SPHK1 was markedly inhibited by either NaCl and KCl, with each causing 50% inhibition at a concentration of 200 mM (Fig. 5B). In contrast, SPHK2 activity was dramatically stimulated by increasing the salt concentration, with a maximal effect at a concentration of 400 mM, although KCl was much more effective than NaCl. However, above this concentration, SPHK2 activity decreased sharply although remaining elevated even at 1 M salt (Fig. 5C). Kinetic analysis of mSPHK2 in the presence and absence of high concentrations of salt indicated that the K_m for sphingosine was unaltered, whereas the V_{max} was increased (Fig. 5, D and E). The physi-

ological significance of these observations remains to be determined but it could be related to different subcellular localizations of the two types of SPHK.

Substrate Presentation—Because sphingolipids are highly lipophilic, in *in vitro* SPHK assays, sphingosine is usually presented in micellar form with Triton X-100 or as a complex with BSA (42, 43). Furthermore, detergents such as Triton X-100 have been shown to stimulate the activity of SPHK in rat brain extracts (37) and the enzyme from rat kidney (29), and we previously found that the stability of rat kidney SPHK was increased in the presence of certain detergents (29). However, when the effect of increasing concentrations of Triton X-100 on the activities of SPHK1 and SPHK2 were compared, some unexpected results were found. Concentrations of detergent up to 0.005% had no effect, but at higher concentrations, SPHK2 activity was inhibited and SPHK1 activity was markedly stimulated (Fig. 6A). At a concentration of Triton X-100 of 0.5%, SPHK1 activity was increased by more than 4-fold, whereas SPHK2 was almost completely inhibited. Thus, Triton X-100 could be used to differentially determine SPHK1 and SPHK2 activities in tissues or cells that express both types.

Interestingly, increasing the BSA concentration from our usual SPHK assay conditions with sphingosine-BSA complex as substrate, *i.e.* 0.2 mg/ml BSA, caused a concentration-dependent inhibition of SPHK2 activity without affecting SPHK1 activity (Fig. 6B). Therefore, when measuring SPHK activity in cell or tissue extracts, the method of substrate presentation, whether in mixed micelles or in BSA complexes, must be carefully optimized because the differential effects of Triton X-100 and BSA on activity could yield different results depending on the relative expression of the two types of SPHK.

Effects of Phospholipids—Acidic phospholipids, particularly phosphatidylserine, phosphatidic acid, and phosphatidylinositol, and cardiolipin to a lesser extent, induced a dose-dependent increase in SPHK activity in Swiss 3T3 fibroblast lysates, whereas neutral phospholipids had no effect (42). In agreement, the enzymatic activity of recombinant SPHK1 and SPHK2 was stimulated by phosphatidylserine; the activity of both was maximally increased 4-fold at a concentration of 40 μ g/ml (Fig. 6C) and inhibited by higher concentrations in a dose-dependent manner. These effects of phosphatidylserine appeared to be specific because other phospholipids, including phosphatidylcholine, had no effect on the enzyme activity. In contrast, the activities of the three major forms of SPHK in human platelets were not affected by phosphatidylserine (32).

The mechanism by which phosphatidylserine enhances the enzymatic activity of SPHK is not yet understood. One possibility is that phosphatidylserine possesses unique membrane-structuring properties, which better present the substrate, sphingosine. A second possibility is that SPHK contains determinants that specifically recognize the structure of the serine headgroup and that these determinants may only become exposed upon interaction of SPHK with membranes. In this regard, the molecular basis for the remarkable specificity of protein kinase C for phosphatidylserine has been the subject of much debate. However, recent data reveal that lipid structure and not membrane structure is the major determinant in the regulation of protein kinase C by phosphatidylserine (44).

Concluding Remarks

The presence of multiple ESTs in the data base with significant homologies to SPHK1 as well as the identification of several genes in *S. cerevisiae* encoding different SPHKs (31) suggested that there may be a large and important SPHK gene

family. In this study, we have cloned and characterized a second type of SPHK that has some unique properties. Although SPHK2 has a high degree of homology to SPHK1, especially in the previously identified conserved domains identified in type 1 SPHKs (30), it is much larger (65.2 and 65.6 kDa for hSPHK2 and mSPHK2, respectively, *versus* 42.4 kDa for mSPHK1) and contains an additional 236 amino acids. Furthermore, its differential tissue expression, temporal developmental expression, cellular localization, and kinetic properties in response to increasing ionic strength and detergents are completely different from SPHK1, suggesting that it most likely has a different function and regulates levels of SPP in a different manner than SPHK1, which is known to play a prominent role in regulating cell growth and survival. Thus, type 2 SPHK might be involved in regulation of some of the numerous biological responses attributed to SPP, such as angiogenesis and allergic responses.

Acknowledgments—We thank Ayako Yamamoto for excellent technical assistance and Drs. Emanuela Lacana and Tom I. Bonner for helpful suggestions.

REFERENCES

1. Spiegel, S. (1999) *J. Leukocyte Biol.* **65**, 341–344
2. Goetzl, E. J., and An, S. (1998) *FASEB J.* **12**, 1589–1598
3. Olivera, A., and Spiegel, S. (1993) *Nature* **365**, 557–560
4. Cuvillier, O., Pirianov, G., Kleuser, B., Vanek, P. G., Coso, O. A., Gutkind, S., and Spiegel, S. (1996) *Nature* **381**, 800–803
5. Bornfeldt, K. E., Graves, L. M., Raines, E. W., Igarashi, Y., Wayman, G., Yamamura, S., Yatomi, Y., Sidhu, J. S., Krebs, E. G., Hakomori, S., and Ross, R. (1995) *J. Cell Biol.* **130**, 193–206
6. Pyne, S., Chapman, J., Steele, L., and Pyne, N. J. (1996) *Eur. J. Biochem.* **237**, 819–826
7. Coroneos, E., Martinez, M., McKenna, S., and Kester, M. (1995) *J. Biol. Chem.* **270**, 23305–23309
8. Edsall, L. C., Pirianov, G. G., and Spiegel, S. (1997) *J. Neurosci.* **17**, 6952–6960
9. Rius, R. A., Edsall, L. C., and Spiegel, S. (1997) *FEBS Lett.* **417**, 173–176
10. Kleuser, B., Cuvillier, O., and Spiegel, S. (1998) *Cancer Res.* **58**, 1817–1824
11. Meyer zu Heringdorf, D., Lass, H., Alemany, R., Laser, K. T., Neumann, E., Zhang, C., Schmidt, M., Rauen, U., Jakobs, K. H., and van Koppen, C. J. (1998) *EMBO J.* **17**, 2830–2837
12. Xia, P., Gamble, J. R., Rye, K. A., Wang, L., Hii, C. S. T., Cockerill, P., Khew-Goodall, Y., Bert, A. G., Barter, P. J., and Vadas, M. A. (1998) *Proc. Natl. Acad. Sci. U. S. A.* **95**, 14196–14201
13. Choi, O., Kim, J.-H., and Kinet, J.-P. (1996) *Nature* **380**, 634–636
14. Melendez, A., Floto, R. A., Gillooly, D. J., Harnett, M. M., and Allen, J. M. (1998) *J. Biol. Chem.* **273**, 9393–9402
15. Mattie, M., Brooker, G., and Spiegel, S. (1994) *J. Biol. Chem.* **269**, 3181–3188
16. Rani, C. S. S., Wang, F., Fuor, E., Berger, A., Wu, J., Sturgill, T. W., Beitner-Johnson, D., LeRoith, D., Varticovski, L., and Spiegel, S. (1997) *J. Biol. Chem.* **272**, 10777–10783
17. Van Brocklyn, J. R., Lee, M. J., Menzeleev, R., Olivera, A., Edsall, L., Cuvillier, O., Thomas, D. M., Coopman, P. J. P., Thangada, S., Hla, T., and Spiegel, S. (1998) *J. Cell Biol.* **142**, 229–240
18. Perez, G. I., Knudson, C. M., Leykin, L., Korsmeyer, S. J., and Tilly, J. L. (1997) *Nat. Med.* **3**, 1228–1232
19. Cuvillier, O., Rosenthal, D. S., Smulson, M. E., and Spiegel, S. (1998) *J. Biol. Chem.* **273**, 2910–2916
20. Prieschl, E. E., Csonga, R., Novotny, V., Kikuchi, G. E., and Baumruker, T. (1999) *J. Exp. Med.* **190**, 1–8
21. Lee, M. J., Van Brocklyn, J. R., Thangada, S., Liu, C. H., Hand, A. R., Menzeleev, R., Spiegel, S., and Hla, T. (1998) *Science* **279**, 1552–1555
22. Spiegel, S., and Milstien, S. (2000) *Biochim. Biophys. Acta* **1484**, 107–116
23. Van Brocklyn, J. R., Tu, Z., Edsall, L. C., Schmidt, R. R., and Spiegel, S. (1999) *J. Biol. Chem.* **274**, 4626–4632
24. Wang, F., Van Brocklyn, J. R., Hobson, J. P., Movafagh, S., Zukowska-Grojec, Z., Milstien, S., and Spiegel, S. (1999) *J. Biol. Chem.* **274**, 35343–35350
25. English, D., Kovala, A. T., Welch, Z., Harvey, K. A., Siddiqui, R. A., Brindley, D. N., and Garcia, J. G. (1999) *J. Hematother. Stem Cell Res.* **8**, 627–634
26. Lee, O. H., Kim, Y. M., Lee, Y. M., Moon, E. J., Lee, D. J., Kim, J. H., Kim, K. W., and Kwon, Y. G. (1999) *Biochem. Biophys. Res. Commun.* **264**, 743–750
27. Lee, M. J., Thangada, S., Claffey, K. P., Ancellin, N., Liu, C. H., Kluk, M., Volpi, M., Sha'afi, R. I., and Hla, T. (1999) *Cell* **99**, 301–312
28. MacLennan, A. J., Marks, L., Gaskin, A. A., and Lee, N. (1997) *Neuroscience* **79**, 217–224
29. Olivera, A., Kohama, T., Tu, Z., Milstien, S., and Spiegel, S. (1998) *J. Biol. Chem.* **273**, 12576–12583
30. Kohama, T., Olivera, A., Edsall, L., Nagiec, M. M., Dickson, R., and Spiegel, S. (1998) *J. Biol. Chem.* **273**, 23722–23728
31. Nagiec, M. M., Skrzypek, M., Nagiec, E. E., Lester, R. L., and Dickson, R. C. (1998) *J. Biol. Chem.* **273**, 19437–19442
32. Banno, Y., Kato, M., Hara, A., and Nozawa, Y. (1998) *Biochem. J.* **335**, 301–304
33. Ausubel, F. M., Brent, R., Kingston, R. E., Moore, D. D., Smith, J. A., Seidman, J. G., and Struhl, K. (1987) *Current Protocols in Molecular Biology*, pp. 9.1.4–9.1.1, Wiley-Interscience, New York
34. Olivera, A., Kohama, T., Edsall, L. C., Nava, V., Cuvillier, O., Poulton, S., and

- Spiegel, S. (1999) *J. Cell Biol.* **147**, 545-558
35. Olivera, A., and Spiegel, S. (1998) in *Methods in Molecular Biology* (Bird, I. M., ed) Vol. 105, pp. 233-242, Humana Press Inc., Totawa, NJ
36. Edsall, L. C., and Spiegel, S. (1999) *Anal. Biochem.* **272**, 80-86
37. Buehrer, B. M., and Bell, R. M. (1992) *J. Biol. Chem.* **267**, 3154-3159
38. Olivera, A., Rosenthal, J., and Spiegel, S. (1994) *Anal. Biochem.* **223**, 306-312
39. Ghosh, T. K., Bian, J., and Gill, D. L. (1994) *J. Biol. Chem.* **269**, 22628-22635
40. Edsall, L. C., Van Brocklyn, J. R., Cuvillier, O., Kleuser, B., and Spiegel, S. (1998) *Biochemistry* **37**, 12892-12898
41. Machwate, M., Rodan, S. B., Rodan, G. A., and Harada, S. I. (1998) *Mol. Pharmacol.* **54**, 70-77
42. Olivera, A., Rosenthal, J., and Spiegel, S. (1996) *J. Cell. Biochem.* **60**, 529-537
43. Olivera, A., Barlow, K. D., and Spiegel, S. (2000) *Methods Enzymol.* **311**, 215-223
44. Johnson, J. E., Zimmerman, M. L., Daleke, D. L., and Newton, A. C. (1998) *Biochemistry* **37**, 12020-12025



Sphingosine generation, cytochrome c release, and activation of caspase-7 in doxorubicin-induced apoptosis of MCF7 breast adenocarcinoma cells

O Cuvillier^{1,2}, VE Nava¹, SK Murthy¹, LC Edsall³, T Levade², S Milstien³ and S Spiegel^{*,1}

¹ Department of Biochemistry and Molecular Biology, Georgetown University Medical Center, 3900 Reservoir Road NW, Washington, DC 20007, USA

² Unité Inserm 466, CHU Rangueil, 1 avenue Jean Poulhes, 31403 Toulouse France

³ Laboratory of Cellular and Molecular Regulation, NIMH, Bethesda, MD 20892, USA

* Corresponding author: S Spiegel, Department of Biochemistry and Molecular Biology, Georgetown University Medical Center, 353 Basic Science Building, 3900 Reservoir Road NW, Washington, DC 20007, USA Tel: 202-687-1432, Fax: 202-687-0260; E-mail: spiegel@bc.georgetown.edu

Received 9.5.00; revised 2.8.00; accepted 20.9.00

Edited by C Thiele

Abstract

Treatment of human breast carcinoma MCF7 cells with doxorubicin, one of the most active antineoplastic agents used in clinical oncology, induces apoptosis and leads to increases in sphingosine levels. The transient generation of this sphingolipid mediator preceded cytochrome c release from the mitochondria and activation of the executioner caspase-7 in MCF7 cells which do not express caspase-3. Bcl-x_L overexpression did not affect sphingosine generation whereas it reduced apoptosis triggered by doxorubicin and completely blocked apoptosis triggered by sphingosine. Exogenous sphingosine-induced apoptosis was also accompanied by cytochrome c release and activation of caspase-7 in a Bcl-x_L-sensitive manner. Furthermore, neither doxorubicin nor sphingosine treatment affected expression of Fas ligand or induced activation of the apical caspase-8, indicating a Fas/Fas ligand-independent mechanism. Our results suggest that a further metabolite of ceramide, sphingosine, may also be involved in mitochondria-mediated apoptotic signaling induced by doxorubicin in human breast cancer cells. *Cell Death and Differentiation* (2001) 8, 162–171.

Keywords: apoptosis; sphingosine; doxorubicin; cytochrome c; caspases

Abbreviations: Ac-DEVD-AMC, acetyl-Asp-Glu-Val-Asp-amino-methylcoumarin; dMAPP, D-erythro-2-(N-myristoylamino)-1-phenyl-1-propanol; FB1, fumonisins B1; PARP, poly(ADP-ribose) polymerase

Introduction

The anthracycline antibiotics constitute an important group of drugs that have been used to successfully produce regression in disseminated neoplasias, including acute lymphoblastic leukemia, acute myeloblastic leukemia, Wilm's tumor, soft tissue and bone sarcomas, breast carcinoma, ovarian carcinoma, and many others. The molecular mechanisms responsible for the cytotoxic effects of anthracyclines in malignant cells are not fully understood but are mainly attributed to their ability to intercalate into DNA and cause localized uncoiling of the double helix or by stabilization of the complex between DNA and topoisomerase II.¹ In addition, anthracyclines can mediate oxygen free radical generation originating from quinone-generated redox activity that can also damage DNA.¹

Ceramide, a sphingolipid produced by the hydrolysis of membrane-associated sphingomyelin, has previously been implicated as a gauge of apoptosis (reviewed in ²). Diverse apoptotic stimuli, including the anthracycline drug daunorubicin,^{3–9} increase ceramide levels, which in turn leads to activation of downstream signals important for the apoptotic process. Daunorubicin triggers apoptosis and ceramide generation by activating a neutral sphingomyelinase in the leukemic cell lines U937 and HL-60,³ whereas other studies suggest that it stimulates ceramide elevation in lymphocytic P388 and U937 cells by activation of ceramide synthase in the *de novo* pathway, rather than by activation of sphingomyelinase.⁴ Although Bcl-2 overexpression inhibits ceramide-mediated apoptosis, it does not intervene in ceramide generation induced by daunorubicin, suggesting that Bcl-2 suppresses apoptosis downstream of ceramide generation.⁵ In agreement, doxorubicin, another member of the anthracycline family, induces apoptosis in cardiac myocytes and activates the sphingomyelin-ceramide pathway.^{10,11}

Sphingosine, formed from ceramide by ceramidase, has also been implicated in cell growth arrest and apoptosis. Indeed, sphingosine is rapidly produced during TNF α -mediated apoptosis in human neutrophils¹² and in cardiac myocytes,¹³ and is capable of inducing apoptosis when added exogenously to many cell types.^{12–18} More recently, we found that sphingosine is also transiently produced during the early phase of Fas- and ceramide-induced apoptosis in Jurkat T cells, acting in a mitochondria-dependent manner.¹⁹

Here, we report that treatment of human breast cancer MCF7 cells with doxorubicin induces transient generation of sphingosine, preceding cytochrome c release and activation of the executioner caspase-7. In addition, exogenous sphingosine recapitulates doxorubicin-induced apoptosis, as well as cytochrome c redistribution and activation of

caspase-7 in a Bcl-x_L-sensitive fashion. Our findings suggest the potential involvement of sphingosine, in addition to ceramide, in mitochondria-dependent apoptosis triggered by doxorubicin in human breast cancer MCF7 cells.

Results

In agreement with previous studies,²⁰ we found that treatment of MCF7 cells with doxorubicin caused extensive cell death (Figure 1A). As sphingosine has been implicated in cytokine-induced apoptosis,^{12,13,19} it was of interest to determine whether treatment with doxorubicin could also induce apoptosis in a manner dependent on sphingosine generation. After treatment with 1 μ g/ml doxorubicin, a therapeutic concentration, sphingosine levels significantly increased by 16 h, peaked at 24 h, and declined thereafter (Figure 1B). Interestingly, sphingosine levels also somewhat increased in untreated cells, probably as a result of changing to fresh serum-free media, in agreement with previous studies demonstrating that sphingolipid synthesis was stimulated by replacement of the media.^{21,22} In line with previous studies in other cell types,^{12,13,15-19,23,24} addition of exogenous sphingosine also induced apoptosis in MCF7/Fas cells in a time- (Figure 1A) and concentration-dependent manner (data not shown).

To examine the possibility that sphingosine-induced cell death might be due to its conversion to ceramide by the action of ceramide synthase, we investigated the effect of the mycotoxin fumonisin B1, a competitive inhibitor of

ceramide synthase.²⁵ Treatment of MCF7/Fas cells with 25 μ M fumonisin B1 had no effect on cell death induced by doxorubicin (Figure 2A) nor did it affect the extent of cell death induced by sphingosine (Figure 2B). However, surprisingly, a higher concentration of fumonisin B1 (100 μ M) inhibited cell death in MCF7/Fas cells treated with doxorubicin to a lesser extent than that induced by sphingosine (Figure 2C). These data suggest that sphingosine- and doxorubicin-induced cell death in MCF7/Fas cells is partially dependent on ceramide synthase activity.

The generation of sphingosine during cell death induced by doxorubicin suggests that the increase in sphingosine might result from degradation of ceramide. This is a likely possibility, as sphingosine is not synthesized *de novo* and can only be produced by metabolism of ceramide.²⁵ To gain further insight into the relative function of endogenous sphingosine, we used the ceramidase inhibitor, dMAPP.²⁶ Treatment of MCF7/Fas cells with 5 μ M dMAPP not only attenuated cell death induced by doxorubicin (Figure 3A), but also surprisingly, that induced by exogenous sphingosine to an even greater extent (Figure 3B).

Because overexpression of Bcl-2 or Bcl-x_L protects against diverse apoptotic stimuli, including ceramide-induced apoptosis,^{5,19,27-30} it was important to determine whether the effects of sphingosine were also blocked by these proteins. MCF7/Fas cells stably overexpressing Bcl-x_L were treated with doxorubicin or sphingosine and cell death was measured. In agreement with the anti-apoptotic effects of Bcl-x_L family members in other cell types,

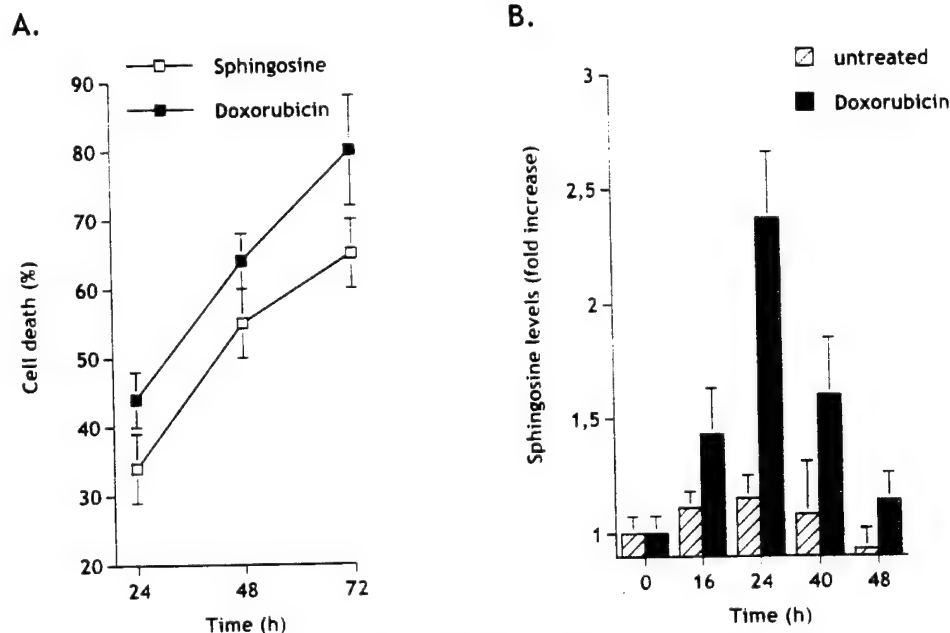


Figure 1 The effect of doxorubicin on cell death and sphingosine levels in MCF7 cells. (A) MCF7/Fas cells were treated with 1 μ g/ml of doxorubicin (filled squares) or 10 μ M sphingosine (open squares) for the indicated times. The percentage of cell death was assessed by the MTT assay. The values are means of triplicate determinations \pm S.D. Similar results were obtained in three additional experiments. (B) Sphingosine levels were measured in MCF7/Fas cells cultured in serum-free media without (untreated) or with 1 μ g/ml doxorubicin for the indicated times. Results are means \pm S.D. of three independent experiments performed in triplicate.

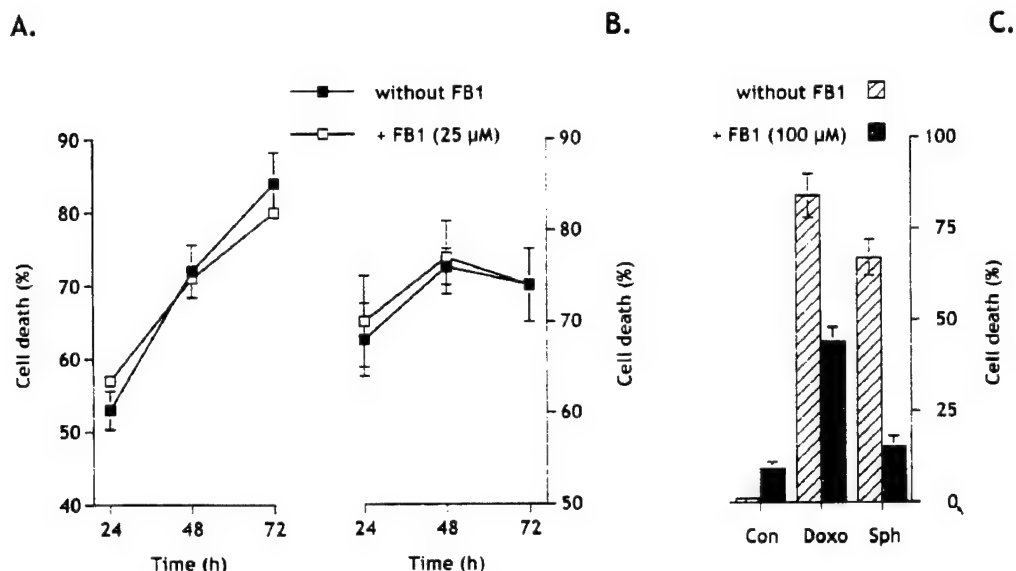


Figure 2 Effects of fumonisins B1 on cell death. (A) MCF7/Fas cells were pre-incubated without (filled squares) or with (open squares) 25 μ M fumonisins B1 for 30 min in serum-free medium and then 1 μ g/ml doxorubicin was added for the indicated times. (B) MCF7/Fas cells were pre-incubated without (filled squares) or with (open squares) 25 μ M fumonisins B1 for 30 min in serum-free medium and then incubated in the presence of 10 μ M sphingosine for the indicated times. (C) MCF7/Fas cells were incubated in the presence of 1 μ g/ml doxorubicin or 10 μ M sphingosine without or with 100 μ M fumonisins B1 for 72 h. The percentage of cell death was assessed by the MTT assay. The values are means \pm S.D. of triplicate determinations.

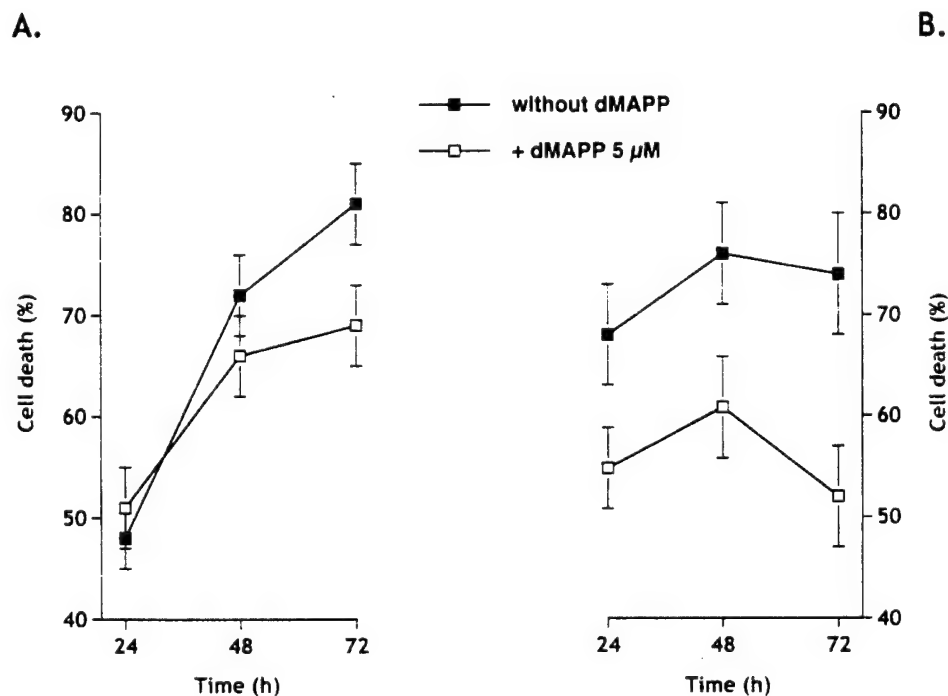


Figure 3 Effects of dMAPP on cell death. MCF7/Fas cells were incubated without (filled squares) or with (open squares) 5 μ M dMAPP for 30 min and then 1 μ g/ml doxorubicin (A) or 10 μ M sphingosine (B) were added for the indicated times. The percentage of cell death was assessed by the MTT assay. The values are means \pm S.D. of triplicate determinations.

including human small cell lung cancer cells,³ neuroblastoma cells,³² myeloid leukemia HL-60 cells^{33,34} and U937 cells.³⁵ overexpression of Bcl-x_L inhibited doxorubicin-

induced cell death and completely protected against sphingosine-induced cell death (Figure 4A). However, Bcl-x_L expression did not have any significant effect on the

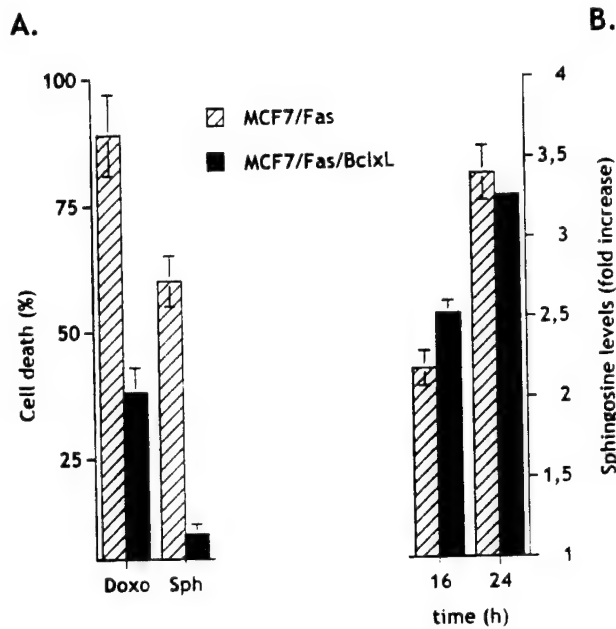


Figure 4 Bcl-x_L overexpression blocks doxorubicin-induced cell death but not sphingosine generation. (A) MCF7/Fas and MCF7/Fas/Bcl-x_L cells were treated with 1 µg/ml doxorubicin or 10 µM sphingosine and cell death was assessed by the MTT assay. The values are means ± S.D. of triplicate determination. This experiment was repeated three times with similar results. (B) Sphingosine levels were determined in MCF7/Fas and MCF7/Fas/Bcl-x_L cells treated with 1 µg/ml doxorubicin for the indicated times. Results are means ± S.D. of three independent experiments performed in triplicate.

increase in sphingosine induced by doxorubicin (Figure 4B). These results suggest that the sphingosine increase is not merely a consequence of cell death as it is also observed in the Bcl-x_L overexpressing cells which do not die and imply that sphingosine may act upstream of Bcl-x_L.

Because our previous findings suggested that sphingosine may function proximal to executioner caspases in Jurkat T lymphoma cells,¹⁹ we next investigated whether doxorubicin and sphingosine activated executioner caspases in MCF7/Fas cells. Based on their substrate specificities, caspase-3, -2, and -7, believed to be the final executioner caspases, belong to the group II subfamily that preferentially cleave the peptide sequence DExD found in numerous death substrates.³⁶ Proteolytic activation of these caspases was examined by Western blotting analysis. Only caspase-7 was activated by both doxorubicin (Figure 5A) and sphingosine (Figure 5C) in MCF7/Fas cells. Surprisingly, although caspase-2 is clearly expressed in MCF7/Fas cells, it was not cleaved after treatment with doxorubicin (Figure 5B) or sphingosine (Figure 5D). Similarly, extracts from MCF7/Fas cells treated with Fas mAb, a strong inducer of apoptosis in this cell line,^{37–40} did not activate caspase-2 (Figure 5F), whereas caspase-7 was processed to the active fragment (Figure 5E). As the MCF7 cell line is devoid of caspase-3 owing to the functional deletion of the *CASP-3* gene,⁴¹ caspase-7 appears to be the only executioner caspase activated in these cells. Despite activation of caspase-7, Ac-DEVD-

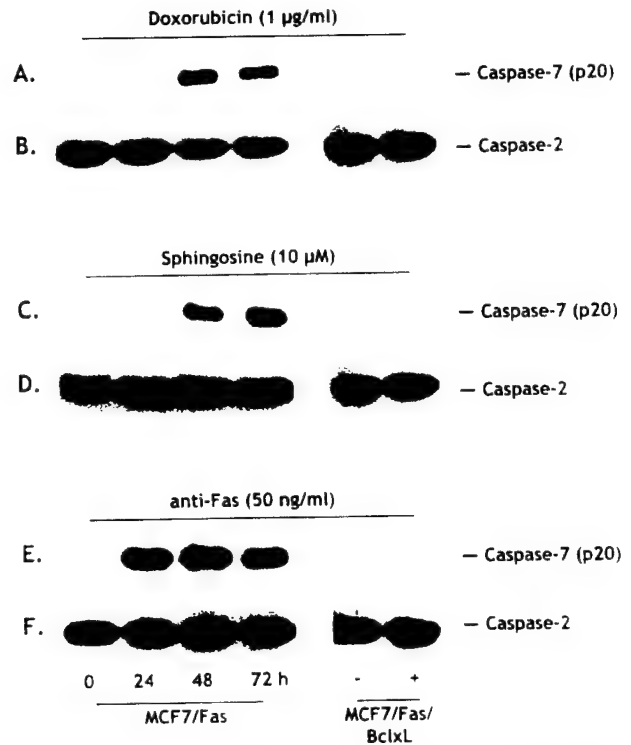


Figure 5 Activation of caspase-7 and caspase-2 in response to doxorubicin, sphingosine, and anti-Fas mAb. MCF7/Fas and MCF7/Fas/Bcl-x_L cells were incubated in serum-free conditions without (–) or with (+) 1 µg/ml doxorubicin (A, B), 10 µM sphingosine (C, D), or 50 ng/ml anti-Fas mAb (E, F) and extracts prepared at the indicated times or 72 h for MCF7/Fas/Bcl-x_L cells. Proteins were resolved by 15% SDS-PAGE, blotted, and probed with anti-caspase-7 antibody (A, C, E), or with anti-caspase-2 antibody (B, D, F). Migrations indicated: active subunit p20 of caspase-7; full-length caspase-2.

AMC-cleaving activity was not detectably increased after treatment of MCF7/Fas cells with sphingosine or doxorubicin (data not shown), likely a result of the deficiency of caspase-3 activity.

Having established that doxorubicin- and sphingosine-induced cell death was prevented by Bcl-x_L overexpression, we also examined caspase activation in MCF7/Fas/Bcl-x_L cells. As shown in Figure 5A, C, E, activation of caspase-7 in these cells was markedly inhibited by overexpression of Bcl-x_L.

After initiation of the apoptotic program, release of cytochrome *c* from mitochondria plays an important role in activation of downstream caspases. Cytochrome *c* binds to Apaf-1, a mammalian homologue of the *Caenorhabditis elegans* death-promoting CED-4 protein, inducing it to associate with caspase-9, thereby triggering its autoactivation into a mature form, which in turn can then directly cleave caspase-3 or -7 (reviewed in^{42–44}). Because expression of Bcl-x_L has been shown to interfere with cytochrome *c* release,⁴⁴ we next determined whether doxorubicin and sphingosine could also trigger mitochondrial cytochrome *c* release. As shown in Figure 6A, treatment with doxorubicin resulted in a significant increase in cytosolic cytochrome *c* levels by 24 h. This is

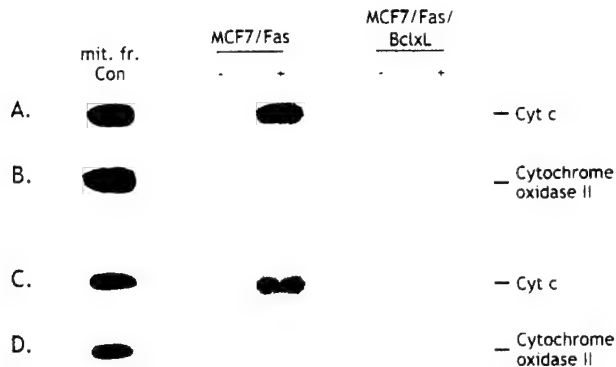


Figure 6 Cytosolic accumulation of cytochrome *c* induced by doxorubicin or sphingosine is inhibited by Bcl-x_L overexpression. MCF7/Fas and MCF7/Fas/Bcl-x_L cells treated without (–) or with (+) 1 µg/ml doxorubicin (A, B) or 10 µM sphingosine (C, D) were harvested after 48 h, and cytosolic and mitochondrial proteins were separated by 15% SDS-PAGE and analyzed by immunoblotting with anti-cytochrome *c* (A, C) or anti-cytochrome oxidase (subunit II; B, D). Cytochrome oxidase serves as a marker for mitochondrial contamination of cytosolic extracts. A mitochondrial extract from nontreated cells (mit. Fr. Con) was used as a positive control for cytochrome *c* and cytochrome oxidase (subunit II).

in agreement with a previous study establishing cytochrome *c* release upon doxorubicin treatment in neuroblastoma cells.³² Similarly, treatment with exogenous sphingosine also caused accumulation of cytochrome *c* in the cytosol (Figure 6C). Cytochrome *c* release induced by doxorubicin or sphingosine was prevented by Bcl-x_L overexpression (Figure 6A,C). The absence of detectable cytochrome oxidase in cytosolic extracts confirmed that our preparations were free of mitochondrial contamination (Figure 6B, D).

As doxorubicin and sphingosine were capable of inducing caspase-7 activation as well as cytochrome *c* translocation to the cytosol, it was important to determine whether cytochrome *c* mediated activation of caspase-7 in caspase-3 null MCF7 cells. When cytochrome *c* was added *in vitro* to cell-free MCF7/L/neo extracts in the presence of 1 mM dATP, cleavage of caspase-7 increased with time of incubation (data not shown) and cytochrome *c* concentration (Figure 7D). However, as recently reported,⁴⁵ DEVDase activity was only slightly increased under these conditions (Figure 7A), presumably owing to the absence of caspase-3 in these cells (Figure 7C). Interestingly, but in line with our results showing that caspase-2 was not processed in apoptotic MCF7/Fas cells (Figure 5B,D,F), no activation of caspase-2 was detected in this *in vitro* system (Figure 7E). These results demonstrate that cytochrome *c*-dependent caspase-7 activation can take place in caspase-3 deficient MCF7 cell lines. In a comparative *in vitro* study performed with MCF7/L cells stably expressing caspase-3 (denoted MCF7/L/casp-3), processing of caspase-3 (Figure 7C) was accompanied by increased cleavage of caspase-7 (Figure 7D). Furthermore, increased processing of caspase-2 (Figure 7E) demonstrates that caspase-3 activation is required for proteolysis of caspase-2. Likewise, MCF7/L/casp-3 extracts have several fold higher DEVDase activity

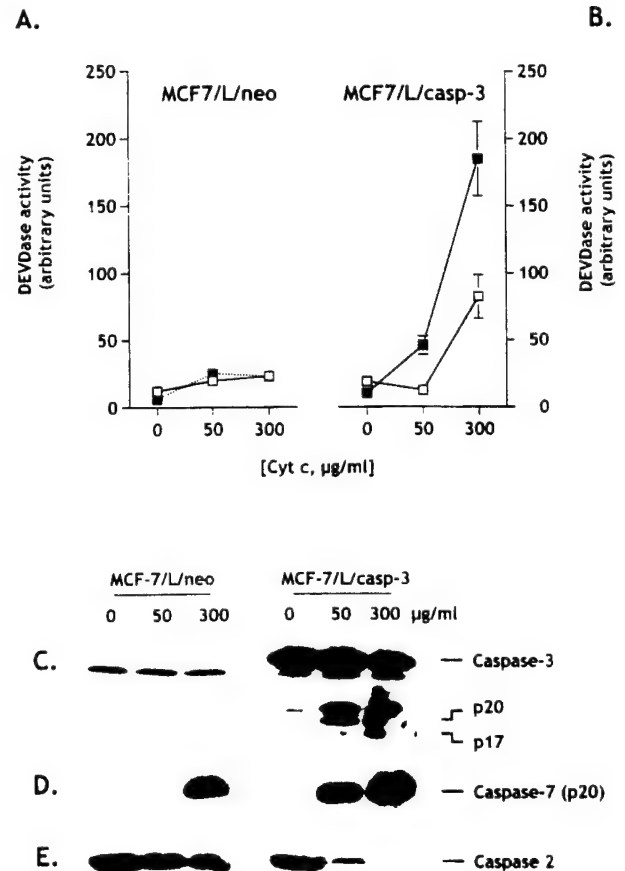


Figure 7 Cytochrome *c*-initiated activation of caspases in a cell-free system from MCF7/L/neo and MCF7/L/casp3 cells. (A) DEVDase activity was measured with the fluorogenic substrate Ac-DEVD-AMC in cytosolic extracts from MCF7/L/neo cells treated without or with the indicated concentrations of horse heart cytochrome *c* for 30 min (open squares) or 90 min (filled squares) at 37 °C. Results are means ± S.D. of at least three independent experiments performed in triplicate. (B) DEVDase activity was measured in cytosolic extracts from MCF7/L/casp3 cells treated without or with the indicated concentrations of horse heart cytochrome *c* for 30 min (open squares) or 90 min (filled squares) at 37 °C. Results are means ± S.D. of at least three independent experiments. Cytosolic extracts from MCF7/L/neo cells treated without or with the indicated concentrations of horse heart cytochrome *c* for 90 min at 37 °C were separated by SDS-PAGE and analyzed by immunoblotting with anti-caspase-3 (C), anti-caspase-7 (D), or anti-caspase-2 (E). Migrations indicated: full-length caspase-3; cleavage intermediate p20; active subunit p17; active subunit p20 of caspase-7; full-length caspase-2.

than MCF7/L/neo extracts, probably as a result of the combined activity of caspase-3 and caspase-7. In contrast to cytosolic extracts prepared from MCF7 cells and in agreement with previous results, complete processing of caspase-9,^{46,47} caspase-7,^{46,47} and -2⁴⁶ was readily observed in cytosolic extracts prepared from Jurkat cells incubated with a concentration of cytochrome *c* as low as 10 µg/ml within 30 min (Figure 8A–D). Moreover, cytochrome *c*-triggered caspase activation resulted in rapid cleavage of PARP (Figure 8E), confirming that this *in vitro* system recapitulates the apoptotic cascade from initiation of executioner caspases activation to cleavage of death

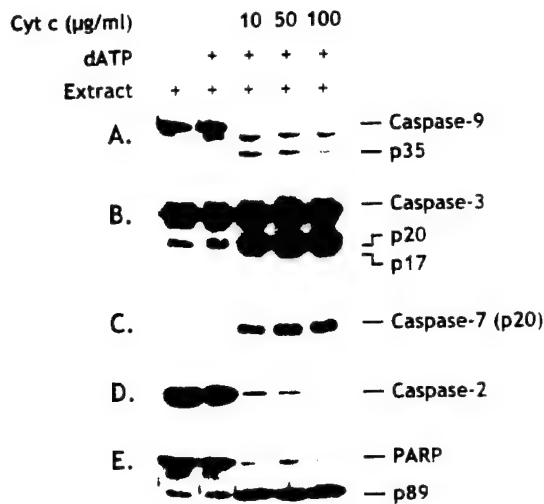


Figure 8 Cytochrome c-initiated activation of casp-9, -3, -7, and -2, and cleavage of PARP in Jurkat cell extracts. Cytosolic extracts from Jurkat T cells treated without or with the indicated concentrations of horse heart cytochrome c for 30 min at 37°C were separated by SDS-PAGE and analyzed by immunoblotting with anti-caspase-9 (A), anti-caspase-3 (B), anti-caspase-7 (C), anti-caspase-2 (D), anti-PARP (E). Migrations indicated: full-length caspase-9, cleavage intermediate p35; full-length caspase-3, cleavage intermediate p20, active subunit p17; active subunit p20 of caspase-7; full-length caspase-2, full-length PARP, active form p89.

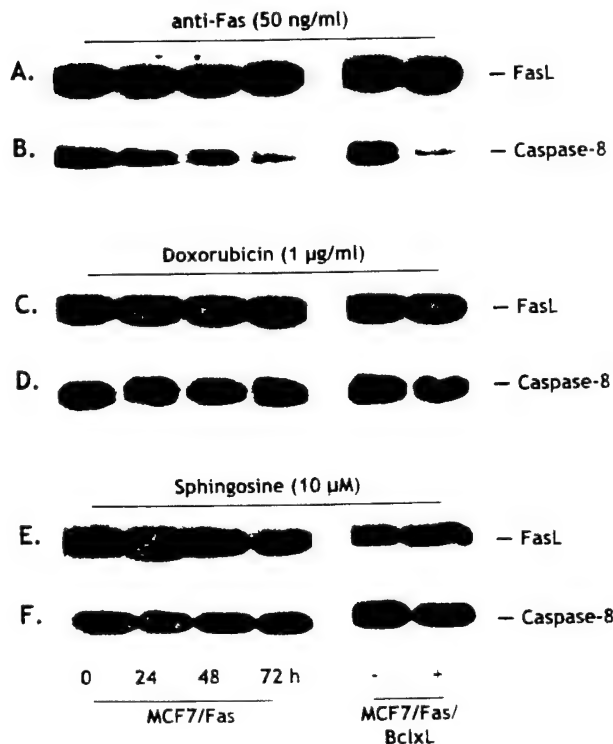


Figure 9 Caspase-8 activation and FasL expression in response to doxorubicin, sphingosine, or anti-Fas mAb. MCF7/Fas and MCF7/Fas/Bcl-x_L cells were incubated in serum-free conditions without (-) or with (+) 50 ng/ml anti-Fas mAb (A, B), 1 µg/ml doxorubicin (C, D), or 10 µM sphingosine (E, F) and extracts prepared at the indicated times or 72 h for MCF7/Fas/Bcl-x_L cells. Proteins were resolved by 15% SDS-PAGE, blotted, and probed with anti-FasL antibody (A, C, E), or with anti-caspase-8 (B, D, F). Migrations indicated: full-length caspase-8; FasL.

substrates. Taken together, these assays demonstrate that caspase-7 does not require the presence of caspase-3 to be activated in MCF7 cells, although overexpression of caspase-3 does enhance its processing.

The Fas receptor/ligand system has been proposed to play a role in doxorubicin-mediated apoptosis.⁴⁸⁻⁵⁰ Levels of FasL protein were examined by Western blotting to determine whether its expression was increased by doxorubicin or sphingosine treatment. There were no detectable changes in FasL protein expression discernible after doxorubicin (Figure 9C) or sphingosine treatment (Figure 9E). To further examine the possible requirement for Fas signaling in cell death induced by doxorubicin in MCF7/Fas cells, we determined whether caspase-8 could be activated. Caspase-8 cleavage often represents the first detectable event in Fas death receptor-mediated apoptosis.⁵¹ Notwithstanding, in type II cells, such as Jurkat T cells, caspase-8 can be activated in a post-mitochondrial manner, and sphingosine treatment can lead to caspase-8 processing in this cell type.¹⁹ As shown in Figure 7B, caspase-8 was only activated in anti-Fas mAb-treated, but not in doxorubicin- (Figure 9D) or sphingosine-treated (Figure 9F) MCF7/Fas cells. In agreement with previous studies,^{37,40,52} Bcl-x_L, which strongly inhibits apoptosis, had no effect on the processing of caspase-8 induced by Fas ligation (Figure 9B). Together, these findings negate a role for the Fas ligand/receptor signaling in doxorubicin-induced cell death in MCF7 carcinoma cells.

Discussion

Accumulating evidence indicates that chemotherapeutic agents such as anthracyclines kill neoplastic cells by the induction of apoptosis. Although the pathways involved in cell death induced by these agents are not fully understood, abundant reports have suggested that the sphingolipid ceramide play an important role in apoptosis initiated by anthracyclines.³⁻¹¹

Accumulation of glucosylceramides, simple glycosylated forms of ceramide, is a feature of some multidrug-resistant cancer cells and tumors from patients who are less responsive to chemotherapy, demonstrating a correlation between cellular drug resistance and alterations in ceramide metabolism.⁵³ Reduction of ceramide levels by transfection with glucosylceramide synthase, the enzyme that converts ceramide to glucosylceramide, confers doxorubicin resistance in MCF7 cells.⁵⁴ Conversely, transfection of antisense glucosylceramide synthase to limit cellular ceramide glycosylation, overcomes doxorubicin resistance.⁵⁵ Hence, tumor cells may have reduced sensitivity to chemotherapy because of an inability to produce sufficient apoptotic signal via sphingomyelin hydrolysis to ceramide.⁵⁶ Indeed, sphingomyelin co-administration potentiates chemotherapy of human cancer xenografts.⁵⁷

In contrast to doxorubicin, which induces apoptosis only in human epidermoid carcinoma KB-3-1 cells and not in a multidrug-resistant subclone that expresses P-glycoprotein, the ceramide breakdown product, sphingosine, induces apoptosis in both cell types.¹⁴ Furthermore, neither the

protein kinase C (PKC) inhibitor H7 nor staurosporine induced apoptosis in these cell lines, suggesting that PKC-independent signaling is involved in apoptosis induced by sphingosine.¹⁴ An analog of sphingosine, L-threo-dihydrosphingosine (known as safingol), enhanced doxorubicin accumulation and sensitivity of MCF7 drug resistant cells. However, this effect correlated with inhibition of PKC rather than interference with P-glycoprotein drug binding.⁵⁸ Because sphingosine and its analogs induce apoptosis regardless of P-glycoprotein expression, they may provide a new strategy for the treatment of anticancer drug-resistant cancers. Indeed, in pilot clinical phase I trials with safingol, which potentiates the effect of doxorubicin in tumor-bearing animals, it was found that safingol can be given safely with doxorubicin at a dose that is potentially pharmacologically active without dose-limiting toxicity.⁵⁹

The results presented here demonstrate that transient generation of endogenous sphingosine also occurs in MCF7 breast cancer cells during apoptosis induced by the anthracycline doxorubicin, preceding release of cytochrome *c* from the mitochondria and activation of the executioner caspase-7. Similar to doxorubicin, exogenous sphingosine induced apoptosis in a caspase-7-dependent manner. Consistent with other studies,^{31–35} overexpression of Bcl-x_L protected MCF7 cells from doxorubicin-induced apoptosis and rendered them resistant to sphingosine-induced apoptosis, even though Bcl-x_L overexpression did not inhibit sphingosine generation after doxorubicin treatment. Despite the lack of caspase-3, MCF7 cells underwent apoptosis suggesting that other executioner caspases, such as caspase-7 or -2 may be activated. In this study, we established that caspase-7 is indeed activated during apoptosis of MCF7 cells. Furthermore, even in a cell-free caspase activation assay, caspase-2, which shares the same substrate specificity, was not detectably activated, in agreement with previous studies showing that caspase-2 was not processed in MCF7 cells following TNF α or staurosporine treatment.⁶⁰ However, introduction of CASP-3 cDNA into MCF7 cells restored caspase-2 cleavage. To date, caspase-3-dependent caspase-2 activation has only been reported in Jurkat T cell extracts immunodepleted of caspase-3.⁴⁶ Thus our results support the notion that activation of caspase-2 but not -7 depend on the presence of caspase-3.

Our observations establish that cytochrome *c*-inducible caspase-7 activation takes place in caspase-3 null MCF7 cells during apoptosis and raises the possibility that caspase-7 may be able to compensate for the lack of caspase-3, as overexpression of caspase-3 in MCF7 cells did not greatly enhance their apoptotic susceptibility (data not shown). Our results also demonstrate that activation of Fas/FasL signaling is not involved in apoptosis triggered by doxorubicin in MCF7 breast carcinoma cells. In addition, caspase-8, the first caspase to be processed in death receptor-mediated apoptosis,⁵¹ was only proteolyzed when cells were treated with anti-Fas mAb, whereas caspase-8 was not activated during doxorubicin-induced apoptosis.

Interestingly, we have found that the involvement of sphingolipid metabolites in cell death machinery triggered by doxorubicin may be more complex than previously

thought. Accumulation of ceramide in anthracycline-mediated cell death has been shown to be due to activation of sphingomyelinase³ or ceramide synthase.⁴ In agreement, our results suggest that doxorubicin might in fact activate both pathways to mediate cell death, *de novo* sphingolipid synthesis⁴ and a sphingolipid degradation pathway mediated by a sphingomyelinase³ and a ceramidase. Unexpectedly, we found that cell death induced by exogenous sphingosine was inhibited by ceramide synthase or ceramidase inhibitors. These findings support the notion that exogenously added sphingosine can first be converted to ceramide, which can then be hydrolyzed to sphingosine by the action of a ceramidase, presumably in another compartment.

In sum, our results suggest that sphingosine, the metabolite of ceramide, is also involved in the doxorubicin-mediated, Bcl-x_L inhibitable pathway of apoptosis in human breast cancer cells.

Materials and Methods

Cell culture and reagents

The MCF7/L cell variant was obtained from the Cell Culture Core Resource (Lombardi Cancer Center, Washington, DC, USA), and was maintained in RPMI 1640 containing 10% fetal bovine serum, 1% L-glutamine and 1% penicillin/streptomycin. MCF7 cells stably transfected to express the Fas antigen (denoted MCF7/Fas) or both Fas and Bcl-x_L (denoted MCF7/Fas/Bcl-x_L) were a kind gift of Dr. Vishva Dixit (Genentech Inc., San Francisco, CA, USA), and were grown in the same media supplemented with 200 μ g/ml G418 and 150 μ g/ml hygromycin. The MCF7/L/neo and MCF7/L/casp-3 cell lines were obtained by transfecting MCF7/L cells with either empty pcDNA3 or pcDNA3 engineered to express caspase-3, respectively (the CASP-3 expression vector was a kind gift of Dr. Donald Nicholson, Merck-Frosst Centre for Therapeutic Research, Pointe Claire-Dorval, Quebec). These cells were propagated in the same media containing 1 mg/ml G418.

Cells were subcultured twice weekly and 48 h prior to the initiation of an experiment. For induction of apoptosis, cells at ≤ 60 –75% confluence were treated in serum-free media with either doxorubicin (Sigma), anti-Fas antibody (Upstate Biotechnology, Lake Placid, NY, USA) or sphingosine (Biomol, Plymouth Meeting, PA, USA). Jurkat T cells were cultured in RPMI 1640 containing 10% FBS.

Ac-DEVD-AMC was from Bachem (King of Prussia, PA, USA), 3-(4,5-Dimethylthiazol-2-yl)-2,5-diphenyltetrazolium bromide (MTT), horse heart cytochrome *c* and phosphocreatine were from Sigma. ATP, dATP and rabbit muscle creatine kinase were from Roche Diagnostics. [γ -³²P]ATP (3000 Ci/mmol) was from NEN Life Science. FB1 and dMAPP were from Biomol (Plymouth Meeting, PA, USA). Other reagents and solvents were analytical grade.

Mass measurement of sphingosine

Sphingosine was measured after phosphorylation to sphingosine-1-phosphate, using recombinant sphingosine kinase as described by Olivera *et al.*⁶¹ For each experiment, known amounts of sphingosine were used to generate a standard curve. Total phospholipids mass in the lipid extracts was quantified as previously described⁶² using a colorimetric phosphate assay.⁶³

Cell death assay

The tetrazolium based MTT assay was used to determine cell death as previously described.⁶⁴ Briefly, approximately 5000 cells per well were plated in 96-well tissue culture plates as described above, and 24 h later, the medium was replaced with 100 μ l serum-free medium containing the indicated amounts of doxorubicin, anti-Fas antibody, or sphingosine. After various times of incubation at 37 °C, 25 μ l of MTT solution (5 mg/ml) was added and the plates were incubated for approximately 4 h. After solubilization for 16 h with 100 μ l of lysis buffer (20% SDS in 50% *N,N*-dimethylformamide), formazan was quantified with a microplate reader at a wavelength of 570 nm.

Preparation of mitochondria and Western blot analysis of cytochrome c

Mitochondrial preparations were carried out as previously described.⁶⁵ In brief, cells were collected by centrifugation at 600 \times *g* for 5 min at 4 °C. After washing once with ice-cold PBS, mitochondrial and cytosolic fractions were prepared by resuspending cell pellets in 5 vol of ice-cold buffer A (20 mM HEPES-KOH pH 7.5, 0.1% BSA, 1 mM sodium EDTA, 1 mM DTT, 0.1 mM PMSF, 20 μ g/ml leupeptin, 10 μ g/ml aprotinin and 10 μ g/ml pepstatin A) containing 250 mM sucrose. After swelling on ice for 15 min, cells were homogenized with 15 to 20 strokes of a number 22 Kontes Dounce homogenizer with a B pestle (Kontes Glass Company, Vineland, NJ, USA), and the homogenates centrifuged at 750 \times *g* for 5 min at 4 °C. Supernatants were then centrifuged at 10 000 \times *g* for 15 min at 4 °C, and the resulting mitochondria pellets resuspended in cold buffer A. For Western blot analysis, equal amounts of mitochondrial and cytosolic proteins were separated on 15% SDS-PAGE and then transblotted to nitrocellulose. Anti-cytochrome c mAb (PharMingen) and anti-cytochrome oxidase subunit II mAb (Molecular Probes, Eugene, OR, USA) were used as primary antibodies.

Western blot analysis

Cell lysate preparation and Western blotting were carried out as previously described.^{65,66} Rabbit anti-caspase-3 (gift of Dr. Donald Nicholson, Merck-Frosst Centre for Therapeutic Research, Pointe Claire-Dorval, Québec), mouse anti-caspase-8 (PharMingen, San Diego, CA, USA), rabbit anti-caspase-7, rabbit anti-caspase-2 (Santa Cruz Biotechnology), rabbit anti-caspase-9 (Research Diagnostic, Flanders, NJ, USA or Oncogene Research), anti-PARP (PharMingen), and anti-FasL (Transduction Laboratories, Lexington, KY, USA) were used as primary antibodies. Proteins were visualized by ECL using anti-rabbit or anti-mouse HRP-conjugated IgG (Bio-Rad).

Fluorogenic DEVD cleavage enzyme assays

Enzyme reactions were performed in 96-well plates with 20 μ g of cytosolic proteins and a final concentration of 20 μ M Ac-DEVD-AMC substrate as previously described.^{65,66}

In vitro assay for cytochrome c-dependent activation of caspases

Cytosolic fractions (40 μ l, 400 μ g proteins), prepared as described above, were incubated at 37 °C for various times in 96-well plates in a final volume of 200 μ l in buffer B (10 mM HEPES pH 7.4, 2 mM MgCl₂, 5 mM sodium EGTA, 5 mM DTT, 1 mM ATP, 1 mM PMSF, 10 μ g/ml leupeptin, 10 μ g/ml aprotinin, 10 μ g/ml pepstatin A, 10 mM phospho-

creatine, 150 μ g/ml creatine kinase) supplemented without or with 1 mM dATP and horse heart cytochrome c. Proteins were then separated by SDS-PAGE, blotted, and probed with anti-caspase and anti-PARP antibodies.

Acknowledgements

This work was supported by a grant from the National Institutes of Health (CA61774) to S Spiegel. Financial support from Inserm (to O Cuvillier and T Levade) and the Association pour la Recherche sur le Cancer (to O Cuvillier) is gratefully acknowledged.

References

- Gewirtz DA (1999) A critical evaluation of the mechanisms of action proposed for the antitumor effects of the anthracycline antibiotics adriamycin and daunorubicin. *Biochem. Pharmacol.* 57: 727–741
- Hannun YA and Luberto C (2000) Ceramide in the eukaryotic stress response. *Trends Cell Biol.* 10: 73–80
- Jaffrézou J, Levade T, Battaieb A, Andrieu N, Bezombes C, Maestre N, Vermeersch S, Rousse A and Laurent G (1996) Daunorubicin-induced apoptosis: triggering of ceramide generation through sphingomyelin hydrolysis. *EMBO J.* 15: 2417–2424
- Bose R, Verheij M, Haimovitz-Friedman A, Scotto K, Fuks Z and Kolesnick R (1995) Ceramide synthase mediates daunorubicin-induced apoptosis: an alternative mechanism for generating death signals. *Cell* 82: 405–414
- Allouche M, Battaieb A, Vindis C, Rousse A, Grignon C and Laurent G (1997) Influence of Bcl-2 overexpression on the ceramide pathway in daunorubicin-induced apoptosis of leukemic cells. *Oncogene* 14: 1837–1845
- Mansat V, Laurent G, Levade T, Battaieb A and Jaffrézou JP (1997) The protein kinase C activators phorbol esters and phosphatidylserine inhibit neutral sphingomyelinase activation, ceramide generation, and apoptosis triggered by daunorubicin. *Cancer Res.* 57: 5300–5304
- Mansat V, Battaieb A, Levade T, Laurent G and Jaffrézou JP (1997) Serine protease inhibitors block neutral sphingomyelinase activation, ceramide generation, and apoptosis triggered by daunorubicin. *FASEB J.* 11: 695–702
- Come MG, Battaieb A, Skladanowski A, Larsen AK and Laurent G (1999) Alteration of the daunorubicin-triggered sphingomyelin-ceramide pathway and apoptosis in MDR cells: influence of drug transport abnormalities. *Int. J. Cancer* 81: 580–587
- Battaieb A, Plo I, Mas VMD, Quillet-Mary A, Levade T, Laurent G and Jaffrézou JP (1999) Daunorubicin- and mitoxantrone-triggered phosphatidylcholine hydrolysis: implication in drug-induced ceramide generation and apoptosis. *Mol. Pharmacol.* 55: 118–125
- Andrieu-Abadie N, Jaffrézou JP, Hatem S, Laurent G, Levade T and Mercadier JJ (1999) L-carnitine prevents doxorubicin-induced apoptosis of cardiac myocytes: role of inhibition of ceramide generation. *FASEB J.* 13: 1501–1510
- Delpy E, Hatem SN, Andrieu N, de Vaumas C, Henaff M, Rucker-Martin C, Jaffrézou JP, Laurent G, Levade T and Mercadier JJ (1999) Doxorubicin induces slow ceramide accumulation and late apoptosis in cultured adult rat ventricular myocytes. *Cardiovasc. Res.* 43: 398–407
- Ohta H, Yatomi Y, Sweeney EA, Hakomori S and Igarashi Y (1994) A possible role of sphingosine in induction of apoptosis by tumor necrosis factor- α in human neutrophils. *FEBS Lett.* 355: 267–270
- Krown KA, Page MT, Nguyen C, Zechner D, Gutierrez V, Comstock KL, Gliembski CC, Quintana PJ and Sabbadini RA (1996) Tumor necrosis factor- α -induced apoptosis in cardiac myocytes. Involvement of the sphingolipid signaling cascade in cardiac cell death. *J. Clin. Invest.* 98: 2854–2865
- Shirahama T, Sweeney EA, Sakakura C, Singhal AK, Nishiyama K, Akiyama S, Hakomori S and Igarashi Y (1997) In vitro and in vivo induction of apoptosis by sphingosine and N,N-dimethylsphingosine in human epidermoid carcinoma KB-3-1 and its multidrug-resistant cells. *Clin. Cancer Res.* 3: 257–264
- Sweeney EA, Sakakura C, Shirahama T, Masamune A, Ohta H, Hakomori S and Igarashi Y (1996) Sphingosine and its methylated derivative N,N-dimethylsphingosine (DMS) induce apoptosis in a variety of human cancer cell lines. *Int. J. Cancer* 66: 358–366

16. Sweeney EA, Inokuchi J and Igarashi Y (1998) Inhibition of sphingolipid induced apoptosis by caspase inhibitors indicates that sphingosine acts in an earlier part of the apoptotic pathway than ceramide. *FEBS Lett.* 425: 61–65
17. Hung WC, Chang HC and Chuang LY (1999) Activation of caspase-3-like proteases in apoptosis induced by sphingosine and other long-chain bases in Hep3B hepatoma cells. *Biochem. J.* 338: 161–166
18. Jarvis WD, Fornari FA, Taylor RS, Martin HA, Kramer LB, Erukulla RK, Bittman R and Grant S (1996) Induction of apoptosis and potentiation of ceramide-mediated cytotoxicity by sphingoid bases in human myeloid leukemia cells. *J. Biol. Chem.* 271: 8275–8284
19. Cuvillier O, Edsall L and Spiegel S (2000) Involvement of sphingosine in mitochondria-dependent Fas-induced apoptosis of type II Jurkat T cells. *J. Biol. Chem.* 275: 15691–15700
20. Ravid A, Rucker D, Machlenkin A, Rotem C, Hochman A, Kessler-Ickson G, Liberman UA and Koren R (1999) 1,25-Dihydroxyvitamin D₃ enhances the susceptibility of breast cancer cells to doxorubicin-induced oxidative damage. *Cancer Res.* 59: 862–867
21. Smith ER, Jones PL, Boss JM and Merrill Jr AH (1997) Changing J774A.1 cells to new medium perturbs multiple signaling pathways, including the modulation of protein kinase C by endogenous sphingoid bases. *J. Biol. Chem.* 272: 5640–5646
22. Smith ER and Merrill Jr AH (1995) Differential roles of de novo sphingolipid biosynthesis and turnover in the 'burst' of free sphingosine and sphinganine, and their 1-phosphates and N-acyl-derivatives, that occurs upon changing the medium of cells in culture. *J. Biol. Chem.* 270: 18749–18758
23. Ohta H, Sweeney EA, Masamune A, Yatomi Y, Hakomori S and Igarashi Y (1995) Induction of apoptosis by sphingosine in human leukemic HL-60 cells: a possible endogenous modulator of apoptotic DNA fragmentation occurring during phorbol ester-induced differentiation. *Cancer Res.* 55: 691–697
24. Shirahama T, Sakakura C, Sweeney EA, Ozawa M, Takemoto M, Nishiyama K, Ohi Y and Igarashi Y (1997) Sphingosine induces apoptosis in androgen-independent human prostatic carcinoma DU-145 cells by suppression of bcl-X(L) gene expression. *FEBS Lett.* 407: 97–100
25. Merrill Jr AH, van Echten G, Wang E and Sandhoff K (1993) Fumonisin B1 inhibits sphingosine (sphinganine) N-acyltransferase and de novo sphingolipid biosynthesis in cultured neurons in situ. *J. Biol. Chem.* 268: 27299–27306
26. Bielawska A, Greenberg MS, Perry D, Jayadev S, Shayman JA, McKay C and Hannun YA (1996) (1S,2R)-D-erythro-2-(N-myristoylamino)-1-phenyl-1-propanol as an inhibitor of ceramidase. *J. Biol. Chem.* 271: 12646–12654
27. Zhang J, Alter N, Reed JC, Borner C, Obeid LM and Hannun YA (1996) Bcl-2 interrupts the ceramide-mediated pathway of cell death. *Proc. Natl. Acad. Sci. USA* 93: 5325–5328
28. Geley S, Hartmann BL and Kofler R (1997) Ceramides induce a form of apoptosis in human acute lymphoblastic leukemia cells that is inhibited by Bcl-2, but not by CrmA. *FEBS Lett.* 400: 15–18
29. Smyth MJ, Perry DK, Zhang J, Poirier GG, Hannun YA and Obeid LM (1996) pRCE: a downstream target for ceramide-induced apoptosis and for the inhibitory action of Bcl-2. *Biochem. J.* 316: 25–28
30. Dbaibo GS, Perry DK, Gamard CJ, Platt R, Poirier GG, Obeid LM and Hannun YA (1997) Cytokine response modifier A (CrmA) inhibits ceramide formation in response to tumor necrosis factor (TNF)- α : CrmA and Bcl-2 target distinct components in the apoptotic pathway. *J. Exp. Med.* 185: 481–490
31. Ohmori T, Podack ER, Nishio K, Takahashi M, Miyahara Y, Takeda Y, Kubota N, Funayama Y, Ogasawara H, Ohira T et al. (1993) Apoptosis of lung cancer cells caused by some anti-cancer agents (MMC, CPT-11, ADM) is inhibited by bcl-2. *Biochem. Biophys. Res. Commun.* 192: 30–36
32. Fulda S, Susin SA, Kroemer G and Debatin KM (1998) Molecular ordering of apoptosis induced by anticancer drugs in neuroblastoma cells. *Cancer Res.* 58: 4453–4460
33. Ruvolo PP, Deng X, Carr BK and May WS (1998) A functional role for mitochondrial protein kinase Calpha in Bcl2 phosphorylation and suppression of apoptosis. *J. Biol. Chem.* 273: 25436–25442
34. Naumovski L, Martinovsky G, Wong C, Chang M, Ravendranath Y, Weinstein H and Dahl G (1998) BCL-2 expression does not correlate with patient outcome in pediatric acute myelogenous leukemia. *Leuk. Res.* 22: 81–87
35. Katoh O, Takahashi T, Oguri T, Kuramoto K, Mihara K, Kobayashi M, Hirata S and Watanabe H (1998) Vascular endothelial growth factor inhibits apoptotic death in hematopoietic cells after exposure to chemotherapeutic drugs by inducing MCL1 acting as an antiapoptotic factor. *Cancer Res.* 58: 5565–5569
36. Nicholson DW (1999) Caspase structure, proteolytic substrates, and function during apoptotic cell death. *Cell Death Differ.* 6: 1028–1042
37. Srinivasan A, Li F, Wong A, Kodandapani L, Smidt Jr R, Krebs JF, Fritz LC, Wu JC and Tomaselli KJ (1998) Bcl-x_L functions downstream of caspase-8 to inhibit Fas- and Tumor Necrosis Factor Receptor 1-induced apoptosis of MCF7 breast carcinoma cells. *J. Biol. Chem.* 273: 4523–4529
38. Jäättelä M, Benedict M, Tewari M, Shayman JA and Dixit VM (1995) Bcl-x and Bcl-2 inhibit TNF and Fas-induced apoptosis and activation of phospholipase A2 in breast carcinoma cells. *Oncogene* 10: 2297–2305
39. Li F, Srinivasan A, Wang Y, Armstrong RC, Tomaselli KJ and Fritz LC (1997) Cell-specific induction of apoptosis by microinjection of cytochrome c. *J. Biol. Chem.* 272: 30299–30305
40. Medema JP, Scaffidi C, Krammer PH and Peter ME (1998) Bcl-x_L acts downstream of caspase-8 activation by the CD95 death-inducing signaling complex. *J. Biol. Chem.* 273: 3388–3393
41. Janicke RU, Sprengart ML, Wati MR and Porter AG (1998) Caspase-3 is required for DNA fragmentation and morphological changes associated with apoptosis. *J. Biol. Chem.* 273: 9357–9360
42. Cecconi F (1999) Apaf1 and the apoptotic machinery. *Cell Death Differ.* 6: 1087–1098
43. Slee EA, Adrain C and Martin SJ (1999) Serial killers: ordering caspase activation events in apoptosis. *Cell Death Differ.* 6: 1067–1074
44. Budihardjo I, Oliver H, Lutter M, Luo X and Wang X (1999) Biochemical pathways of caspase activation during apoptosis. *Annu. Rev. Cell Dev. Biol.* 15: 269–290
45. Wolf BB, Schuler M, Echeverri F and Green DR (1999) Caspase-3 is the primary activator of apoptotic DNA fragmentation via DNA fragmentation factor-45/ inhibitor of caspase-activated DNase inactivation. *J. Biol. Chem.* 274: 30651–30656
46. Slee EA, Harte MT, Kluck RM, Wolf BB, Casiano CA, Newmeyer DD, Wang HG, Reed JC, Nicholson DW, Alnemr ES, Green DR and Martin SJ (1999) Ordering the cytochrome c-initiated caspase cascade: hierarchical activation of caspases-2, -3, -6, -7, -8, and -10 in a caspase-9-dependent manner. *J. Cell. Biol.* 144: 281–292
47. Hampton MB, Zhivotovsky B, Slater AF, Burgess DH and Orrenius S (1998) Importance of the redox state of cytochrome c during caspase activation in cytosolic extracts. *Biochem. J.* 329: 95–99
48. Herr I, Wilhelm D, Bohler T, Angel P and Debatin K (1997) Activation of CD95 (APO-1/Fas) signaling by ceramide mediates cancer therapy-induced apoptosis. *EMBO J.* 16: 6200–6208
49. Friesen C, Fulda S and Debatin KM (1997) Deficient activation of the CD95 (APO-1/Fas) system in drug-resistant cells. *Leukemia* 11: 1833–1841
50. Fulda S, Scaffidi C, Prietsch T, Krammer PH, Peter ME and Debatin K-M (1998) Activation of the CD-95 (APO-1/Fas) pathway in drug- and γ -irradiation-induced apoptosis of brain tumor cells. *Cell Death Differ.* 5: 884–893
51. Peter ME and Krammer PH (1998) Mechanisms of CD95 (APO-1/Fas)-mediated apoptosis. *Curr. Opin. Immunol.* 10: 545–551
52. Li H, Zhu H, Xu CJ and Yuan J (1998) Cleavage of BID by caspase 8 mediates the mitochondrial damage in the Fas pathway of apoptosis. *Cell* 94: 491–501
53. Lavie Y, Cao H, Bursten SL, Giuliano AE and Cabot MC (1996) Accumulation of glucosylceramides in multidrug-resistant cancer cells. *J. Biol. Chem.* 271: 19530–19536
54. Liu YY, Han TY, Giuliano AE and Cabot MC (1999) Expression of glucosylceramide synthase, converting ceramide to glucosylceramide, confers adriamycin resistance in human breast cancer cells. *J. Biol. Chem.* 274: 1140–1146
55. Liu YY, Han TY, Giuliano AE, Hansen N and Cabot MC (2000) Uncoupling ceramide glycosylation by transfection of glucosylceramide synthase antisense reverses adriamycin resistance. *J. Biol. Chem.* 275: 7138–7143
56. Bezombes C, Maestre N, Laurent G, Levade T, Bettaieb A and Jaffrézou JP (1998) Restoration of TNF- α -induced ceramide generation and apoptosis in resistant human leukemia KG1a cells by the P-glycoprotein blocker PSC833. *FASEB J.* 12: 101–109
57. Modrak DE, Lew W, Goldenberg DM and Blumenthal R (2000) Sphingomyelin potentiates chemotherapy of human cancer xenografts. *Biochem. Biophys. Res. Commun.* 268: 603–606
58. Sachs CW, Safa AR, Harrison SD and Fine RL (1995) Partial inhibition of multidrug resistance by safinolol is independent of modulation of P-glycoprotein substrate activities and correlated with inhibition of protein kinase C. *J. Biol. Chem.* 270: 26639–26648

59. Schwartz GK, Ward D, Saltz L, Casper ES, Spiess T, Mullen E, Woodworth J, Venuti R, Zervos P, Storniolo AM and Kelsen DP (1997) A pilot clinical pharmacological study of the protein kinase C-specific inhibitor safingol alone and in combination with doxorubicin. *Clin. Cancer Res.* 3: 537–543
60. Janicke RU, Ng P, Sprengart ML and Porter AG (1998) Caspase-3 is required for alpha-fodrin cleavage but dispensable for cleavage of other death substrates in apoptosis. *J. Biol. Chem.* 273: 15540–15545
61. Olivera A, Rosenthal J and Spiegel S (1994) Sphingosine kinase from Swiss 3T3 fibroblasts: a convenient assay for the measurement of intracellular levels of free sphingoid bases. *Anal. Biochem.* 223: 306–312
62. Edsall LC, Pirianov GG and Spiegel S (1997) Involvement of sphingosine 1-phosphate in nerve growth factor-mediated neuronal survival and differentiation. *J. Neurosci.* 17: 6952–6960
63. van Veldhoven PP and Mannaerts GP (1987) Inorganic and organic phosphate measurements in the nanomolar range. *Anal. Biochem.* 161: 45–48
64. Cuvillier O, Pirianov G, Kleuser B, Vanek PJ, Coso OA, Gutkind JS and Spiegel S (1996) Suppression of ceramide-mediated programmed cell death by sphingosine-1-phosphate. *Nature* 381: 800–803
65. Cuvillier O, Mayhew E, Janoff AS and Spiegel S (1999) Induction of a cytochrome c-mediated apoptosis in liposome-associated ether lipid ET-18-O-CH₃. *Blood* 94: 3583–3592
66. Cuvillier O, Rosenthal DS, Smulson ME and Spiegel S (1998) Sphingosine 1-phosphate inhibits activation of caspases that cleave poly(ADP-ribose) polymerase and lamins during Fas- and ceramide-mediated apoptosis in Jurkat T lymphocytes. *J. Biol. Chem.* 273: 2910–2916

Edg-1, the G protein-coupled receptor for sphingosine-1-phosphate, is essential for vascular maturation

Yujing Liu,¹ Ryuichi Wada,¹ Tadashi Yamashita,¹ Yide Mi,¹
Chu-Xia Deng,¹ John P. Hobson,² Hans M. Rosenfeldt,²
Victor E. Nava,² Sung-Suk Chae,³ Menq-Jer Lee,³
Catherine H. Liu,³ Timothy Hla,³ Sarah Spiegel,² and Richard L. Proia¹

¹Genetics of Development and Disease Branch, National Institute of Diabetes and Digestive and Kidney Diseases, NIH, Bethesda, Maryland, USA

²Department of Biochemistry and Molecular Biology, Georgetown University Medical Center, Washington, DC, USA

³Center for Vascular Biology, Department of Physiology, University of Connecticut Health Center, Farmington, Connecticut, USA

Address correspondence to: Richard L. Proia, Building 10, Room 9N-314, National Institutes of Health, 10 Center DR MSC 1821, Bethesda, Maryland 20892-1821, USA. Phone: (301) 496-4391; Fax: (301) 496-9878; E-mail: proia@nih.gov.

Received for publication July 28, 2000, and accepted in revised form September 12, 2000.

Sphingolipid signaling pathways have been implicated in many critical cellular events. Sphingosine-1-phosphate (SPP), a sphingolipid metabolite found in high concentrations in platelets and blood, stimulates members of the endothelial differentiation gene (Edg) family of G protein-coupled receptors and triggers diverse effects, including cell growth, survival, migration, and morphogenesis. To determine the *in vivo* functions of the SPP/Edg signaling pathway, we disrupted the *Edg1* gene in mice. *Edg1*^{-/-} mice exhibited embryonic hemorrhage leading to intrauterine death between E12.5 and E14.5. Vasculogenesis and angiogenesis appeared normal in the mutant embryos. However, vascular maturation was incomplete due to a deficiency of vascular smooth muscle cells/pericytes. We also show that Edg-1 mediates an SPP-induced migration response that is defective in mutant cells due to an inability to activate the small GTPase, Rac. Our data reveal Edg-1 to be the first G protein-coupled receptor required for blood vessel formation and show that sphingolipid signaling is essential during mammalian development.

J. Clin. Invest. 106:951-961 (2000).

Introduction

Sphingolipids have emerged as important signaling molecules in a variety of biologic processes (1-3). SPP in particular has come to the fore as a mediator of an extracellular signaling pathway through its interaction with the family of G protein-coupled receptors known by the acronym, Edg (endothelial differentiation gene) (4). Edg-1, the first of these receptors described, was identified as a gene induced during human endothelial cell differentiation (5). Activation of the Edg receptors triggers diverse effects including proliferation, survival, migration, morphogenesis, adhesion molecule expression, and cytoskeletal changes and has led to the view that the Edg receptor signaling pathways may have important roles in many physiological and pathological events (reviewed in refs. 6-10).

The Edg family can be subdivided into either receptors for SPP or for lysophosphatidic acid. The Edg receptors for SPP activate different and sometimes overlapping G protein-mediated intracellular signaling pathways. For instance, Edg-1 couples directly to the G_i pathway, whereas Edg-3 and -5 stimulate G₁₂, G₁₃

and G₁₃ pathways with differing degrees of potency (4, 11-14). Moreover, the expression pattern of individual Edg receptors changes during development and differentiation, leading to different combinations on cells and tissues (15-18). The diverse receptor expression and activation of divergent signaling pathways may explain the pleiotropic responses to SPP but have made functional analysis difficult.

To determine the functions of the SPP/Edg-1 signaling pathway, we have disrupted *Edg1* in mice. Homozygous *Edg1* mutant mice die in utero due to massive embryonic hemorrhage. They undergo normal vasculogenesis and angiogenesis but are severely impaired in vessel maturation due to a defect in the recruitment of mural cells to vessel walls. The results reveal the SPP receptor Edg-1 as mediating a novel G protein-coupled signaling pathway required for blood vessel development.

Methods

Generation of *Edg1* mutant mice. To generate the *Edg1* knockout mice, we cloned a 10-kb genomic DNA fragment containing the entire *Edg1* gene from a 129/Sv

library. As shown in Figure 1a, the *Edg1* gene is composed of two exons and an intron (16). The second large exon contains a 5'-UTR region, the entire open reading frame region, and approximately 1.8 kb of the 3'-UTR region. For knocking-in the *LacZ* reporter gene and targeted inactivation of the *Edg1* gene, a *NcoI* site in the beginning of the *Edg1* open reading frame was used to insert a *LacZ-neo* (neomycin-resistant gene) cassette (19). In the construct used for disruption of the *Edg1* gene, the *LacZ* coding region is preceded by an internal ribosomal entry sequence (20). Therefore, targeted insertion generates a bi-cistronic transcription unit in which the expression of the β -galactosidase reporter protein is under the control of *Edg1* transcriptional regulatory elements. The herpes simplex virus thymidine kinase (TK) gene was located outside the homologous sequence to prevent random integration.

Gene targeting in TC1 embryonic stem (ES) cells and generation of chimeric and heterozygous mice were as described previously (21). One targeted ES clone was used to establish chimeric mice, which were crossed with C57BL/6 mice to obtain *Edg1* heterozygotes. All mice analyzed were obtained from intercrosses of the *Edg1* heterozygotes. *Edg1* genotypes were determined by Southern blot and PCR analyses of genomic DNA isolated from ES cells, yolk sacs and tail biopsies. For genotyping by PCR, the primers were: 5'TAGCAGCTATGGTGTCCACTAG3' (Primer 1), 5'GATCCTGCGAGTAGAGGATGGC3' (Primer 2), 5'TTGGAGTGACGGCAGTTATCTGGA3' (Primer 3), and 5'TCAACCACCGCAGATAGAGATTC3' (Primer 4). Primers 1 and 2 detected the wild-type *Edg1* allele and amplified an approximately 630-bp fragment. Primers 3 and 4 detected the *Edg1^{LacZ}* allele and amplified an approximately 350-bp fragment. Forty-five cycles of 94°C (1 minute), 55°C (1 minute), and 72°C (3 minutes) were used.

Histological analysis. Embryos at embryonic days (E) 9.5–16.5 were removed from the mother after heterozygous mating. Then the embryos were fixed and processed to be embedded in paraffin. Serial sections (5- μ m-thick) were made at 15- μ m intervals and stained with hematoxylin and eosin (H&E).

Paraffin sections were deparaffinized and rehydrated. Antigen retrieval was accomplished by 30-minute incubation at 95°C in Target Retrieval Solution (DAKO Corp., Carpinteria, California, USA). Endogenous peroxidase activity was quenched by incubation with 5% hydrogen peroxide in methanol for 5 minutes. Specimens were incubated with anti-smooth muscle α actin (EPOS anti-SMA/HRP; no. U7033; DAKO Corp.) for 1 hour at room temperature. After washing with PBS, peroxidase reaction was visualized with diaminobenzidine/hydrogen (DAB/hydrogen) peroxide.

To define the developmental and tissue-specific expression patterns of *Edg1* through X-Gal staining, embryos dissected out from the decidua at various developmental stages were fixed in 2% formaldehyde/2% glutaraldehyde in PBS for 10 minutes. They

were washed in PBS and then incubated in PBS containing 5 mM $K_3Fe(CN)_6$, 2 mM $MgCl_2$, and 1 mg/ml X-Gal at 37°C overnight. Reactions were stopped by rinsing embryos with PBS, followed by further fixation in 4% paraformaldehyde.

Whole-mount embryo immunostaining. Embryos were dissected out and fixed in 4% paraformaldehyde in PBS at 4°C overnight. They were then dehydrated through a methanol series and stored in 100% methanol at -20°C. The embryos were bleached in 6% hydrogen peroxide/methanol for 1 hour at room temperature and rehydrated through a methanol series to PBS + 0.1% Tween 20 (PBST). They were incubated in a blocking solution (4% BSA in PBST) twice, for 1 hour each time. The embryos were incubated with rat mAb's (anti-PECAM-1: no.1951D; anti-CD34: no. 09431D; anti-VE-cadherin: no. 28091D; PharMingen, San Diego, California, USA), diluted 1:200 in 10% goat serum and 4% BSA in PBST at 4°C overnight. Embryos were washed with 4% BSA in PBST at room temperature and then incubated with peroxidase-conjugated goat anti-rat Ig in 10% goat serum and 4% BSA in PBST at 4°C overnight. Peroxidase reaction was visualized with DAB/hydrogen peroxide.

RT-PCR and immunoblotting. Total RNA was isolated from E12.5 mouse embryos and cultured cells using Trizol (Life Technologies Inc., Gaithersburg, Maryland, USA) and treated with DNaseI (Life Technologies). Total RNA (5 μ g) was reverse transcribed using Superscript Preamplification System (Life Technologies) according to the manufacturer's instructions. PCR was performed on 2 μ l of the RT reaction in a volume of 50 μ l using AmpliTaq Gold polymerase (Perkin-Elmer Corp., Norwalk, Connecticut, USA). The PCR conditions were as follows: initial denaturation at 95°C for 10 minutes followed by up to 35 cycles of denaturation at 95°C (1 minute), annealing at 55°C (1 minute), and extension at 72°C (1 min). Amplified PCR products were analyzed by electrophoresis on a 2% agarose gel. PCR primer pairs were as follows:

Flt-1: (5'TGTGGAGAACTTGGTGACCT3', 5'TGGAGAACAGCAGGACTCCTT3')
Flk-1: (5'TCTGTGGTTCTGCGTGGAGA3', 5'GTATCATTTCCAACCACCCT3')
Tie-1: (5'TCTTTGCTGCTCCCCACTCT3', 5'ACACACACATTCGCCATCAT3')
Tie-2: (5'CCTTCCTACCTGCTACTTTA3', 5'CCACTACACCTTTCTTTACA3')
Ang-1: (5'AAGGGAGGAAAAAGAGAAGAAGAG3', 5'GTTAGCATGAGAGCGCATTTG3')
Ang-2: (5'TGCCTACACTACCAGAAGAAC 3', 5'TATTTACTGCTGAACCTCCAC 3')
PECAM-1: (5'GTCATGGCCATGGTGCAGTA3', 5'CTCCTCGGCATCTTGCTGAA3')
VE-cadherin: (5'GGATGCAGAGGCTCAGAG3', 5'CTGGCGGTTACGTTGGACT3')
Smad5: (5'CTTTCCACCAACCAACAAC3', 5'TCATAGGCGACAGGCTGAAC3')
endoglin: (5'TACTCATGTCCCTGATCCAGCC3',

5'GTCGATGCACTGTACCTTTTCC3')
 LKLF: (5'CCACACATACTTGACGTACAC3',
 5'CCATCGTCTCCCTTATAGAAATA3')
 Edg-1: (5'TAGCAGCTATGGTGTCCACTAG-3',
 5'GATCCTGCAGTAGAGGATGGC3')

For immunoblotting, detergent extracts of E12.5 embryos were analyzed for protein expression using antibodies against the following proteins: VE-cadherin (catalog no. 28091D; PharMingen); N-cadherin (catalog no. SC-7939; Santa Cruz Biotechnology Inc., Santa Cruz, California, USA); and P-cadherin (catalog no. SC-7893), PDGF-B (catalog no. SC-7878), and VEGF (catalog no. SC-507; all from Santa Cruz Biotechnology). A peroxidase-conjugated secondary antibody was used, and the reaction was visualized with the ECL + Plus Western blotting system (Amersham Pharmacia Biotech, Piscataway, New Jersey, USA).

In vitro assays. Chemotactic migration of cells was measured in a modified Boyden chamber as described previously using polycarbonate filters (25 × 80 mm; 12 µm pore size) coated with collagen type I (50 µg/ml in 5% acetic acid), which promotes uniform attachment to and migration across the filter without formation of a barrier (22). SPP or medium without serum was placed in the lower chamber as chemoattractants. Mouse embryonic fibroblasts were harvested and added to the upper chamber at 5 × 10⁴ cells per well. Each data point was the average number of cells in four random fields, each counted twice. Each determination represents the average ± SD of three individual wells. For the detection of GTP-bound activated Rac, embryonic fibroblasts were serum-starved for 24 hours before they were treated with SPP (200 nM) for 5 minutes. The cell lysates were used for affinity precipitation with the PAK-1 p21 binding domain-conjugated (PDB-conjugated) agarose beads (Upstate Biotechnology Inc., Lake Placid, New York, USA) as described elsewhere (23), or were used without fractionation to determine total Rac levels. Rac was visualized by immunoblotting with an mAb.

Results

Generation of *Edg1* knockout mice with an inserted β -galactosidase (*LacZ*) reporter gene. *Edg1* consists of two exons (16), with the entire coding region in the second exon (Figure 1a). To disrupt *Edg1* in mouse ES cells, we constructed a replacement-type targeting vector in which the *Edg1* coding region, containing 382 amino acids, was disrupted after the first 42 amino acids by a *LacZ-Neo* cassette containing a internal ribosome entry sequence (19). This targeting strategy should both create a disrupted *Edg1* allele and enable analysis of *Edg1* expression in mice by creation of an *Edg1-LacZ* hybrid transcript driven by the endogenous *Edg1* promoter elements. The targeting vector was linearized and electroporated into the TC-1 ES cell line. Genomic DNA from G418- and ganciclovir-resistant clones was analyzed by Southern blotting. Of the 120 clones examined, about 60% contained the 2.5-kb BamHI band diagnostic of a homologous recombina-

tion event. Targeted ES cells were injected into C57BL/6 mouse blastocysts and produced highly chimeric male mice that transmitted the targeted allele through the germ line (Figure 1b). No *Edg1^{LacZ}* homozygotes were found among more than 100 newborn animals from heterozygous crosses (Table 1), indicating an embryonic lethal phenotype. Heterozygous *Edg1* mice appeared at the expected frequency and were phenotypically normal.

Edg1^{LacZ} homozygous embryos were present in utero as determined by Southern analysis. To confirm that *Edg1* was disrupted by the targeting scenario, RT-PCR was performed on total embryonic RNA using primers flanking the disrupted sequence (RT-5' and RT-3' in Figure 1a). The predicted 630-bp product was amplified from RNA of both wild-type and heterozygous embryos (Figure 1c). No PCR amplified band was detected from RNA of homozygous mutant embryos, indicating disruption of the normal *Edg1* transcripts.

Expression patterns of *Edg1* gene during mice embryogenesis. *LacZ* expression, under the control of native *Edg1* regulatory elements, was visualized by X-Gal staining in heterozygous embryos. At E9.5, intense expression was observed in the common ventricular chamber of heart, dorsal aorta, intersomitic arteries, and capillaries (Figure 1d). Weak expression was detected in the forebrain and common atrial chamber of the heart. Very weak or no expression was found in the anterior and posterior cardinal veins (Figure 1d). In addition to the expression pattern observed in the E9.5 embryo, E10.5 embryos showed prominent *LacZ* expression in the forebrain and a weaker level of expression in the spinal cord (Figure 1e). To examine the expression of the *Edg1* gene in detail, histological sections of X-Gal stained embryos were evaluated. The expression was most prominent in the endothelial cells of arteries and capillaries (Figure 1f), cardiomyocytes, and neuronal cells of the telencephalon (data not shown). No expression was found in the endothelial cells of veins (Figure 1g). Low levels of expression were detected the smooth muscle layers surrounding the aorta (Figure 1h).

Characterization of *Edg1^{-/-}* embryos. To determine the time of embryonic lethality, embryos at various stages of gestation were isolated. Genotyping of E9.5 to E11.5 embryos from *Edg1* heterozygous intercrosses

Table 1

Genotype analysis of offspring from *Edg1* heterozygous intercrosses

Age	Total	Genotype +/+	Genotype +/-	Genotype -/-	(%)
E9.5	74	19	31	24	(32)
E10.5	42	8	23	11	(26)
E11.5	30	8	14	8	(27)
E12.5	113	32	55	26 ^A	(23)
E13.5	45	9	28	8 ^A	(18)
E14.5	33	12	21	0	(0)
E15.5-16.5	35	12	23	0	(0)
Adult	115	38	77	0	(0)

^AHemorrhage.

revealed inheritance of the *Edg1* mutant allele at the expected mendelian frequency (Table 1). Up to E11.5, *Edg1*^{+/+} embryos appeared phenotypically normal. At E12.5, the *Edg1*^{+/+} embryos could be identified by their abnormal yolk sacs, which were edematous, with less blood in the otherwise normal looking, highly branched, vasculature (Figure 2a, arrows). After removing the yolk sac, intraembryonic bleeding was evident in the *Edg1*^{+/+} embryos (Figure 2b). The pericardial cavity of mutant embryos was enlarged and

filled with fluid. The limbs of mutant embryos were underdeveloped and rounded with areas of bleeding. In comparison, age-matched wild-type embryos had more developed, fan-shaped limbs. Much less blood was found in the yolk sac blood vessels of E13.5 *Edg1*^{+/+} embryos compared with those of the mutant embryos obtained 1 day earlier (Figure 2c, arrows). At E13.5, massive intraembryonic bleeding could be observed through the yolk sac. In addition to widespread hemorrhage, severe edema was observed

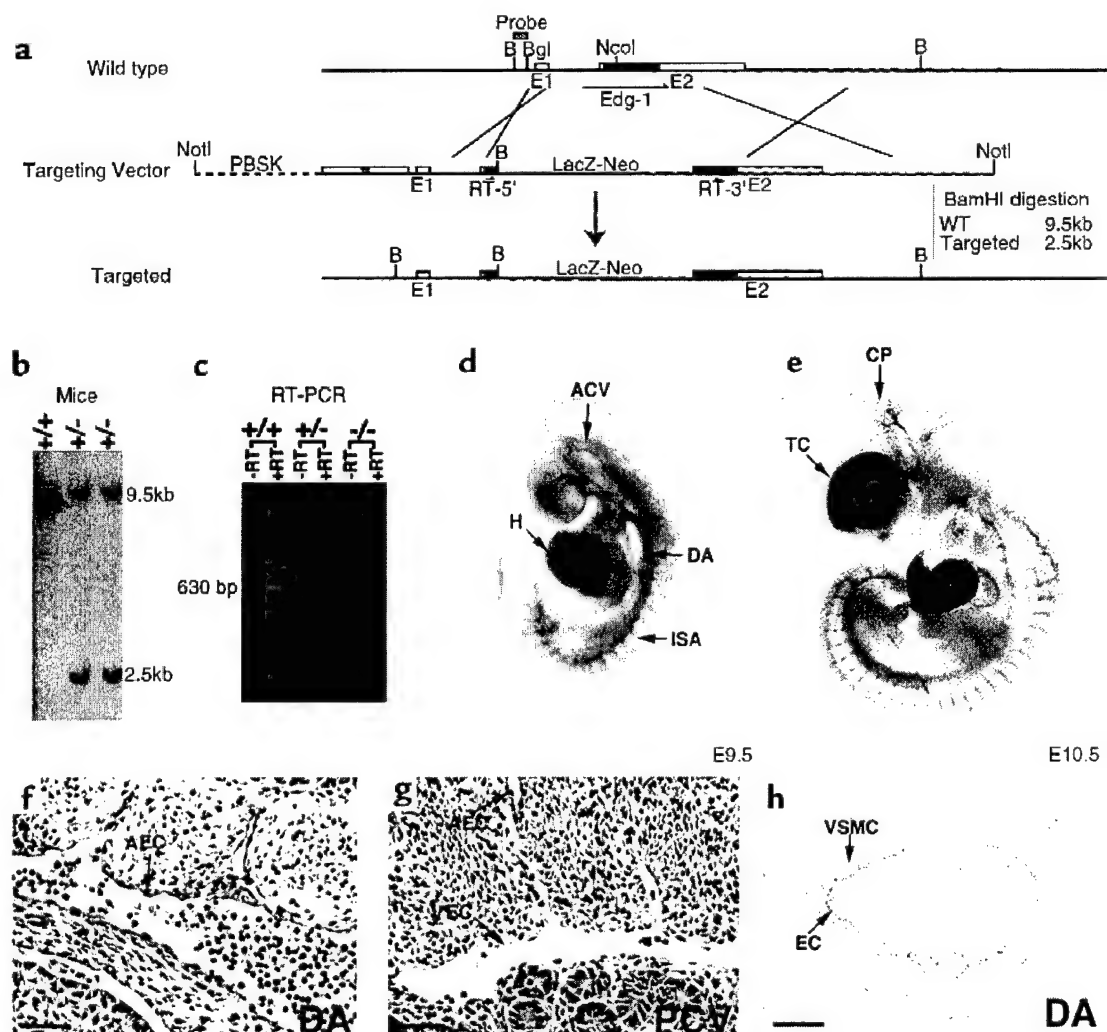
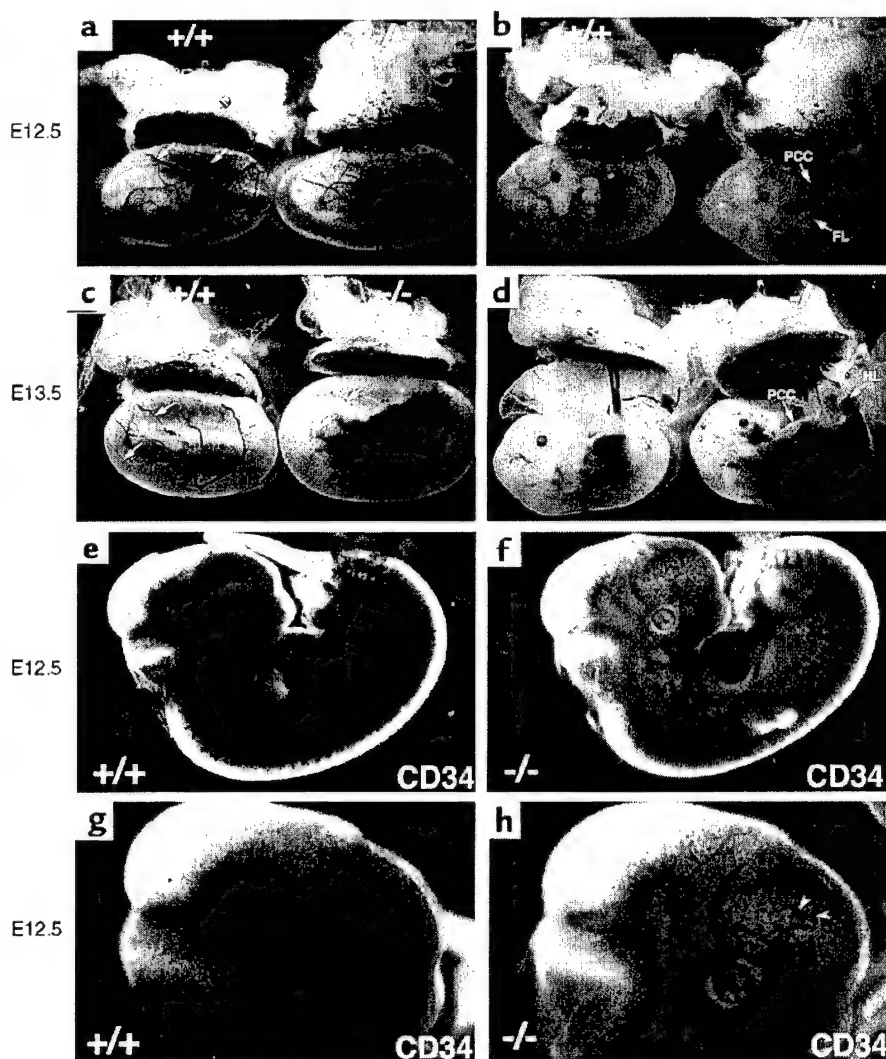


Figure 1

Targeted disruption and embryonic expression of the *Edg1* gene. (a) Schematic representation of the *Edg1* targeting strategy. The structure of the mouse *Edg1* locus is shown at the top, the structure of the *Edg1* targeting vector in the middle, and the predicted structure of the homologous recombined locus on the bottom. RT-5' and RT-3', primers for RT-PCR. B, BamHI; Bgl, BglII; PBSK, pBluescript vector. (b) Genotyping of mouse offspring from the *Edg1* heterozygous mating. Wild-type *Edg1* locus yielded a 9.5-kb BamHI band. Disrupted *Edg1* locus yielded a 2.5-kb BamHI band. No *Edg1*^{-/-} mice were found born alive. (c) RT-PCR analysis of total RNA from E12.5 mouse embryos by using RT-5' and RT-3'. *Edg1*^{+/+} and *Edg1*^{+/+} RNA yielded the predicted 630-bp amplification product. No amplification product was detected from *Edg1*^{-/-} RNA. (d, e) Whole-mount of *Edg1*^{-/-} E9.5 and E10.5 embryos stained with X-Gal. H, heart; DA, dorsal aorta; ISA, intersomatic arteries; CP, capillaries; TC, telencephalon; ACV, anterior cardinal vein. (f) Longitudinal section of dorsal aorta (DA) from E10.5 *Edg1*^{-/-} embryo. LacZ staining is seen in arterial ECs (AEC). (g) Longitudinal section of posterior cardinal vein (PCV) from E10.5 *Edg1*^{-/-} embryo. LacZ staining is seen in arterial endothelial cells (AEC) but not in venous endothelial cells (VEC). (h) Transverse section of dorsal aorta from E12.5 *Edg1*^{-/-} embryo. Vascular ECs and VSMCs are stained. EC, endothelial cell; VSMC, vascular smooth muscle cell. Scale bars = 50 μ m.

Figure 2

Phenotype of *Edg1*^{-/-} embryos and normal vascular network in the *Edg1*^{-/-} embryos. Photomicrographs of E12.5 and E13.5 embryos with the amnion, yolk sac, and placenta intact (a and c), or with extraembryonic membranes removed (b and d). *Edg1*^{-/-} embryos show normal yolk sac vasculature but with less blood (arrows). Yolk sacs of *Edg1*^{-/-} embryos display progressive edema. E12.5 *Edg1*^{-/-} embryo shows intraembryonic hemorrhages in the body and limbs. FL, front limb; HL, hind limb. E13.5 *Edg1*^{-/-} embryo demonstrates severe intraembryonic hemorrhages and edema. Both E12.5 and E13.5 *Edg1*^{-/-} embryos display pericardial cavity (PCC) edema. (e-h) E12.5 wild-type and *Edg1*^{-/-} embryos were stained with an anti-CD34 mAb and visualized by low-power (e and f) or higher-power (g and h) magnification. Note the normal vascular patterning, capillary plexus, and capillary sprouting (black arrowheads) in the *Edg1*^{-/-} embryos. Small blood vessels in the forebrain of *Edg1*^{-/-} embryos are slightly dilated (white arrowheads).



throughout the body of *Edg1*^{-/-} embryos (Figure 3d). No *Edg1*^{-/-} embryos survived beyond E14.5 (Table 1).

Normal vasculogenesis in *Edg1*^{-/-} embryos. To define the vascular system in the *Edg1*^{-/-} embryos, the morphology of the vasculature was characterized by whole-mount immunohistochemical staining using mAb's against markers for endothelial cells. Antibodies to CD34 (Figure 2, e and f) and platelet endothelial cell adhesion molecule-1 (PECAM-1) (data not shown) revealed a substantially normal arborized vascular network both in the mutants and age-matched control embryos. High magnification views showed capillary sprouts in the head of mutant embryos (Figure 2, g and h, black arrowhead). However, the small vessels in the forebrain of mutant embryos appeared dilated and stained darker than controls with antibodies against PECAM-1 and CD34 (white arrowheads).

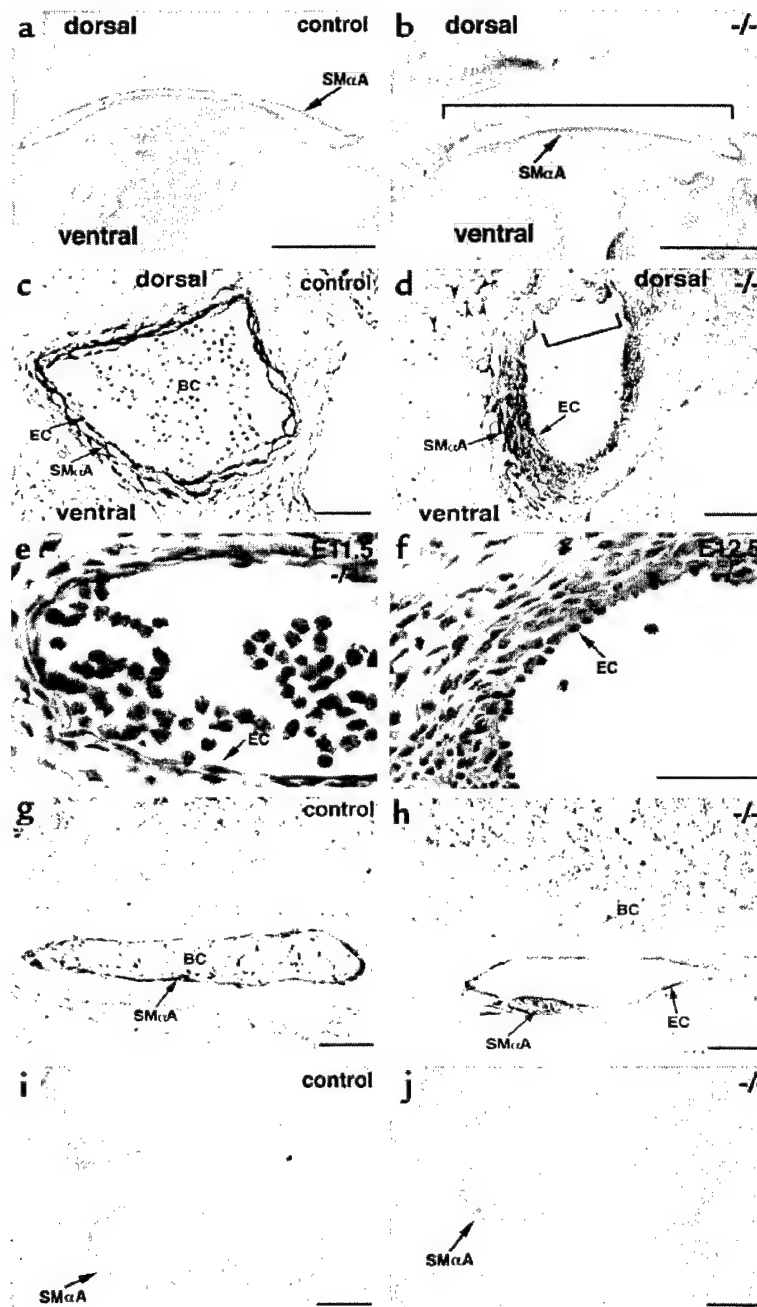
Because SPP signaling through Edg-1 was shown to be involved in adherens junction assembly in HUVEC cells in vitro (24), we investigated the expression of VE-cad-

herin, P-cadherin, E-cadherin, N-cadherin, and PECAM-1 in *Edg1*^{-/-} embryos by using whole-mount immunohistochemistry and Western blot analysis. No obvious difference was observed in expression patterns between mutant and control embryos. Disruption of VE-cadherin function causes increased endothelial apoptosis (25); however, there was no apparent enhancement of endothelial cell death in E12.5 *Edg1*^{-/-} embryos as determined by TUNEL staining (data not shown).

Because *Edg1* is highly expressed in vascular endothelial cells, endothelial cell proliferation and differentiation signaling factors, including *VEGF*, *Flt-1*, *Flk-1*, *Tie-1*, *Tie-2*, *Ang-1*, and *Ang-2*, were analyzed by Western blot and RT-PCR methods. All of these genes were expressed in *Edg1*^{-/-} embryos at levels similar to those of control embryos (data not shown). Thus the expression of genes required for early differentiation and assembly of endothelial cells into the vascular network was not impaired in the *Edg1*^{-/-} embryos. Our data indicate that in *Edg1*^{-/-} embryos, vasculogenesis

Figure 3

Vascular smooth muscle defects in the *Edg1*^{-/-} embryos. (a and b) Aortae of E12.5 embryos, sectioned longitudinally and stained with anti-SM α A antibody. Note the lack of SM α A-positive smooth muscle cells (bracket) on the dorsal side of aorta in the *Edg1*^{-/-} embryo. (c and d) Transverse sections of aortae from E12.5 embryos stained with anti-SM α A. Smooth muscle cells have accumulated at the ventral site of the aorta in the *Edg1*^{-/-} embryo. Note the discontinuous endothelial cell (EC) layer (bracket) in the *Edg1*^{-/-} embryo. Many blood cells have leaked out to the surrounding tissues in the *Edg1*^{-/-} embryo (arrowheads). BC, blood cells. (e and f) H&E staining of aorta from E11.5 and 12.5 *Edg1*^{-/-} embryos. Arrows point to ECs. Note their normal, flattened morphology in e and abnormal, cuboidal morphology in f. (g and h) Cranial arteries from E12.5 embryos stained with anti-SM α A antibody. Note the clustering of smooth muscle cells and nearly naked endothelial tube from the *Edg1*^{-/-} embryo. (i and j) Sections of intestine from E12.5 embryos stained with anti-SM α A. Note that that coverage of intestine by smooth muscle is similar in control and mutant embryos. Scale bars = 1 mm (a and b); 50 μ m (c and d); 50 μ m (e and f); 50 μ m (g and h); 500 μ m (i and j).



and the phase of angiogenesis that entails vessel sprouting and penetration had occurred.

Vascular smooth muscle defects in *Edg1*^{-/-} embryos. After the initial formation of the vascular plexus, vessels mature by the stabilization of the endothelial vascular network through a recruitment and differentiation process that ultimately results in the investment of vessel walls with mural cells (26).

Vascular smooth muscle cells (VSMCs) first appear on the ventral side of the aorta in E10.5 embryos, followed by migration to the dorsum (27). By E11.5, the aorta is completely enveloped by VSMCs (27). To

assess this aspect of vessel development in the *Edg1* mutant embryos, VSMCs were identified using an antibody to SM α A. In longitudinal sections of E12.5 control embryos stained with anti-SM α A, the dorsal aortae were found to be completely surrounded by VSMCs (Figure 3a). The aortae of *Edg1*^{-/-} mice were strikingly different. SM α A-positive VSMCs were present on the ventral surface; however, VSMCs were deficient along the entire length of the dorsal surface examined (Figure 3b).

Transverse sections of aortae from control embryos showed two to three layers of VSMCs surrounding the

vessel (Figure 3c). In contrast, similar sections from *Edg1*^{-/-} embryos showed that the aortae were covered only ventrally by poorly organized SM α A-expressing cells (Figure 3d). SM α A-expressing cells were not found on the dorsal side of the mutant aortae. These results suggested initial recruitment and differentiation had taken place to produce VSMCs on the ventral side of the mutant aorta, but that the process leading to the complete envelopment of the vessel was defective. Endothelial cell morphology appeared normal in E11.5 embryos, before the onset of bleeding (Figure 3e). In the E12.5 embryos, after the onset of bleeding, the dorsal aortic surface (uncovered by VSMCs) appeared abnormal and discontinuous (Figure 3, d and f).

In E12.5 control embryos, the majority of medium-sized arteries, identified by association with SM α A-positive VSMCs, were surrounded by a continuous layer of VSMCs (Figure 3g). Only rare vessels were found with an incomplete covering by VSMCs. In contrast, a substantial fraction of intracerebral arteries in the mutant embryos displayed a discontinuous or patchy covering by VSMCs (Figure 3h). Bleeding from these arteries was apparent by the presence of blood cells in the surrounding tissue space (Figure 3h).

The muscular layers in the gastrointestinal tract (Figure 3, i and j) and bronchial tree (data not shown) were well developed in the mutant embryos, indicating that there was not a generalized defect in smooth muscle.

The blood vessel defects in the *Edg1*^{-/-} embryos were further analyzed by electron microscopy. Small blood vessels from the limb of E12.5 *Edg1*^{-/-} embryos illustrated a marked reduction of VSMCs/pericytes adjacent to the endothelial cells (Figure 4, a and b). The endothelial cell body was very thin, and in some areas, fragmented (data not shown). Intracerebral capillaries of mutant embryos appeared without associated microvascular pericytes (Figure 4, c and d). The endothelial cell nuclei of the mutant capillaries were abnormally rounded and enlarged. The areas surrounding these vessels were generally much less densely packed with cells. Mutant blood vessels contained normal-appearing, electron-dense interendothelial junctions (Figure 4, e and f), suggesting that endothelial cell-cell junctions formation occurred in the absence of Edg-1. Given that PDGF-B and its receptor β are critical for the investment of capillaries with pericytes (28-30), we determined their expression in mutant embryos. We found that in *Edg1*^{-/-} embryos PDGF-B expression was normal as determined by Western analysis and that PDGF-receptor β was highly expressed in mesenchymal cells by immunohistochemical analysis (data not shown). Mice deficient in the transcription factor LKLF also show marked reductions in VSMCs and pericytes around vessels (31). RT-PCR of E12.5 *Edg1*^{-/-} RNA indicated that LKLF expression was similar to control levels (data not shown).

SPP induced migration in *Edg1*^{-/-} fibroblasts. Our analysis of *Edg1* embryos demonstrated a defect in blood vessel maturation that appeared to involve the ability of

mural cells to properly organize and reinforce endothelial walls. Recently, Edg-1 has been implicated as the mediator of an SPP-induced migration response in different cell types (32-35). We investigated whether cells derived from the mutant embryos were defective in their migration response to SPP.

Fibroblasts were obtained from control and *Edg1*^{-/-} embryos. RT-PCR revealed that wild-type fibroblasts expressed transcripts for *Edg1*, -3, and -5 genes (Figure 5a). *Edg1*^{-/-} fibroblasts, as expected, were devoid of the authentic *Edg1* transcript but contained transcripts for *Edg3* and -5. The mutant cells adhered normally to tissue culture plates and exhibited a normal mitogenic response to SPP (data not shown).

As shown in Figure 5b, 100 nM SPP induced a significant increase in the chemotaxis of wild-type fibroblasts. In contrast, the *Edg1*^{-/-} fibroblasts did not display a significant migratory response to SPP, proving that Edg-1 is required for SPP-induced migration in these cells. Because Rac activation, which has been shown to be stimulated by SPP (24), is critical for cell migration responses (36), we compared the effect of

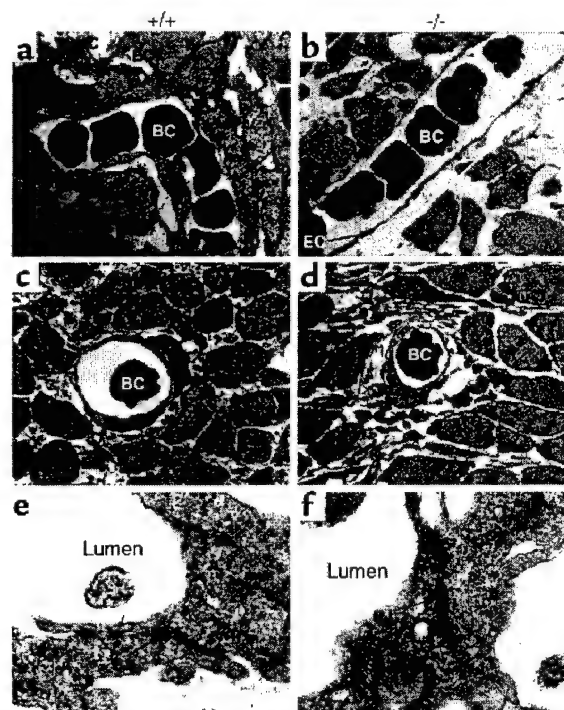


Figure 4 Reduced VSMCs and pericytes in the *Edg1*^{-/-} vessels. (a-d) EM microscopic analyses of representative small blood vessels from the limb (a and b) and brain capillaries (c and d) from E12.5 wild-type and *Edg1*^{-/-} embryos. Reduced number of VSMCs (bracket in b) and the lack of capillary pericytes (PC) were found in the *Edg1*^{-/-} embryos. Notice the abnormally rounded EC nucleus in the *Edg1*^{-/-} capillary (d). (e and f) EC junctions (arrows) in wild-type and mutant embryos. Note the normal EC junction (EJ) in the *Edg1*^{-/-} embryo (f). BC, blood cell. $\times 2,000$ (a-d); $\times 50,000$ (e and f).

Figure 5

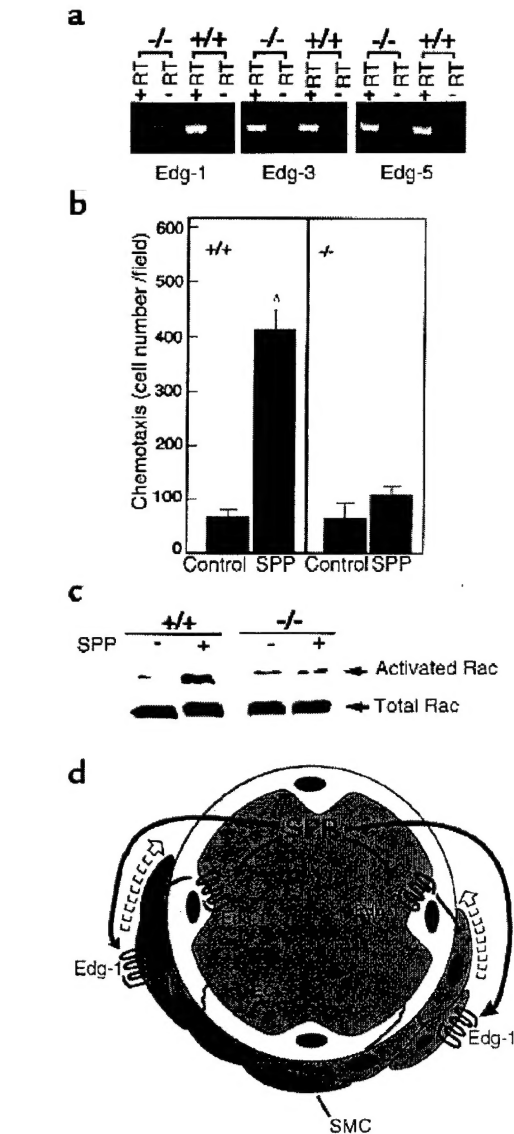
Migration and Rac activation defects in *Edg1*^{-/-} embryonic fibroblasts. (a) RT-PCR analysis of *Edg1*, -3, and -5 expression was carried out with total RNA isolated from *Edg1*^{+/+}, *Edg1*^{+/-}, and *Edg1*^{-/-} embryonic fibroblasts. (b) SPP chemotactic responses of embryonic fibroblasts. Serum-starved *Edg1*^{+/+} and *Edg1*^{-/-} fibroblasts were allowed to migrate toward a gradient produced by SPP (100 nM). Control (Cont.) indicates medium without serum was used as the chemoattractant. Chemotaxis was measured as described in Methods. Data are means \pm SD of triplicate determinations. *Statistically significant difference compared with the control, determined by Student's *t* test (*P* < 0.01). (c) Rac activation in fibroblasts. *Edg1*^{+/+} and *Edg1*^{-/-} fibroblasts were serum-starved and then treated with SPP for 5 minutes. The cell lysates were used both for affinity precipitation with the PAK-1-conjugated agarose to pull down activated, GTP-bound Rac (top panel) and without fractionation to determine total Rac levels (bottom panel) by SDS-PAGE and immunoblotting. (d) Model of Edg-1 functions in blood vessel development. The *Edg1* knockout demonstrates that Edg-1 is essential for vascular maturation by impairing the recruitment of smooth muscle cells to vessel walls. SPP, found in blood, may directly stimulate Edg-1 on VSMCs, facilitating their migration to vessels walls. In a second mechanism, which does not exclude the first, SPP could stimulate Edg-1 expressed on endothelial cells, which in turn recruit may VSMCs. EC, endothelial cell; SMC, smooth muscle cell.

SPP on Rac activation in wild-type and *Edg1*^{-/-} fibroblasts (Figure 5c). In wild-type fibroblasts, SPP treatment resulted in a substantial increase in the amount of activated Rac. By contrast, no increase in activated Rac could be detected after SPP treatment of *Edg1*^{-/-} fibroblasts, demonstrating that Edg-1 is required for the SPP induction of activated Rac.

Discussion

A number of receptor-mediated signaling pathways have been identified that coordinate the stages of blood vessel formation. Disruption of the genes encoding these receptors and ligands in mice has been instrumental in defining their roles (reviewed in refs. 26, 37, 38). Vasculogenesis is dependent on VEGF and its receptor tyrosine kinases, Flk-1 and Flt-1, expressed in endothelial cells (39–42). *VEGF*, *Flk-1*, and *Flt-1* knockout mice die between E8.5 and E9.5 as a result of defects in the formation of the primitive vasculature. Angiogenesis and vascular remodeling require the Tie-2 receptor tyrosine kinase on endothelial cells and its ligand, angiopoietin-1. Without Tie-2, mice have normal vasculogenesis but defective vessel sprouting, branching, and remodeling; they die at E10.5. Mice devoid of angiopoietin-1 have a similar phenotype (43–45).

Signaling pathways have also been implicated in the recruitment and differentiation of mural cells during vessel maturation. PDGF-B and its receptor- β have been shown to be essential for the recruitment of mesenchymally derived mural cell precursors to vessel walls (30, 46). Disruption of the *PDGF-B* or *PDGF receptor- β* genes in mice leads to lethal hemorrhage and edema in the perinatal stage owing to a lack of microvasculature pericytes (28–30). TGF- β 1 induces differentiation of VSMCs



(47) after their recruitment to endothelial walls (48, 49). The endothelial TGF- β 1 binding protein, endoglin, and its downstream signaling molecule, SMAD5, both important in the TGF- β 1 signaling pathway, also have essential roles in VSMC differentiation (50, 51). *Endoglin*- and *Smad5*-deficient mice die between E10.5 and E11.5 with a lack of VSMCs around major vessels.

These studies point to the critical roles played by receptor tyrosine kinases during vascular development. In contrast, the involvement of G-protein-coupled signaling pathways have not been as well characterized during development. Such pathways are important because disruption of the *G α_{13}* gene results in defects in embryonic vasculature formation, presumably due to a migration defect (52). However, upstream receptors involved had not been defined.

Role of Edg-1 during early vascular system development. We found that *Edg1* was highly expressed in the cardiovas-

cular system during early embryonic development. Vascular endothelial cells expressed *Edg1* at relatively high levels, although expression was almost exclusively found in the endothelial cells of arteries rather than of veins. A low but detectable expression was also found in VSMCs surrounding the aorta. Expression of *Edg1* was prominent in cardiomyocytes, although no gross abnormalities were detected in the developing heart. In addition to the vascular system, *Edg1* was found highly expressed in the developing central nervous system as has been shown previously (16, 18).

Severe bleeding caused lethality in *Edg1*^{-/-} embryos between E12.5 and E14.5. However, the mutant embryos showed a substantially normal blood vessel network when stained with antibodies to markers specific for differentiated endothelial cells such as PECAM-1 and CD34. The expression of genes known to be important for vasculogenesis and angiogenesis was not measurably affected in *Edg1*^{-/-} embryos. These genes included *VEGF*, *Flk-1*, *Flt-1*, *Ang-1*, and *Tie-2*. Each phenotype of these knockout mice is quite distinct from that of the *Edg1*^{-/-} mice, which develop a relatively normal appearing vascular network and die between E12.5 and E14.5. These results indicate that *Edg1* is dispensable for vascular endothelial cell differentiation, proliferation, migration, and tube formation during vasculogenesis and for the stage of angiogenesis involving vessel sprouting and branching. The morphology and viability of endothelial cells in the mutants appeared normal until the onset of severe bleeding, suggesting that the morphology changes were secondary to the lack of supporting VSMCs and subsequent disruption of the vessels in the mutant embryos.

Although SPP signaling through Edg-1 has been shown to regulate adherens junction formation in vitro in human endothelial cells, we found no evidence of aberrant endothelial junctions in *Edg1* mutant mice during development. Ultrastructural analysis of mutant endothelial cells revealed normal appearing cell-cell junctions. The phenotype of the *Edg1* mutant embryos was also not in keeping with significant defects in endothelial cell junctions. Recently, it was shown that VE-cadherin, an important component of adherens junctions, controls an endothelial cell survival pathway through its intracellular interaction with β -catenin (25). Disruption of this pathway in mice resulted in impaired angiogenesis, increased endothelial apoptosis, and embryonic death by E9.5. The *Edg1* mutant mice exhibited none of these characteristics. Thus the formation of functional endothelial junctions apparently proceeds normally during early development in the absence of Edg-1. This could indicate that there is functional redundancy among members of the Edg family for this process and that other Edg proteins may substitute for Edg-1. It may also indicate that the SPP-Edg regulation of adherens junction assembly is not required for blood vessel formation during development. However, this would not preclude a role for the pathway during angiogenesis in the adult.

Functions of Edg-1 during vessel maturation. In dorsal aorta, VSMC investment is initiated on the ventral side with a condensation of SM α A-positive cells. The recruitment process continues dorsally until VSMCs have completely enveloped the endothelial tube (27). We found that the aortae of wild-type and heterozygous embryos were surrounded by several layers of elongated VSMCs. The aortae in the *Edg1*^{-/-} embryos were strikingly abnormal in VSMC investment. Aortic sections demonstrated the presence of multiple layers of SM α A-positive cells, but only at the ventral surface. These results suggest that the defect in VSMC investment of vessel walls in *Edg1* mutant embryos was expressed after the initial VSMC recruitment to the ventral aortic surface has taken place. This vessel abnormality was distinct from that observed in mice deficient in endoglin, the TGF- β binding protein on endothelial cells, and in SMAD5, the TGF- β 1 signaling molecule. Both of these proteins are required for VSMC differentiation; the respective knockout mice have severely defective VSMC development with almost no SM α A-positive cells around vessels (50, 51).

In addition to a defect in mural cell recruitment in dorsal aorta, the *Edg1*^{-/-} mice exhibited defects in the smaller vessels and in the microvasculature. By electron microscopy, we found evidence of a lack of pericytes associated with capillaries. When pericytes are deficient as in *PDGF-B*^{-/-} mice, dilated microvessels develop that are prone to rupture (53). Similarly, in the *Edg1*^{-/-} mice, dilation of small cranial vessels and bleeding were evident.

How does Edg-1 so dramatically influence the recruitment of VSMCs to vessels during development? With fibroblasts from the *Edg1* mutant mice, we found that in the absence of Edg-1, the SPP-induced activation of Rac seen in wild-type cells did not occur. Rac is a key regulator of the actin cytoskeleton and of associated activities such as cell motility (36, 54). Thus, the *Edg1*^{-/-} fibroblasts, without this signaling pathway, were unable to mount a migration response to SPP. This signaling pathway may also operate in VSMCs, and its disruption could be responsible for the defect in vascular maturation seen in the *Edg1*^{-/-} mice. Consistent with this hypothesis, we found that Edg-1 mediates migration of normal VSMCs toward SPP (data not shown). SPP is abundantly stored in platelets and secreted after stimulation (55). Other blood cells, including erythrocytes, neutrophils, and mononuclear cells, produce and secrete SPP constitutively (56), resulting in significant SPP levels in blood. During maturation of the dorsal aorta and possibly other vessels, plasma containing SPP could escape from immature, leaky vessels and act as a signal to recruit VSMCs that are differentiating in the proximity of vessel walls (Figure 5d).

Recently, it was shown that the zebra fish gene, *mil*, encodes an SPP-binding, G protein-coupled receptor of the Edg family that directs the migration of heart precursors to the midline during embryonic development (57). Interestingly, *mil* does not function in the

migrating precursor cells, but in the paraxial cells at the midline, presumably by creating a permissive environment for migration. Sequence and functional similarities suggest that *mil* may be the ortholog of the mammalian *Edg5* gene. However, the indirect influence of *mil* on migrating cells, as well as the high level of expression of *Edg1* in arterial endothelial cells, raises the possibility that Edg-1 stimulation on endothelial cells may regulate the recruitment of VSMCs (Figure 5d). This might occur via the upregulation of adhesion molecules on endothelial cells, or by stimulating the secretion of recruitment factors for VSMCs. Further studies using tissue-specific knockouts of *Edg1* will be required to address precisely how Edg-1 functions. Nevertheless, our data demonstrate an indispensable role of *Edg1* in vascular maturation and, together with the results showing *mil* is essential for heart organogenesis, indicate that different members of the Edg receptor family regulate distinct aspects of cardiovascular development through sphingolipid signaling pathways.

In summary, we have uncovered a unique and vital role for the G protein-coupled receptor, Edg-1, in blood vessel formation during development. The SPP-Edg signaling pathway may also have important functions in adult vascular biology. SPP stimulation of Edg receptors on endothelial cells in vitro results in proliferation, migration, and tube formation (24, 32, 58), all requisite for the angiogenic process. Thus, the release of SPP after platelet activation, with subsequent stimulation of the Edg receptors on both endothelial cells and VSMCs, may drive blood vessel formation during wound healing and solid tumor growth (59, 60). If so, the SPP-Edg signaling pathway is a potential target for therapeutic manipulation during these and other processes that are dependent on angiogenesis.

Acknowledgments

We thank J. Van Brocklyn for help in the early stages of this project and A. Howard for producing the figures.

- Shayman, J.A. 2000. Perspectives in basic science: sphingolipids. *Kidney Int.* **58**:11-26.
- Huwyler, A., Kolter, T., Pfeilschifter, J., and Sandhoff, K. 2000. Physiology and pathophysiology of sphingolipid metabolism and signaling. *Biochim. Biophys. Acta.* **1485**:63-99.
- Spiegel, S., and Merrill, A.H., Jr. 1996. Sphingolipid metabolism and cell growth regulation. *FASEB J.* **10**:1388-1397.
- Lee, M.J., et al. 1998. Sphingosine-1-phosphate as a ligand for the G protein-coupled receptor EDG-1. *Science.* **279**:1552-1555.
- Hla, T., and Maciag, T. 1990. An abundant transcript induced in differentiating human endothelial cells encodes a polypeptide with structural similarities to G-protein-coupled receptors. *J. Biol. Chem.* **265**:9308-9313.
- Goetzl, E.J., and An, S. 1998. Diversity of cellular receptors and functions for the lysophospholipid growth factors lysophosphatidic acid and sphingosine 1-phosphate. *FASEB J.* **12**:1589-1598.
- Spiegel, S., and Milstien, S. 2000. Functions of a new family of sphingosine-1-phosphate receptors. *Biochim. Biophys. Acta.* **1484**:107-116.
- Hla, T., et al. 1999. Sphingosine-1-phosphate: extracellular mediator or intracellular second messenger? *Biochem. Pharmacol.* **58**:201-207.
- Chun, J., Contos, J.J., and Munroe, D. 1999. A growing family of receptor genes for lysophosphatidic acid (LPA) and other lysophospholipids (LPs). *Cell Biochem. Biophys.* **30**:213-242.
- Moolenaar, W.H. 1999. Bioactive lysophospholipids and their G protein-coupled receptors. *Exp. Cell Res.* **253**:230-238.
- Lee, M.J., Evans, M., and Hla, T. 1996. The inducible G protein-coupled receptor edg-1 signals via the G(i)/mitogen-activated protein kinase pathway. *J. Biol. Chem.* **271**:11272-11279.
- Ancellin, N., and Hla, T. 1999. Differential pharmacological properties and signal transduction of the sphingosine 1-phosphate receptors EDG-1, EDG-3, and EDG-5. *J. Biol. Chem.* **274**:18997-19002.
- An, S., Bleu, T., and Zheng, Y. 1999. Transduction of intracellular calcium signals through G protein-mediated activation of phospholipase C by recombinant sphingosine 1-phosphate receptors. *Mol. Pharmacol.* **55**:787-794.
- Windh, R.T., et al. 1999. Differential coupling of the sphingosine 1-phosphate receptors Edg-1, Edg-3, and H218/Edg-5 to the g(i), g(q), and G(12) families of heterotrimeric G proteins. *J. Biol. Chem.* **274**:27351-27358.
- Hecht, J.H., Weiner, J.A., Post, S.R., and Chun, J. 1996. Ventricular zone gene-1 (*vzg-1*) encodes a lysophosphatidic acid receptor expressed in neurogenic regions of the developing cerebral cortex. *J. Cell Biol.* **135**:1071-1083.
- Liu, C.H., and Hla, T. 1997. The mouse gene for the inducible G-protein-coupled receptor edg-1. *Genomics.* **43**:15-24.
- Galer, M.H., Bernhardt, G., and Lipp, M. 1998. EDG6, a novel G-protein-coupled receptor related to receptors for bioactive lysophospholipids, is specifically expressed in lymphoid tissue. *Genomics.* **53**:164-169.
- Zhang, G., Contos, J.J., Weiner, J.A., Fukushima, N., and Chun, J. 1999. Comparative analysis of three murine G-protein coupled receptors activated by sphingosine-1-phosphate. *Gene.* **227**:89-99.
- Nehls, M., et al. 1996. Two genetically separable steps in the differentiation of thymic epithelium. *Science.* **272**:886-889.
- Mountford, P.S., and Smith, A.G. 1995. Internal ribosome entry sites and dicistronic RNAs in mammalian transgenesis. *Trends Genet.* **11**:179-184.
- Liu, Y., et al. 1999. A genetic model of substrate deprivation therapy for a glycosphingolipid storage disorder. *J. Clin. Invest.* **103**:497-505.
- Wang, F., Nohara, K., Olivera, A., Thompson, E.W., and Spiegel, S. 1999. Involvement of focal adhesion kinase in inhibition of motility of human breast cancer cells by sphingosine 1-phosphate. *Exp. Cell Res.* **247**:17-28.
- Benard, V., Bohl, B.P., and Bokoch, G.M. 1999. Characterization of rac and cdc42 activation in chemoattractant-stimulated human neutrophils using a novel assay for active GTPases. *J. Biol. Chem.* **274**:13198-13204.
- Lee, M.J., et al. 1999. Vascular endothelial cell adherens junction assembly and morphogenesis induced by sphingosine-1-phosphate. *Cell.* **99**:301-312.
- Carmeliet, P., et al. 1999. Targeted deficiency or cytosolic truncation of the VE-cadherin gene in mice impairs VEGF-mediated endothelial survival and angiogenesis. *Cell.* **98**:147-157.
- Carmeliet, P. 2000. Mechanisms of angiogenesis and arteriogenesis. *Nat. Med.* **6**:389-395.
- Takahashi, Y., Imanaka, T., and Takano, T. 1996. Spatial and temporal pattern of smooth muscle cell differentiation during development of the vascular system in the mouse embryo. *Anat. Embryol. (Berl.)* **194**:515-526.
- Leveen, P., et al. 1994. Mice deficient for PDGF B show renal, cardiovascular, and hematological abnormalities. *Genes Dev.* **8**:1875-1887.
- Soriano, P. 1994. Abnormal kidney development and hematological disorders in PDGF beta-receptor mutant mice. *Genes Dev.* **8**:1888-1896.
- Lindahl, P., Johansson, B.R., Leveen, P., and Berrholzt, C. 1997. Pericyte loss and microaneurysm formation in PDGF-B-deficient mice. *Science.* **277**:242-245.
- Kuo, C.T., et al. 1997. The LKLF transcription factor is required for normal tunica media formation and blood vessel stabilization during murine embryogenesis. *Genes Dev.* **11**:2996-3006.
- Wang, F., et al. 1999. Sphingosine 1-phosphate stimulates cell migration through a G(i)-coupled cell surface receptor. Potential involvement in angiogenesis. *J. Biol. Chem.* **274**:35343-35350.
- Panetti, T.S., Nowlen, J., and Mosher, D.F. 2000. Sphingosine-1-phosphate and lysophosphatidic acid stimulate endothelial cell migration. *Arterioscler. Thromb. Vasc. Biol.* **20**:1013-1019.
- English, D., et al. 1999. Induction of endothelial cell chemotaxis by sphingosine 1-phosphate and stabilization of endothelial monolayer barrier function by lysophosphatidic acid. potential mediators of hematopoietic angiogenesis. *J. Hematother. Stem Cell Res.* **8**:627-634.
- Kon, J., et al. 1999. Comparison of intrinsic activities of the putative sphingosine 1-phosphate receptor subtypes to regulate several signaling pathways in their cDNA-transfected Chinese hamster ovary cells. *J. Biol. Chem.* **274**:23940-23947.
- Hall, A. 1998. Rho GTPases and the actin cytoskeleton. *Science.* **279**:509-514.
- Folkman, J., and D'Amore, P.A. 1996. Blood vessel formation: what is its molecular basis? *Cell.* **87**:1153-1155.

38. Hanahan, D. 1997. Signaling vascular morphogenesis and maintenance. *Science*. **277**:48-50.
39. Carmeliet, P., et al. 1996. Abnormal blood vessel development and lethality in embryos lacking a single VEGF allele. *Nature*. **380**:435-439.
40. Ferrara, N., et al. 1996. Heterozygous embryonic lethality induced by targeted inactivation of the VEGF gene. *Nature*. **380**:439-442.
41. Shalaby, F., et al. 1995. Failure of blood-island formation and vasculogenesis in Flk-1-deficient mice. *Nature*. **376**:62-66.
42. Fong, G.H., Rossant, J., Gertsenstein, M., and Breitman, M.L. 1995. Role of the Flt-1 receptor tyrosine kinase in regulating the assembly of vascular endothelium. *Nature*. **376**:66-70.
43. Dumont, D.J., et al. 1994. Dominant-negative and targeted null mutations in the endothelial receptor tyrosine kinase, tek, reveal a critical role in vasculogenesis of the embryo. *Genes Dev*. **8**:1897-1909.
44. Sato, T.N., et al. 1995. Distinct roles of the receptor tyrosine kinases Tie-1 and Tie-2 in blood vessel formation. *Nature*. **376**:70-74.
45. Suri, C., et al. 1996. Requisite role of angiopoietin-1, a ligand for the TIE2 receptor, during embryonic angiogenesis. *Cell*. **87**:1171-1180.
46. Hellstrom, M., Kal, M., Lindahl, P., Abramsson, A., and Besholtz, C. 1999. Role of PDGF-B and PDGFR-beta in recruitment of vascular smooth muscle cells and pericytes during embryonic blood vessel formation in the mouse. *Development*. **126**:3047-3055.
47. Shah, N.M., Groves, A.K., and Anderson, D.J. 1996. Alternative neural crest cell fates are instructively promoted by TGF-beta superfamily members. *Cell*. **85**:331-343.
48. Hirschi, K.K., Rohovsky, S.A., Beck, L.H., Smith, S.R., and D'Amore, P.A. 1999. Endothelial cells modulate the proliferation of mural cell precursors via platelet-derived growth factor-BB and heterotypic cell contact. *Circ. Res*. **84**:298-305.
49. Hirschi, K.K., Rohovsky, S.A., and D'Amore, P.A. 1998. PDGF, TGF-beta, and heterotypic cell-cell interactions mediate endothelial cell-induced recruitment of 10T1/2 cells and their differentiation to a smooth muscle fate [erratum, 1998. **141**:1287]. *J. Cell Biol.* **141**:805-814.
50. Li, D.Y., et al. 1999. Defective angiogenesis in mice lacking endoglin. *Science*. **284**:1534-1537.
51. Yang, X., et al. 1999. Angiogenesis defects and mesenchymal apoptosis in mice lacking SMAD5. *Development*. **126**:1571-1580.
52. Offermanns, S., Mancino, V., Revel, J.P., and Simon, M.I. 1997. Vascular system defects and impaired cell chemokinesis as a result of Galpha13 deficiency. *Science*. **275**:533-536.
53. Lindahl, P., Hellstrom, M., Kalen, M., and Betsholtz, C. 1998. Endothelial-perivascular cell signaling in vascular development: lessons from knockout mice. *Curr. Opin. Lipidol.* **9**:407-411.
54. Nobes, C.D., and Hall, A. 1995. Rho, rac, and cdc42 GTPases regulate the assembly of multimolecular focal complexes associated with actin stress fibers, lamellipodia, and filopodia. *Cell*. **81**:53-62.
55. Yatomi, Y., Ruan, F., Hakomori, S., and Igarashi, Y. 1995. Sphingosine-1-phosphate: a platelet-activating sphingolipid released from agonist-stimulated human platelets. *Blood*. **86**:193-202.
56. Yang, L., Yatomi, Y., Miura, Y., Satoh, K., and Ozaki, Y. 1999. Metabolism and functional effects of sphingolipids in blood cells. *Br. J. Haematol.* **107**:282-293.
57. Kupperman, E., An, S., Osborne, N., Waldron, S., and Stainier, D.Y.R. 2000. A sphingosine-1-phosphate receptor regulates cell migration during vertebrate heart development. *Nature*. **406**:192-195.
58. Lee, O., et al. 1999. Sphingosine 1-phosphate induces angiogenesis: its angiogenic action and signaling mechanism in human umbilical vein endothelial cells. *Biochem. Biophys. Res. Commun.* **264**:743-750.
59. Folkman, J. 1995. Angiogenesis in cancer, vascular, rheumatoid and other disease. *Nat. Med.* **1**:27-31.
60. Pinedo, H.M., Verheul, H.M., D'Amato, R.J., and Folkman, J. 1998. Involvement of platelets in tumour angiogenesis? *Lancet*. **352**:1775-1777.